

SCUOLA DI SCIENZE

Dipartimento di Chimica Industriale “Toso Montanari”

Corso di Laurea Magistrale in

Chimica Industriale

Classe LM-71 - Scienze e Tecnologie della Chimica Industriale

**Evaluation of recycled carbon fibers as PLA
reinforcement for additive manufacturing applications**

Tesi di laurea sperimentale

CANDIDATO

Daniele Giuliani

RELATORE

Chiar.ma Prof. Laura Mazzocchetti

CORRELATORE

Prof. Francesco Picchioni

Dott. Niccolò Giani

Summary

1.Introduction	1
1.1 Composite materials	1
1.2 CFRPs market	1
1.3 CFRPs' recycling challenges	2
1.4 Recycling methods	3
1.4.1 Mechanical recycling	5
1.4.2 Thermal recycling	5
1.4.3 Chemical recycling.....	8
1.4.4 Future challenges of recycling CFRPs	8
1.5 Composites re-manufacturing	9
1.5.1 Types and characteristics of waste carbon fibers	9
1.5.2 Introduction to processing technologies for recycled carbon fibers.....	12
1.5.3 Injection molding	13
1.5.4 Nonwoven technologies	14
1.5.5 Tape technology	17
1.5.6 Hybrid yarn technologies	19
1.6 Additive manufacturing.....	22
1.6.1 Material extrusion – FFF	25
1.6.2 3D printing (Material extrusion) of PLA	32
2.Thesis object.....	40
3. Results and discussion.....	41
3.1 Production of carbon fiber reinforced PLA filament	41
3.1.1 Carbon fibers pre-treatment	41
3.1.2 Compounding of composite materials.....	42
3.2 Filament characterization	43

3.3 3D printing of carbon fiber reinforced PLA.....	52
3.4 3D-printed specimens characterization	53
4. Conclusions	60
5. Experimental procedure	61
Bibliography.....	65

1.Introduction

1.1 Composite materials

A composite is a material made of two or more phases which are distinguishable thanks to the presence of a net interface so that the resulting material has different properties from its constituents.

The structure of a composite is divided into the following parts.

- matrix: the continuous phase
- reinforcement: the dispersed phase
- reinforcement/matrix interface, eventually modified by coupling agents.
- fillers, that reduce/modify the matrix content.

A broad class of composite materials is represented by reinforced plastics, among which a relevant group is represented by fiber-reinforced polymers (FRPs). FRPs include, among the other, carbon fiber reinforced polymer (CFRP) and glass reinforced plastic (GRP).

Polymer composites can be also classified based on the type of matrix, i.e. thermoplastic or thermoset.

1.2 CFRPs market

In recent decades, carbon fibers (CFs) have found widespread application in a growing number of fields, such as automotive, aerospace and defense, sea vehicles, wind turbines, storage tanks, sport and leisure ^{1, 2}. The utilization of CFs as high-performance light-weight reinforcement, mainly in high-added-value applications, has had a boost. The CF industry has been steadily growing and lately spreading toward more mass-oriented market segments, such as the mainstream automotive and motorcycle, building construction, and wind energy. In all these fields CFs are used for the production of CF reinforced polymers (CFRPs) leading to the reduction of weight, and thus CO₂ emission, but still providing high strength and stiffness.

Due to this trend, the world production of carbon fibers has already almost doubled in the 2009-2014 time span, from 27 to 53 ktons, and is expected to reach a peak of 117 ktons by 2022. The CF composite market is expected to grow at a rate of 6,6% and reach a market value of \$12 billion ³, with an obvious parallel expansion of the CFRP segment, which, according to the previsions, will top a production of about 194 ktons in 2022 ^{4, 5}, leading to a global market increment of 48.7 billion ⁶.

1.3 CFRPs' recycling challenges

The increased exploitation of CFRPs is inevitably bringing about an increase in production waste (e.g. off-cuts) and end-of-life (EoL) components (e.g., decommissioned aircraft). According to some projections, an important number of aircraft will soon reach their EoL. This means that there will be a sharp increase in CFRP waste (about 34.2 ktons in 2050), with the highest cumulative growth in Europe, North America, and Asia ⁷.

Landfill and incineration are two traditional waste treatment methods ^{8,9}, with the majority of FRP wastes currently treated through landfill in specific sites. Accordingly to a review of composite waste in the UK supply chain in 2015, almost 98% of the EoL components and manufacturing composite wastes were buried in landfills ¹⁰. On the other hand, incineration of CFRP waste allows to recover approximately 30MJ/Kg ¹¹ and the quantity of recovered energy depends on the efficiency of the incinerator and energy content of the material ⁶. Despite these two techniques are, at the moment, the most used, they can't be considered as recycling since they do not involve operations by which waste materials are reprocessed into products, materials or substances to be used for some purpose.

It should also be noted that the current European Union (EU) legislation lacks of a specific regulation for composite waste treatment. The End-of-Life Vehicle Directive (ELV 2000/53/EC) states that a minimum of 95% in weight of a new vehicle must be recycled at the EoL stage, and 85% of the waste must be re-used by the European Commission ⁸, but no specific instruction on how to treat EoL CFRP, when involved in car production, is specifically addressed.

Given the high expected growth in waste production, it's of extreme importance to find alternatives to incineration and landfilling. These techniques have a notable environmental impact and imply the loss of all the high-added-value carbon fibers ¹²⁻¹⁸. Therefore, it is clear that alternative recycling methods for CFRPs should be implemented in order to minimize any potential environmental issue and to recover at least the most precious CF. Efficiently recover CF from CFRP and use them to develop other composite materials would allow to diminish the amount of landfilled CFRP waste. Moreover, a part of virgin carbon fibers (vCF) utilized as reinforcement in CFRPs could be replaced with recycled carbon fibers (rCF), minimising in turn the production of vCFs, which is a process that involves the utilization of fossil raw material and leads to strong energy consumption.

Researchers are recently struggling to find new ways to make composites more sustainable, but they are mostly focusing on the study of new, more "green" matrices. Indeed, there is a growing

number of literature articles about the production of biobased resins ¹⁹⁻²³. This type of resins can be synthesized starting from biobased resources but, being thermosetting, they still have the problem of hard recyclability, since it cannot happen by disassembling of its component neither by remelting and remolding. This problem can be avoided utilizing green chemistry to obtain biobased thermoplastic materials ²⁴⁻²⁶, producing so composites, nanocomposites, and green nanocomposites ²⁷⁻²⁹ that, however, do not have the same performance as CFRP and do not increase the recyclability of EoL parts.

Thus, although a lot of effort has been made on matrices, there is no significant improvement in the sustainability of reinforcement. For this reason, it's fundamental to find efficient ways to recycle CFRP.

At present, several recycling methods for treating CFRPs are available, but none of them has been optimized and they are characterized by some serious drawbacks (*figure 1*).

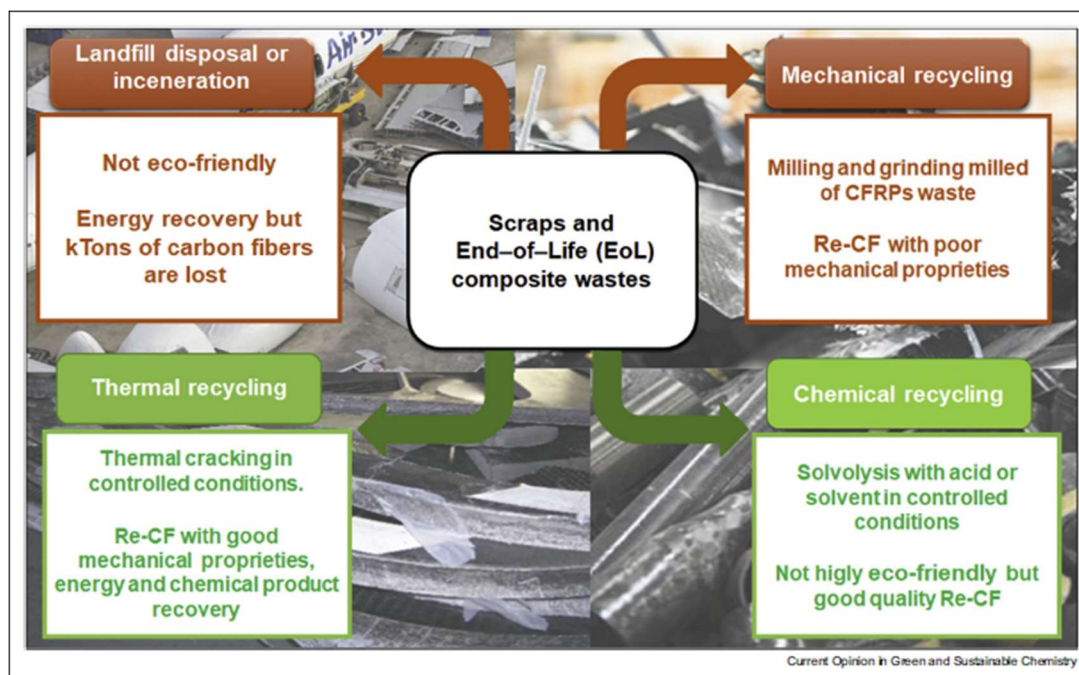


Figure 1. Landfill disposal and the principal advantages and critical issue of CFRP recycling methods to recover and reuse scraps of EoL ³⁰.

1.4 Recycling methods

CFRP recycling can be categorized into three broad methods: mechanical, thermal, and chemical, using the corresponding energy source to separate carbon fibers from the thermoset resin ³¹⁻³⁵ (*fig. 2*).

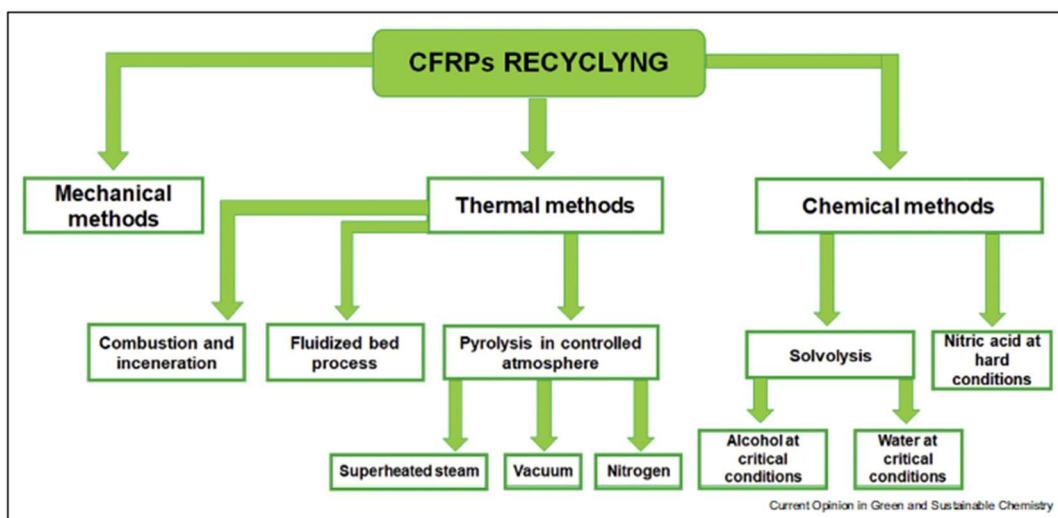


Figure 2. The principal recycling methods of CFRPs. CFRP, carbon fiber reinforced polymers ³⁰.

Currently, several companies (table 1) are performing CFRP recovery and recycling, with the pyrolysis process dominating thanks to technological development, commercial feasibility, and adaptability to different stages of composite manufacturing ^{6, 35-39}.

Table 1. Current CFRP composite recycling companies, their technologies, and capacity ³⁰.

Table 1		
Current CFRP composite recycling companies, their technologies, and capacity.		
Company	Technology	Capacity (tons/year)
Alpha Recyclage Composites (France)	Steam thermolysis process	300
Carbon Conversions Inc. (Toyota Tsusho America, US)	Pyrolysis	2000
CFK Valley Stade Recycling GmbH & Co. KG (Germany)	Pyrolysis	1000
Curti SpA (Italy)	Pyrolysis	12
ELG Carbon Fibre (UK)	Pyrolysis	2000
Hitachi Chemical	Solvolysis	12
KARBOREK RCF (Italy)	Pyrolysis	1000
Procotex (Belgium)	Mechanical (pulling, milling, and precision cutting to length)	N/A
SGL Automotive Carbon Fibres (US)	Pyrolysis	1500
Takayasu	Pyrolysis	60
Toray Industries	Pyrolysis	1000
University of Manchester (UK)	Mechanical	20
University of Nottingham (UK)	Fluidized bed	100
V-Carbon (US)	Solvolysis	1.7

CFRPs, carbon fiber reinforced polymers.

1.4.1 Mechanical recycling

Mechanical recycling is a simple technique consisting of 2 phases: first, the CFRP size is reduced to 50-100 mm with the aid of low-speed cutting tools or crushing mills; then the resulting wastes are milled or grinded to obtain small pieces of about 50 μm (powder) or 10 mm (fibrous size)³². This recycling method does not give excellent results since the obtained Re-CFs lose their integrity, leading to a significant decrement of mechanical properties and, consequently, economic value. Moreover, the energy demand of this process is high because shredding fibers is not easily attained⁴⁰. An alternative way to obtain mechanical recycling is by electromagnetic fragmentation, a technique that utilizes high voltage impulses (50-200 kV) in ionized water^{41, 42}.

Mechanically Re-CFs find application mainly as low-value fillers or particle reinforcement because the product is still rich in resin. However, the specific field of application is strongly correlated to the obtained particle size^{33, 43}. Sometimes, mechanical recycling is applied as a pretreatment to facilitate the subsequent chemical or thermal recycling process^{44, 45}.

1.4.2 Thermal recycling

Thermal recycling consists in the use of high temperatures to degrade the polymer matrix, in order to release the fibers, recovered as a residue (*fig. 3*). Thermal recycling techniques can be divided into three main types: combustion and incineration, fluidized bed process, and pyrolysis in a controlled atmosphere. In general, the process parameters of thermal treatments need to be accurately controlled (atmosphere, temperature, and residential time) to minimize loss of valuable products and undesired chemical modifications or damages to the recovered fraction (Re-CFs)^{34, 46, 47}.

Thermal recycling can be operated as an incineration or combustion treatment when the only purpose is to recover energy, but these methods lead to the complete loss of valuable material (CF) and produce polluting emissions that require the use of expensive gas cleaning devices, as well as a large quantity of ashes that need to be disposed of.

On the other hand, pyrolysis and fluidized bed processes⁴⁸ allow the recovery of clean Re-CFs. The residential time in the reactor and the reactor temperature (450-700°C) determine the result of the recycling process and vary based on the polymer resin present in the CFRP. An excessively low temperature would lead to the formation of an amorphous carbon layer (char) on the Re-CFs surface and an incomplete matrix degradation, resulting in poor mechanical properties and low fiber-matrix interaction when reimpregnated. On the other hand, an overly high temperature would lead to a partial damaging of CF surface, with a consequent reduction

in fiber diameter and thus mechanical properties.^{29, 49, 50}

The fluidized bed recycling has been introduced and developed by Pickering et al⁴⁶ in the 2000s. This technology has now reached a pilot-scale stage, being effectively utilized also for the recycling of CFRPs. The process starts with a mechanical step, where the parts are shredded to a dimension of around 6-25 mm. Subsequently, the waste is fed into a silica bed (silica sand size of around 0.85 mm), at about 450-550 °C and the system is subject to hot air flow (0.4-1.0 m/s). The high temperature and the air flow lead to the separation of CFRP waste into fibers and a volatile fraction. The air flow removes volatile compounds and forces them into a second oxidation chamber at a temperature of 1000 °C⁴⁶.

Re-CFs with a length between 5 and 10 mm are recovered through this process, with an energy consumption lower than that corresponding to the production of virgin carbon fibers⁵¹. Unfortunately, the recovered Re-CFs are characterized by degraded mechanical properties (10-75% retention of the pristine tensile strength), limiting their range of application.

Pyrolysis (*fig. 3*), another relevant thermal approach, seems to be quite appealing. This technique, consisting in the application of strong heat (450-700 °C) under an inert atmosphere, produces thermal decomposition of organic materials into simpler components. In the case of CFRPs treatment by pyrolysis, the matrix (thermoset or thermoplastic) undergoes thermal cracking, producing volatile molecules. This volatile fraction flows away from the reactor and can be thus further separated into two portions: a noncondensable one (gas) and a condensable one (pyrolysis oil). These two fractions can both be used as starting material for further chemical modifications (platform molecules)⁵² or as fuel. In the latter case, the process can be technologically modified to obtain an auto-sustained system, exploiting the high calorific value of both volatile and non-volatile compounds⁵⁰.

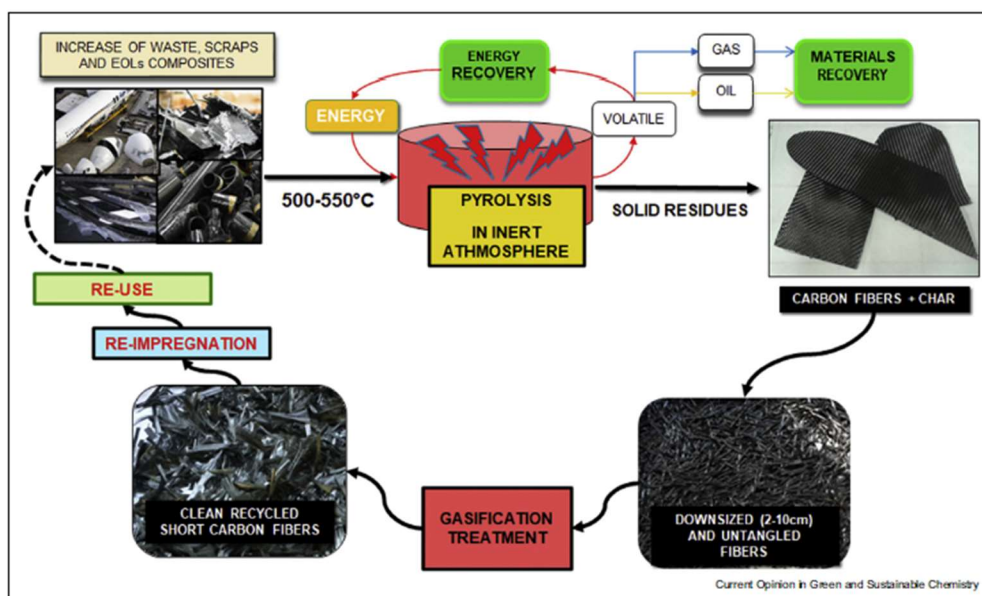


Figure 3. Thermal recovery method in two steps (pyrolysis and gasification) and reuse of CFs. CFs, carbon fibers³⁰.

The solid residue of CFs can be easily recovered at the end of the process. Some studies made by industries have demonstrated that Re-CFs obtained by pyrolysis of CFRPs have a much lower cost with respect to virgin carbon fibers. In fact, the process consumes only 5-10% of the energy required for the production of v-CFs^{34, 35}. The pyrolytic process can lead to the formation of a char layer on the surface of the fibers^{34, 53}. This layer would make inefficient the sequent reimpregnation, decreasing fiber/matrix adhesion, and is thus usually removed by an additional step in oxidative conditions^{52, 54}.

Several companies specialized in the recovering of carbon fibers from waste material have optimized their plants to assure removal of the pyrolytic carbon layer. ReFiber, a danish company that recycles aircraft CFRP waste, has implemented its semi-industrial pyrolysis plant with a secondary heating system that aims to eliminate the char. CFK Valley Stade Recycling GmbH (Germany) and Materials Innovation Technologies-Reengineered Carbon Fiber (US) use an industrial continuous pyrolysis process that exploits a large furnace and continuous flow to obtain longer and cleaner Re-CFs³⁴. ELG Carbon Fibre (UK) utilizes a different approach that completely avoids the char formation on Re-CFs surface through the utilization of a semi-open continuous belt furnace with a controlled atmosphere^{34, 55}. Curti SpA (Italy) recently modified its bed batch pilot reactor^{56, 57} into a continuous process that is able to operate at 500-550 °C both pyrolysis and oxidation steps, combining the different disposal techniques into a more efficient one (fig. 3). This plant allows to carry out the pyrolysis without priorly shredding the wastes, saving a lot of energy, and recovering Re-CFs with 95% of their original strength

and a longer dimension ^{58, 59}.

Recently, another thermal recycling method, exploiting superheated steam (at 550 °C), has been utilized to obtain high-quality Re-CFs ⁶⁰. Char removal can be effectively obtained also utilizing different reaction conditions, such as CO₂ or water vapor ⁶¹.

1.4.3 Chemical recycling

Chemical recycling process, usually called solvolysis, consists in the degradation of the polymer matrix caused by a solution of acids, bases, and solvents. The type of medium has to be chosen based on the matrix chemical composition ^{34, 62} (*fig. 2*). Before operating the dissolution itself, CFRPs undergo a shredding step to increase the surface area in contact with the solution and promote the reaction. After the process, a washing step allows to obtain Re-CFs without decomposed polymer or solvent residues ^{62, 63}. Chemical recycling is usually more gentle compared to other recycling methods and for this reason, the recovered Re-CFs can be long and show tensile strength almost equal to that of virgin CFs ^{64, 65}. The main drawback of this technique is the utilization of hazardous chemicals, that has a significant environmental impact ³⁴. Epoxy resins can be easily dissolved using HNO₃, with better results in Re-CFs quality with respect to H₂SO₄ and HCl dissolution ^{66, 67}. Another efficient method that permits to reach a matrix's decomposition extent of about 95% is based on the use of ultrasonic solvolysis in diluted HNO₃ and H₂O₂ at temperatures below 60°C ⁶⁸. Other solutions such as acetone + H₂O₂ ⁶⁸, DMF + H₂O₂ ⁶⁹, and an aqueous mixture of peracetic acid lead to the dissolution of the matrix with good results (from 90 to 97% of matrix removed) ⁶⁹⁻⁷¹. Novel solvolysis methods contemplate the use of fluids like water or alcohols in supercritical or subcritical conditions (temperature and pressure exceeding values corresponding to the critical point) ⁷²⁻⁷⁴. The environmental impact of this process would be smaller than that of other classic dissolution methods but it has not been commercialized yet and the energy required to generate critical conditions is high.

1.4.4 Future challenges of recycling CFRPs

In order to seek objectives such as environmental sustainability and circular economy and to replace the obsolete landfill and incineration approaches, several CFRP recycling technologies have been implemented (mechanical, thermal, and chemical recycling). The next necessary step is the technological development of the processes to increase the economical feasibility and plant-scale. From this point of view, the pyrolysis process seems to be the most promising, having an actual capacity of 7 kt/y. In addition, as already analyzed, pyrolysis allows to obtain recycled CFs, together with liquid and gaseous fractions that can be used as starting

material or as fuel to sustain the process itself.

The step after CFRP recycling, and also the key to build a solid and sustainable CFRP recycling market, is represented by the utilization of Re-CFs. Currently, according to several researchers, it is possible to efficiently replace virgin CFs with Re-CFs in some applications (Non-wovens, Sheet Molding Compound – SMC, and Bulk Molding Compound – BMC – technologies) ^{5, 51, 54}. To efficiently close the life cycle loop of CFRPs there are the following objectives to be achieved: development of low-environmental-impact recycling technologies capable of producing large quantities of high quality Re-CFs; use Re-CFs as reinforcement to build recycled CFRPs that still have good mechanical properties; find new applications for the Re-CFs.

1.5 Composites re-manufacturing

The second phase of CF reclamation processes (*fig. 4*) consists in utilizing a new matrix to re-impregnate the recovered fibers.

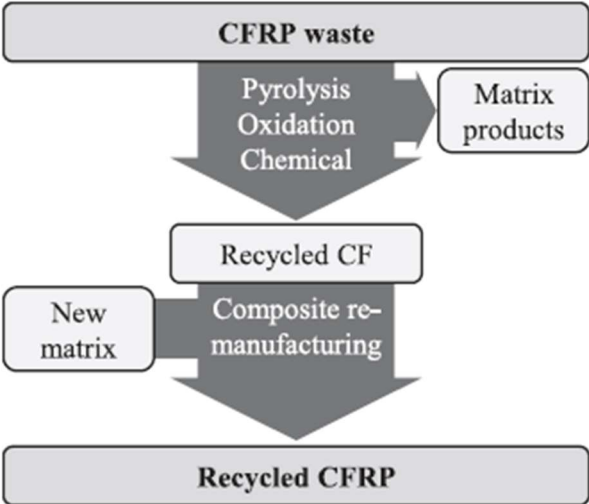


Figure 4. Fiber reclamation ³⁴

1.5.1 Types and characteristics of waste carbon fibers

Recovered carbon fibers can be obtained mainly from two sources: the manufacturing process operated in the composite industry and EoL CFRPs. The manufacturing process can lead to the generation of two types of waste, known as dry waste and wet waste. The dry waste originates from production offcuts, selvages, and bobbin ends and, being not treated yet, has properties identical to those of virgin CFs. Therefore, CFs coming from this type of waste does not require any type of recycling treatment. Instead, the wet waste consists of expired prepreg rolls (virgin CF fabrics pre-impregnated with resin precursor). This type of waste has to be recycled to

eliminate the resin. The other significant source of carbon fiber waste, corresponding to EoL CFRPs such as dismissed aircrafts and wind turbine blades, also contains resin and needs to be recycled before being remanufactured ^{32,34}.

The characteristics of recovered carbon fibers are strictly correlated to the recycling technique used to reclaim the fibers. One of the most important aspects of the Re-CFs is the length and based on this parameter CFs can be classified into three broad groups, i.e short (<6 mm), medium (6-25 mm), and long (25-300 mm) fibers.

The dry waste carbon fibers, not requiring a recycling treatment before remanufacturing, can be cut into any desired length. Contrarily, the lengths of wet waste and EoL parts intimately depend on the utilized recycling technique. Overall, pyrolysis and solvolysis yield random fiber length, while mechanical recycling produces short CFs, ranging from powder to short fiber fragments ⁷⁵. The length of the obtained Re-CFs is crucial because it determines the mechanical properties of the re-manufactured CFRP, but also because several technologies used for the processing of waste carbon fibers are dependent on fiber length (e.g. spun yarn technology) ⁷⁶. Another fundamental characteristic of recycled carbon fibers is the tensile strength and it is determined once again by the fiber source and the recycling treatment. Fibers obtained from dry waste does not suffer from any decrease in mechanical properties while fibers reclaimed from wet waste or EoL CFRPs through chemical or thermal recycling are subjected to a decrease in strength, in different measures depending on the recycling conditions ⁷⁷. *Table 2* shows the effect of recycling processes on the strength of the fibers.

Table 2. Influence of recycling technique on fibre strength ³⁶. Type-II: wet waste; Type-III: EoL

References	Technique	Fibre type	Strength (%)
Pimenta ³⁰	Pyrolysis	Type-II	96
Nahil ³¹	Pyrolysis	Type-II	90
Greco et al. ³²	Pyrolysis	Type-III	86–88
Stoeffler et al. ³³	Pyrolysis	Type-III	90
Holmes ³⁴	Pyrolysis	Type-II	90
Pinero-Hernanz et al. ³⁵	Solvolysis	Type-II	90–98
Jiang et al. ³⁶	Solvolysis	Type-II	97
Bai et al. ³⁷	Solvolysis	Type-III	95–96
Maa et al. ³⁸	Solvolysis	Type-II	96
Okajima and Sako ³⁹	Solvolysis	Type-III	97

The amount of residual resin present on the fiber surface after the recycling treatment also plays an important role. In the case of thermal recycling, the purity of the recovered fibers is generally

lower than that obtained with chemical recycling and it depends on the process conditions (temperature, atmosphere...) ³². Another characteristic of recycled carbon fibers that has to be considered is the presence of the sizing. Usually, before the impregnation and consolidation step, virgin carbon fibers are treated with different chemicals to protect their surface and to enhance interfacial adhesion between matrix and fibers. This sizing layer is present on the surface of dry waste, while is usually removed by the recycling process (pyrolysis or solvolysis) of wet waste and EoL CFRPs ⁷⁸. As a result, recycled carbon fibers recovered from wet waste or EoL CFRPs have scarce interfacial bonding properties, due to the loss of the sizing layer caused by the reclamation process. Thus, they are usually subjected to pretreatment to change the chemical composition of the fiber interface and assure better fiber-matrix adhesion.

Recycled carbon fibers pre-treatment

Several studies have been conducted to find the best system to efficiently increase the interfacial bonding between Re-CFs and different types of matrix.

Altay et al. investigated the effect of MAPP (maleic anhydride-grafted polypropylene) content on morphology, thermal, and mechanical properties of recycled carbon fibers reinforced PP composite. Tensile strength and modulus have been observed to increase with the addition of 2, 4, and 8 wt. % of MAPP. Furthermore, morphology studies have shown an improvement of PP-CF interface after the introduction of the compatibilizer ⁷⁹. The same research group has also conducted a study on the use of atmospheric plasma at different plasma powers (100, 200, and 300 W) to increase the mechanical properties of Re-CF reinforced PP composites. Recycled carbon fibers were subjected to plasma treatment before the compounding step and the results showed an increment of surface roughness and oxygen-containing groups. Enhancement in mechanical properties was observed at plasma power of 100 W while higher powers caused a decrement in flexural and tensile strength values due to the etching of recycled carbon fibers ⁸⁰. The plasma technique was proved to be efficient also by Lee et al. ^{81, 82}. Chen et al. developed an effective approach to clean and treat Re-CFs surface with a concentrated solution of nitric acid, followed by a solution of diglycidyl ether of bisphenol A as a macromolecular coupling agent, in order to improve the fiber-matrix adhesion in the prepared Re-CF/PBT composite. Results showed a significant improvement in mechanical properties, heat distortion temperature, and thermal stability of PBT thanks to the incorporation of surface-treated Re-CFs. SEM observations showed a fine dispersion of fibers in the PBT matrix and good interaction between matrix and fibers ⁸³. The same strategy (treatment with nitric acid followed by treatment with DGEBA) was adopted by Feng et al. to increase the fiber/matrix adhesion

and the results were positive as in the previous case ⁸⁴. Greco et al. compared two different treatments to enhance the adhesion of Re-CFs to an epoxy matrix. First, thermal oxidizing treatment at different operative temperatures (450 and 600 °C) was used. From the results, it can be seen that at 600°C fibers suffered from severe damaging, while at a lower temperature (450°C) fiber integrity has not been affected but also the adhesion properties have remained unchanged. On the other hand, chemical treatment with nitric acid caused very limited damage to the fibers, coupled with a significant modification of surface chemistry (oxygen enrichment), which in turn involved a further increase of fiber/matrix adhesion ⁸⁵. Han et al. exploited a silanization treatment to efficiently increase the adhesion of Re-CFs to two different matrixes (PLLA and PBS) ^{86, 87}, while Nie et al. and Qian et al. used the same method to prepare an optimized Re-CF/POM composite ^{88, 89}. A different approach was adopted by Huan et al., who used a mild oxidative polymerization of dopamine to obtain surface-modified recycled short CF (pDop-ReCF). The high quantity of chemical groups (amine groups and phenolic hydroxyl groups) introduced with the pDop modification led to a strengthened interfacial adhesion between fibers and epoxy matrix ⁹⁰. Li et al. studied the effect of epoxy resins of different molecular weight as in-situ coupling agents and found an optimal strengthening effect caused by the synergic effect of improved interfacial adhesion and in-situ extended chain reaction of PBT matrix with the epoxy coupling agent ⁹¹. Another innovative solution to revalorize recycled carbon fibers, through CVD synthesis of carbon nanotubes on the surface of the fibers, was introduced by Montes et al. ⁹². Szpieg et al. and Wong et al. added a maleic anhydride grafted polypropylene as a coupling agent to improve fiber/matrix adhesion ^{93, 94}.

1.5.2 Introduction to processing technologies for recycled carbon fibers

Recycled carbon fibers, as explained in the previous paragraph, are usually fragmented into shorter lengths during the entire recycling process. Different mechanisms lead to the size reduction of the fibers: a) size reduction of CFRP waste before reclamation, b) fiber breakage caused by the reclamation process, c) chopping of the fibers after reclamation. Furthermore, all fiber-reclamation processes cause the sizing removal from the fibers surface, so the resulting Re-CFs are in a filament-like, random, fluffy form (*fig. 5*).



Figure 5. RCFs in a typical unsized, random, low-density-packing (“fluffy”) form ⁹⁵.

As a result, the manufacturing processes for the processing of Re-CFs must be adapted to their peculiar characteristics ^{95, 96}.

The principal re-manufacturing technologies for waste carbon fibers, when used in thermoplastic matrices, are injection molding, nonwoven, tape development, and hybrid yarn technologies (fig. 6).

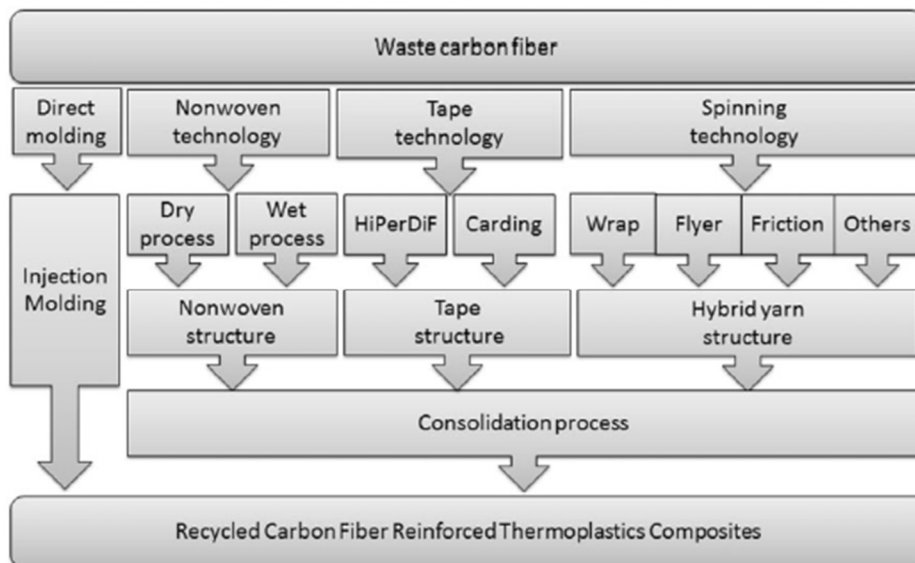


Figure 6. Processing technologies for waste carbon fiber ³⁶.

1.5.3 Injection molding

The injection molding technology is extensively used to produce CFRPs and it is an efficient method also for the production of Re-CFRPs. This technique consists of mixing carbon fibers (chopped, milled, or fragmented) obtained from any type of waste (dry, wet, or EoL) with a thermoplastic polymer and then inject the obtained viscous fluid into a mold to produce the final composite. ³³. A certain pressure is usually applied to force the polymer flowing between

the fibers.

Injection molding is a versatile technique that allows using a broad range of thermoplastic polymers, in addition to classically used thermosets, to produce recycled CFRPs. One of the main drawbacks of injection molding is represented by the length of fiber that can be treated. The technique can process only short carbon fibers, leading to random fiber orientation in the final composite and a consistent quantity of voids. Consequently, the mechanical properties of recycled CFRPs obtained through injection molding are quite limited, ranging from 20 to 200 MPa³⁶.

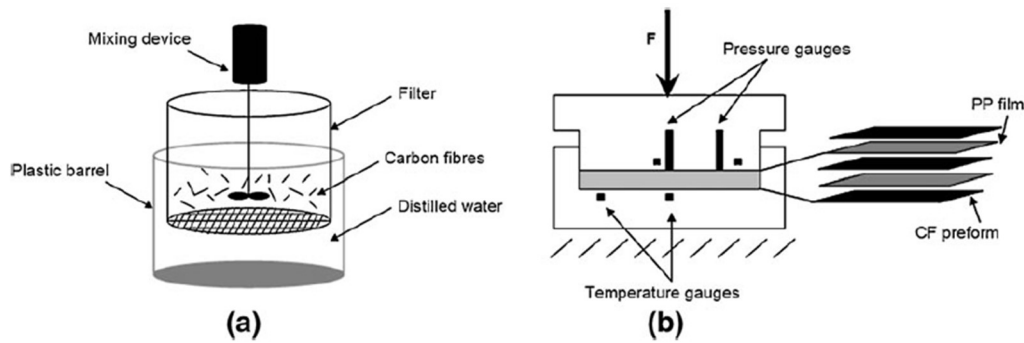
1.5.4 Nonwoven technologies

Nonwovens are a type of fabric in which the fibers are commonly bonded by thermal, mechanical, or chemical treatments. In the case of CF, they are entangled and kept together with the help of sizing coatings. Since, anyway, they do not require yarn, short fibers can be used. The main methods to build nonwovens are represented by wet and dry nonwoven technologies. The obtained recycled carbon fiber nonwovens can be subsequently impregnated with a polymeric matrix to produce Re-CFRPs⁹⁷.

Wet technology

The most exploited wet process able to process recycled carbon fibers is the papermaking technology. This technique consists in dispersing short carbon fibers in a solvent with the help of a stirrer or propeller. In the second step, the fibers are filtered, dried, and solidified to obtain an isotropic web structure. The so obtain structure can be then combined with a thermoplastic polymer to produce the desired composite. Alternatively, it can be impregnated with thermoset precursor to produce and SMC prepreg. The wet-laying method is more gentle towards the fibers in comparison to a dry method like carding, and this is an important aspect in the case of more brittle fibers such as carbon, which tend to break during the carding operation⁹⁸. In addition, the utilization of a solution, as required in the wet method, eliminates several environmental problems correlated to the manufacturing process, since Re-CFs reclaimed by pyrolysis can contain very fine carbon particles that could contaminate the air and the equipment^{99, 100}. The main disadvantages of the papermaking method consist in the relatively low thickness of the obtained recycled carbon fiber mats and the high pressure required to adjust the composite thickness and increase the fiber volume fraction^{101, 102}. A considerable number of researchers have conducted their studies on CFRPs obtained by a paper making method. Giannadakis et al. employed papermaking principles to obtain preforms with uniformly

distributed carbon fibers and then, after having stacked the nonwovens with polypropylene films, used press-forming technique for the manufacture of the final composite (*fig. 7*)⁹⁹.



*Figure 7. Dispersion of carbon fibers for preform manufacture and press forming of thermoplastic composite plate*⁹⁹.

Goergen et al. introduced resin transfer pressing (RTP). In this innovative composite manufacturing process, a recycled carbon fiber nonwoven fabric is oversaturated with a thermoset resin and then used as a resin carrier in a press process, where it is placed in a heated mold together with a dry textile-based preform. The applied pressure makes the resin flowing from the nonwoven into the non-impregnated preform¹⁰³. Huan et al. prepared polydopamine surface-modified recycled short CFs and exploited the enhanced hydrophilicity of modified Re-CFs to obtain, through paper making method, a nonwoven characterized by high structural uniformity. The fabric was then utilized to prepare an epoxy composite⁹⁰. Szpieg et al. developed a fully recycled carbon fiber reinforced MAPP-modified polypropylene composite material building a nonwoven (papermaking technique) and then press-forming these mats combined with recycled PP films. A series of tensile tests using rectangular specimens cut in four different dimensions (0, 90, 45) in the composite plate were performed to analyze the in-plane material isotropy⁹³. Tse et al. mixed short recycled carbon fibers with flax and poly-lactic acid (PLA) fibers, acting as the matrix, to form nonwoven mats through wet-laying and then used compression molding to produce composites with different ratios of Re-CFs and flax fibers in the PLA matrix. Results showed that the replacement of 25% of the carbon fibers content with flax fibers helped to increase the compactability of the nonwoven, resulting in lowering the void content without increasing the pressure in the compression molding step¹⁰⁴. Van De Werken et al. upgraded the classic wet-laying process coupling it with a centrifugal alignment rig that allows to obtain unidirectional aligned recycled carbon fiber mats. The degree of alignment was found to have, as expected, a large influence on the strength and elastic modulus of the final composites, obtained impregnating the mats with an epoxy resin¹⁰⁵. Wei et al. analyzed the properties of a composite made by compression molding a nonwoven of Re-CFs

and PA6 fibers and subsequently, in another paper, discussed the effect of residual contamination of glass fibers on the application of discontinuous recycled carbon fibers ^{106, 107}. A novel application of Re-CFs was introduced by Wong et al. through the development of an electromagnetic interference shielding composite material. A paper making technique has been utilized to produce a nonwoven mat and then a resin transfer molding (RTM) process has been exploited to impregnate the mat with polyester resin and obtain the final composite ¹⁰⁸. Overall, data collected from the analyzed papers show that composites based on wet nonwoven technologies have mechanical properties that are identical to those of injection-molded composites, ranging from 15 to 150 MPa. In addition, it's common to obtain poor fiber orientation, short fiber lengths, and low fiber volume fraction.

Dry technology

Carding is a technique that allows to easily obtain highly oriented nonwoven structures and it can be used to process recycled CFRPs, combining hybrid materials based on waste carbon fibers and thermoplastic fibers. The process exploits a carding machine that transforms the blended fibers into a fibrous sheet called web. The second step consists in using cross lappers to combine multiple sheets of web and prepare an anisotropic nonwoven structure (*fig. 8*). A card machine is composed of several metallic wire cylinders that permit, through carding action, to align the fibers in the machine direction. It can also be used to mix hybrid fibers at fiber-to-fiber level producing intralayer hybrid composites, which are characterized by different fiber types in one layer, resulting in a higher dispersion of fibers. The particular hybrid anisotropic structure leads to an enhancement of fiber-matrix adhesion in composites ⁹⁷.

All the listed advantages made this technique appealing for the processing of recovered carbon fibers and therefore, numerous studies are present.

Bachmann et al. used the carding process to combine natural flax fibers and Re-CFs and obtain a hybrid composite through impregnation of the prepared nonwoven with epoxy resin. The effect on flexural mechanical properties was then evaluated ¹⁰⁹. Wei et al. provided a comparison between papermaking and carding processes analyzing the mechanical properties of PA6 composite specimens reinforced by card and paper made recycled carbon fiber structures ¹¹⁰. Yin et al. treated recycled carbon fibers and PA-66 fibers with a carding machine and used a compression molding process to transform the web in the final thermoplastic composite. The results confirmed the anisotropy of the material due to the higher orientation of the fibers in the machine direction ¹¹¹. Lützkendorf exploited the carding technique to produce a hybrid composite made of recycled carbon fibers, natural fibers, and thermoplastic fibers. The study

confirmed the possibility to use thermoplastic composites for the manufacturing of automotive interiors, obtaining light-weight pieces with still high mechanical properties ¹¹². Cornacchia et al. recovered carbon fibers from EoL sources through a thermal treatment and then utilized a carding mechanism to integrate the recovered fibers into hybrid fibrous mats. The so obtained web structures were then compression molded to obtain a recycled carbon fiber reinforced PP composite ¹¹³. Xiao et al. developed an innovative carding and stretching system to improve the fiber alignment of Re-CFs during the generation of the nonwoven. The key to the success of the stretching step resides in the structure of the matrix fibers, that are formed by a PA-66 core and a PA6/PE shell. The different T_g of the core and the shell allows to stretch the system in a step that follows the nonwoven formation ¹¹⁴.

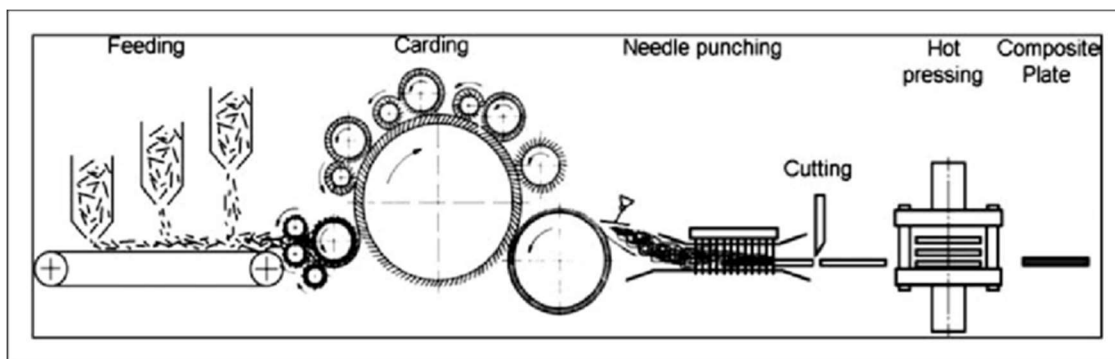


Figure 8. Composite manufacturing through carding process ¹¹⁵.

On the contrary of the papermaking method, the dry nonwoven technology leads to the production of Re-CFRPs with better mechanical properties than injection molding and wet-laid nonwoven based composites, with these properties strictly correlated to matrix type, fiber volume fraction, and fiber orientation.

1.5.5 Tape technology

The tape development technology is a technique that focuses on providing pre-consolidated prepregs, that allows producing recycled CFRPs in short times. A tape or tow structure can be obtained by means of different methods, leading to highly oriented structures that show better mechanical properties than composites prepared from nonwovens.

High-performance discontinuous fiber method (HiPerDiF)

This new process for the production of tapes, starting from short carbon fibers, was developed at the University of Bristol. The HiPerDiF method works with a low concentration suspension of carbon fibers in water, introducing a new concept to orient fibers under wet conditions. The suspension is accelerated by a peristaltic pump through nozzles directed towards the orientation

head placed above a perforated conveyor belt with a suction system underneath. The orientation head is made of a series of parallel plates spaced by a controllable gap. When the fibers hit the plates, their orientation changes transversely to the water jet direction, provided that the gap between the parallel plates is a maximum of 1/3 of the fiber length. As they fall on the conveyor belt, the fibers realign themselves to the movement direction of the belt to produce the preform. The water is removed by vacuum suction (*fig. 9*). Finally, aligned fiber tows or tape are impregnated with resin to produce the desired composite ¹¹⁶.

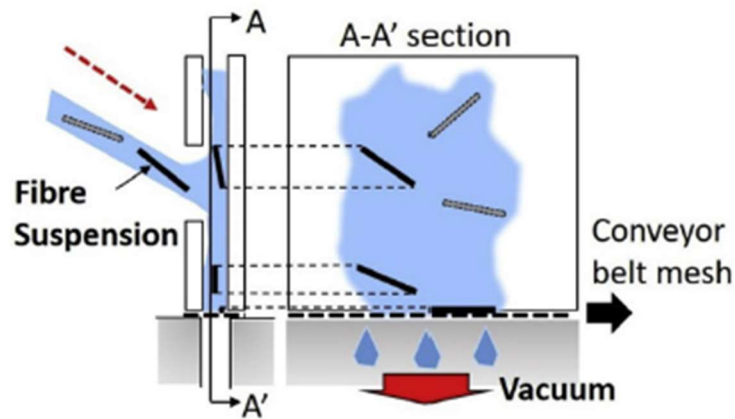


Figure 9. The HiPerDiF working principle ¹¹⁶.

A recycling process for discontinuous carbon fiber polypropylene composites was developed by Tapper et al. After the recycling step, the HiPerDiF method has been used to process the recovered materials and obtain a thermoplastic composite ¹¹⁷.

Carding technology

A modified carding machine can be directly used to produce a tape structure. The modification usually consists in installing a consolidation unit in the carding system. After obtaining the pre-consolidated tape, further steps can lead to the production of woven structures, used as reinforcements in the final composite.

Akonda et al. utilized a modified carding process to obtain a novel thermoplastic pre-consolidated, unidirectional tape, starting from long (60 mm) waste carbon fibers and polyester fibers. The tape has then been processed to form a woven architecture and the dry prepreg has been compression-molded to form a thermoplastic composite showing good mechanical properties ¹¹⁸. Khurshid et al. introduced a new technique based on carding and drawing processes able to produce unidirectional tape structures. The whole process consists in several steps: production of card slivers from recycled carbon and PA fibers through a carding machine, drawing process to obtain a homogeneous sliver, formation of multiple slivers and thermo-

fixation to develop a unidirectional tape structure, and finally laying-up of tape structures to produce the thermoplastic composite ¹¹⁹. A modified carding process was exploited also by Hehl, who integrated a consolidation unit between drafting rollers. After having obtained woven structures, the thermoplastic composites were formed through compression molding ¹²⁰.

1.5.6 Hybrid yarn technologies

In the last decade, a lot of effort has been put into the development of technologies able to produce hybrid yarn from recovered carbon fibers and thermoplastic fibers, in order to exploit the whole potential of waste carbon fibers. Conventional or advanced spinning machinery can be used to process these hybrid yarns, obtaining a fibrous structure with better properties such as higher compactness, fiber orientation, and fiber volume fraction. The process begins with the transformation of blended fibers (reinforcement and matrix fibers) in hybrid slivers through the use of carding and drawing techniques. The so obtained slivers undergo different spinning technologies (wrap, flyer, and friction) to spin hybrid yarns. The final step consists in wounding the hybrid yarns onto a winding frame. At this point, hybrid yarns can be subjected to compression molding to produce anisotropic thermoplastic composites ¹²¹⁻¹²³.

Wrap spinning

Hybrid yarns produced by wrap spinning present high fiber orientation and uniformity. The wrap spinning process can be divided into three steps: drafting, wrapping, and winding. A series of rollers initially draft the hybrid yarn sliver to obtain a yarn structure with the desired number of fibers. Subsequently, a filament called binder wraps the fibers through a hollow spindle ¹²¹ (*fig. 10*).

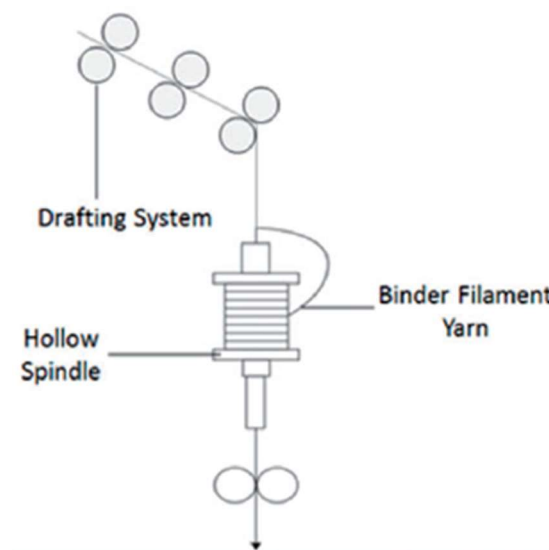


Figure 10. Wrap spinning process ³⁶.

Wrap spinning technique leads to the formation of a yarn structure without a twisting mechanism and thus all the fibers are longitudinally aligned through the yarn body. Furthermore, the produced yarn is particularly uniform compared to other spinning techniques. Akonda et al. used a modified carding and wrap spinning process, followed by a compression molding step, to process recycled carbon fibers and matrix polypropylene staple fibers into the desired recycled CFRP. The analysis of the produced hybrid yarn showed that more than 90% of the Re-CFs are aligned through the yarn axis, providing good mechanical properties to the final composite ⁹⁸. A hybrid yarn made of recycled carbon fibers and PA-6 staple fibers was developed by Goergen et al. The yarn was then utilized to produce fiber-reinforced thermoplastic sheets (also called organic sheets) through thermoforming ¹²⁴.

Flyer spinning

The flyer spinning technique leads to the production of rovings, which are twisted and uniform fibrous structures. The flyer machine is composed of a drafting, twisting, and winding unit. First of all, the drawn slivers are drafted by 3/3 or 4/4 rollers to achieve the desired number of fibers in the cross section. Then, a flyer twists the drafted fibrous structure and finally, the yarn is wound onto a bobbin ⁷⁶ (*fig. 11*)

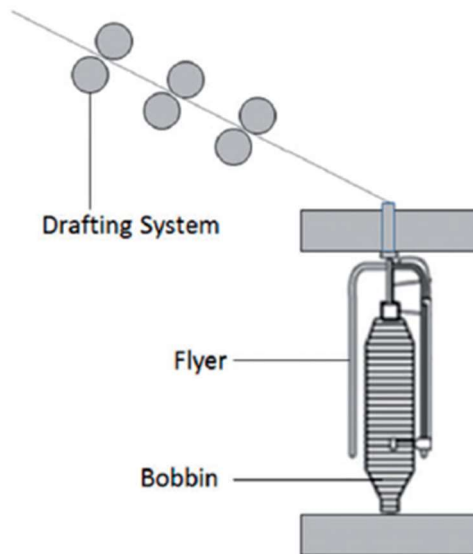


Figure 11. Flyer spinning process ³⁶.

Hengstermann et al. reported the successful manufacturing of hybrid yarns consisting of carbon fiber and PA-6 fibers through carding and drawing techniques, followed by a flyer spinning step. The results have shown that fiber length, mixing ratio of reinforcement and matrix fibers, and orientation of fibers in the card web play a predominant role in the carding process ¹²³. Subsequently, Hengstermann et al. also studied the influence of yarn parameters, founding that

CF length, yarn twist, and CF content determine the tensile properties of the produced thermoplastic composites ¹²⁵. Furthermore, the sizing effect of Re-CFs utilized for hybrid yarn production was assessed. Recycled carbon fibers with thermoplastic and thermoset matrix compatible sizing were used, along with Re-CFs without sizing, to manufacture the final composite. As expected, the sizing developed for thermoplastic matrixes was found to enable the highest tensile and flexural strength in thermoplastic composites ¹²⁶. Miyake et al. introduced a novel method for the manufacture of hybrid yarns, combining drafting and combing processes. In order to obtain high production rates and application for long fibers, the suspending and carrying media, constituted by a fluid, was substituted by fluffy synthetic fibers. After having obtained the yarn, unidirectional thermoplastic composites were fabricated by placing the yarn in one direction and hot-pressing at 200°C. Analysis of the composites revealed that approximately 70% of the fibers were aligned within an angle of $\pm 14^\circ$ in the drafting direction ¹²⁷. A new approach to produce Re-CFs reinforced epoxy composites was introduced by Hasan et al. In the first step recycled carbon fibers and water-soluble PVA fibers were used to obtain a hybrid yarn through a flyer machine. Then, thanks to a water treatment, the PVA fibers contained in the yarn were dissolved and the resulting structure was impregnated with an epoxy resin to produce the composite ¹²⁸.

These studies show that composites made from flyer spun yarns can reach tensile properties up to 1000 MPa.

Friction spinning

Friction spinning is an open-end-spinning technique and it is efficiently used for the production of hybrid yarns characterized by high fiber orientation. An advantage of the friction spinning process consists in the possibility to create core-sheath yarns, through the insertion of a filament into the core of the yarn during the twisting step. This technique allows to stabilize the spinning process and to increase yarn strength. The produced yarn is therefore composed of a core structure (staple fiber and endless filament) that is confined and covered by staple fibers forming the sheath structure. The working principle of the friction spinning process is based on two perforated spinning drums that move in opposite directions to contact the yarn surface. A suction air system is also present to promote the adhesion of the fibers on the spinning drums. The process is characterized by high productivity (up to 250 meters per minute) and can produce very compact yarn structures thanks to a regulation system of the suction air pressure ^{121, 129} (*fig. 12*).

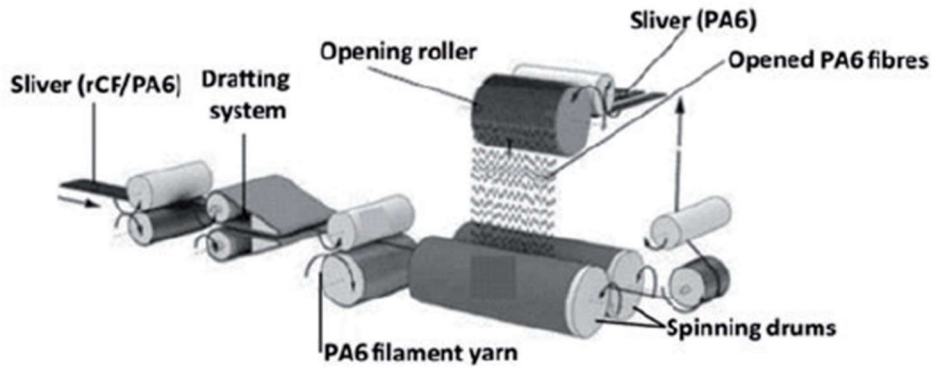


Figure 12. Friction spinning process ³⁶.

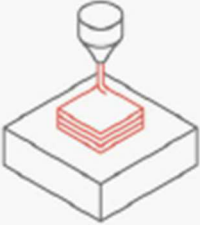

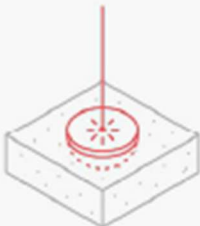
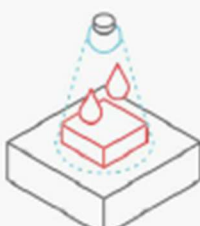
Hasan et al. developed an innovative core-sheath hybrid yarn structure from staple carbon fiber and PA-6 fibers of 60 mm lengths exploiting the friction spinning method. The produced hybrid yarns were then used to obtain CFRPs and the influence of the processing parameters (core to sheath ratio and suction air pressure) on tensile properties of the composite was evaluated ^{122, 130}. A study of the different spinning techniques made by Abdkder et al. at the Institute of Textile Machinery (ITM) concluded that wrap, flyer, and friction spinning technologies are optimal for the processing of hybrid yarns ¹³¹.


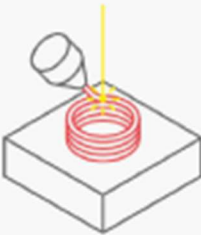

1.6 Additive manufacturing

Another promising field in the production of CFRPs that could lead to the development of new efficient methods to integrate recycled carbon fibers in the manufacturing chain is represented by 3D printing. Additive manufacturing, also known as 3D printing, is the process that allows producing a part additively building it up one layer at a time. A part can be printed from different materials, resulting in several 3D printing technologies, each having their own advantages and drawbacks. The main benefit of 3D printing processes consists in the possibility of producing almost any geometry, even though each additive manufacturing technology has some limitations. In addition, 3D printing does not need other expensive tools besides a 3D printing machine, leading to the rapid development of prototypes and low-volume production parts. On the other hand, 3D printing can produce parts only with materials characterized by limited properties compared to materials manufactured through subtractive (CNC, turning, drilling) or formative (injection molding, casting, stamping, and forging) techniques. Furthermore, 3D printed parts are usually anisotropic or not fully dense and have slight variations due to differential cooling or warping during curing or deposition, decreasing the repeatability of the process ¹³².

Additive manufacturing processes can be categorized into seven groups: material extrusion, vat polymerization, powder bed fusion, material jetting, binder jetting, direct energy deposition, and sheet lamination (table 3). A further distinction can be made also based on the type of material used in the 3D printing process (fig. 13).

Table 3. Classification of 3D printing technologies ¹³².

Process	Description	Technologies
<p data-bbox="264 622 491 645">Material Extrusion</p> 	<p data-bbox="635 622 954 763">Additive manufacturing process in which material is selectively dispensed through a nozzle or orifice.</p>	<p data-bbox="1002 622 1321 763">Fused Filament Fabrication (FFF), more commonly referred to as Fused Deposition Modeling (FDM)</p>
<p data-bbox="264 947 491 969">Vat Polymerization</p> 	<p data-bbox="635 947 954 1111">Additive manufacturing process in which a liquid photopolymer in a vat is selectively cured by light-activated polymerization.</p>	<p data-bbox="1002 947 1305 1021">Stereolithography (SLA), Direct Light Processing (DLP)</p>
<p data-bbox="264 1261 491 1283">Powder Bed Fusion</p> 	<p data-bbox="635 1261 954 1373">Additive manufacturing process in which thermal energy selectively fuses regions of a powder bed.</p>	<p data-bbox="1002 1261 1321 1424">Selective Laser Sintering (SLS), Direct Metal Laser Sintering (DMLS), Selective Laser Melting (SLM), Electron Beam Melting (EBM)</p>
<p data-bbox="264 1574 491 1597">Material Jetting</p> 	<p data-bbox="635 1574 954 1715">Additive manufacturing process in which droplets of material are selectively deposited and cured on a build plate.</p>	<p data-bbox="1002 1574 1273 1626">Material Jetting (MJ), Drop On Demand (DOD)</p>

Process	Description	Technologies
<p>Binder Jetting</p> 	<p>Additive manufacturing process in which a liquid bonding agent selectively binds regions of a powder bed.</p>	<p>Binder Jetting (BJ)</p>
<p>Direct Energy Deposition</p> 	<p>Additive manufacturing process in which focused thermal energy is used to fuse materials by melting as they are being deposited.</p>	<p>Laser Engineering Net Shaping (LENS), Laser-Based Metal Deposition (LBMD)</p>
<p>Sheet Lamination</p> 	<p>Additive manufacturing process in which sheets of material are bonded to form a part.</p>	<p>Ultrasonic Additive Manufacturing (UAM), Laminated Object Manufacturing (LOM)</p>

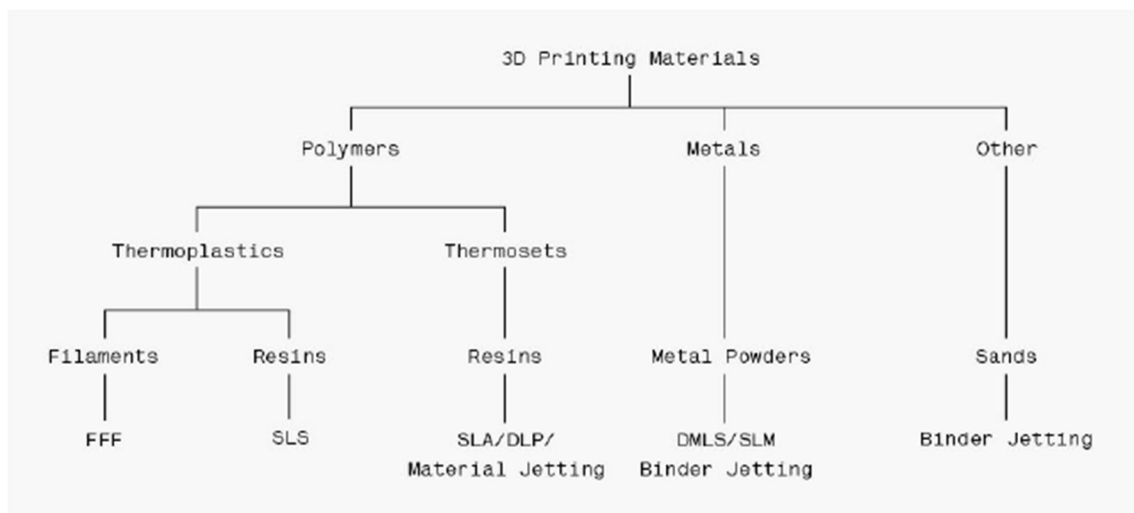


Figure 13. 3D printing material classification ¹³².

1.6.1 Material extrusion – FFF

Fused filament fabrication (FFF), also called fused deposition modeling (FDM), is a technique that prints using a string of solid thermoplastic material (filament). The filament is loaded into the printer and fed through to the extrusion head. The printer nozzle reaches the desired temperature and a motor drives the filament through the heated nozzle melting it. The printer then moves the extrusion head following a predetermined path, laying down melted material at a precise location, where it cools down and solidifies. After having completed a layer, the build platform moves down and the process is repeated building up the part layer-by-layer (*fig. 14*). The produced part can be subjected to some post-processing procedures, which are different based on the utilized printer technology.

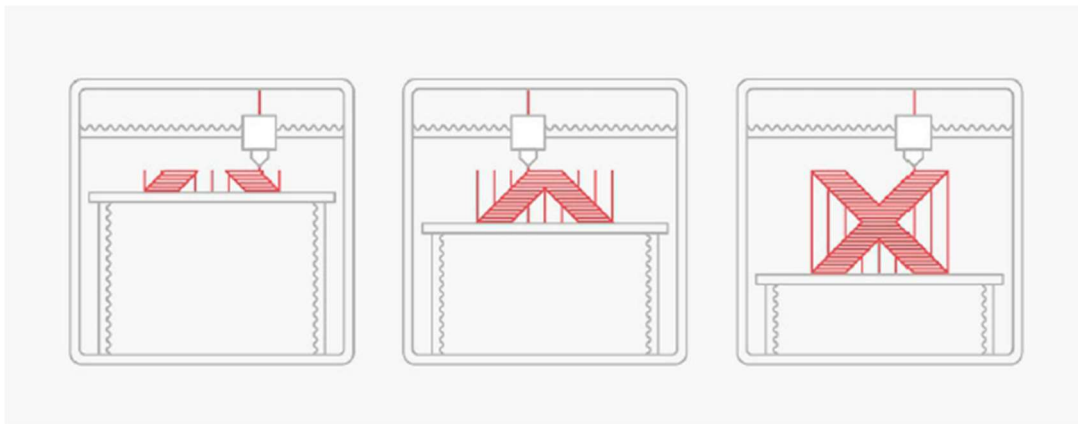


Figure 14. FFF printing process ¹³².

Before the 3D printing process itself, a digital model has to be produced, usually through Computer-Aided Design (CAD) (*fig. 15*). Then the CAD model has to be converted into a format that a 3D printer can interpret. Thus, the CAD model is converted into a STereoLitography (STL) file (*fig. 16*), which essentially uses triangles to describe the surface of an object, simplifying the CAD model. Subsequently, the STL file is imported into a slicer program, that slices the designed part into the printable layers. Finally, the slicer program converts the STL file into G-code, which is a numerical control programming language used in Computer-Aided Manufacturing (CAM) to control automated machines like 3D printers.

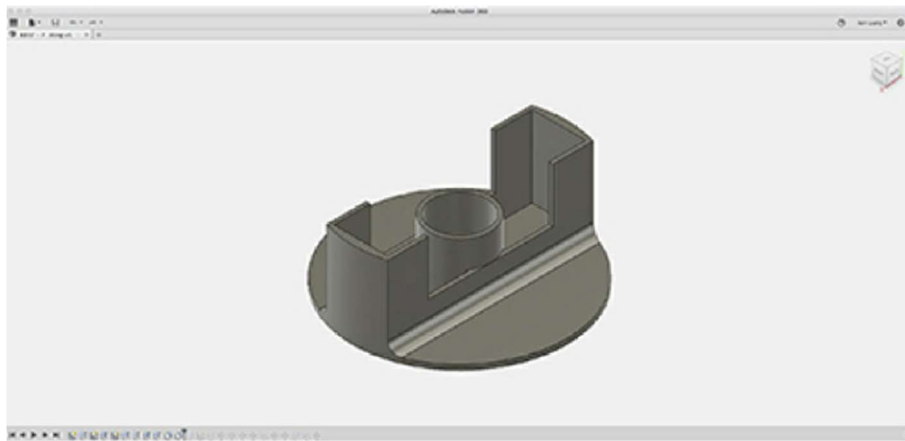


Figure 15. A 3D CAD model of a shaft end cap produced in Autodesk Fusion 360 ¹³²

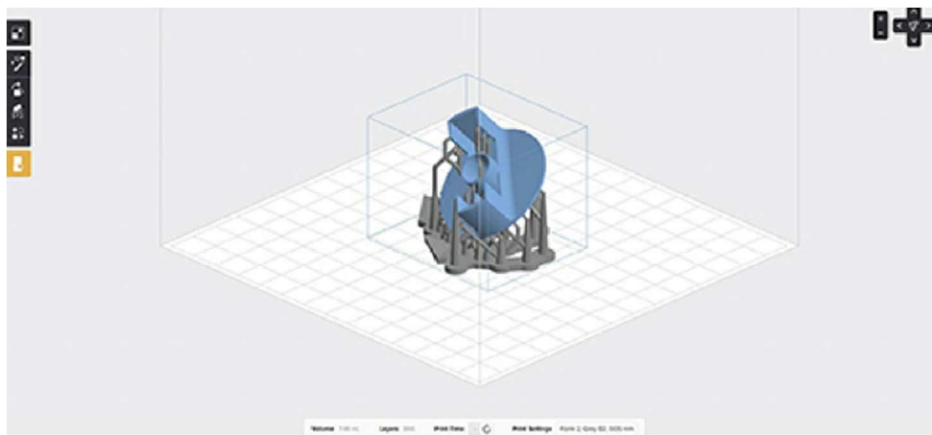


Figure 16. STL file imported into the slicing program Preform ¹³²

Materials

The FFF printing is a technology that produces parts starting from thermoplastic materials in the form of filaments on spools, typically with a diameter of 1,75 or 3 mm. The cost of FFF filaments is generally very low (20- 40 \$ per 1kg spool), except for high-performance polymers such as PEEK (up to 500\$/kg). In general, it can be stated that thermoplastic materials characterized by high mechanical properties have a higher melting temperature, resulting in a more difficult printing process. Higher printing temperatures make the printed part cooling at a faster rate due to a greater temperature gradient, generating more internal stresses and causing undesirable phenomena like warping and distortion. Going from commodities such as ABS and PLA to high-performance polymers such as PEEK and PEI, the printing temperature increase, and so the engineering properties do. Therefore, industrial machines, that guarantee better control over the printing environment, are usually preferred to print hard-printable thermoplastics (*fig. 17*).

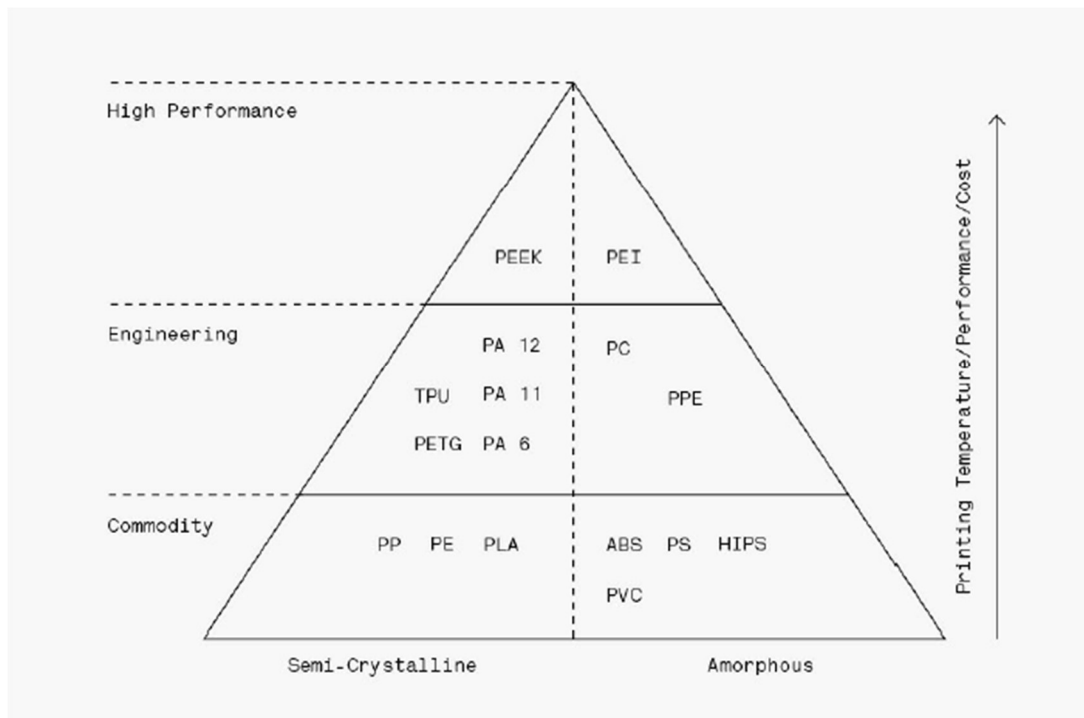


Figure 17. Thermoplastic material pyramid.

Some of the commonly used FFF thermoplastic materials and their main characteristics are presented in *table 4*. In general, FFF materials must have some basic characteristics to be efficiently printed: the mechanical properties of the filament must be adequate, in order to permit the filament to work as a piston and push the melted material toward the extrusion head and the viscosity of the melted material must fall into certain limits to allow a proper extrusion of the material through the heated nozzle¹³³. In fact, a too high viscosity would lead to a scarce adhesion between printed layers, while a too low viscosity would cause the instability of the extruded material width. A 3D printer is also able to process thermoplastic elastomers, which are a class of polymers with intermediate properties between those of plastics and elastomers and seem to be good substitutes for classic vulcanized rubbers.

Table 4. Common FFF materials ¹³².

Material	Common Brands	Characteristics
ABS	eSun Stratasys Ultimaker	<ul style="list-style-type: none"> - Good mechanical properties - Good temperature resistance - Susceptible to warping
PLA	ColorFabb (PLA/PHA) Formfutura Innofil Polymaker Ultimaker	<ul style="list-style-type: none"> - Most common 3D printing plastic - Easy to print with - Lower impact strength, elongation and temperature resistance than ABS
Nylon (PA)	Stratasys Taulman3D Ultimaker	<ul style="list-style-type: none"> - Suitable for end-use prints - Good flexibility - Excellent chemical resistance
PETG	ColorFabb (XT) eSun	<ul style="list-style-type: none"> - High impact & chemical resistance - Good thermal properties - Susceptible to warping
TPU	Ninjabflex Ultimaker TPU 95A Polymaker Polylex	<ul style="list-style-type: none"> - Flexible and rubber-like parts - Good elongation - Difficult to print accurately
PEI	Stratasys (ULTEM)	<ul style="list-style-type: none"> - Excellent strength to weight - Fire and chemical resistance - High cost

Printer parameters

An accurate printing process requires the adjustment of many parameters such as build speed, extrusion speed and nozzle temperature. These parameters are set by the operator and are fundamental to achieve a good quality of the printed item. Another parameter with a large influence on the process is the nozzle diameter. A smaller nozzle diameter and lower layer height usually lead to the production of FFF printed parts characterized by a smooth surface and higher level of detail. The available build volume must also be considered when printing using FFF. Desktop printers have a smaller build chamber (200x200x200 mm) compared to industrial machines (1000x1000x1000 mm). In general, the best solution to deal with the printing of very large parts is breaking the design down into components that can be later assembled.

Warping

Warping of FFF printed parts occurs, as previously mentioned, due to differential cooling. This problem is more common in materials characterized by high crystallinity and is caused by the

different cooling rates of printed part zones. The perimetral zones cool at a faster rate compared to central zones and this reflects in the creation of internal stresses, with an entity proportional to the coefficient of thermal expansion (CTE) of the material. When these stresses are too elevated the printed part undergoes a structural distortion called warping (*fig. 18*).

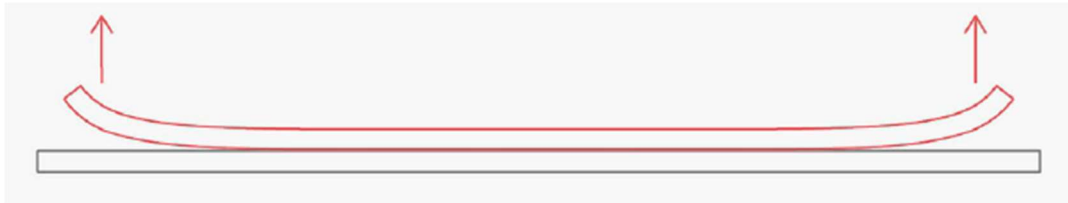


Figure 18. Warping of FFF parts ¹³².

A heated bed, as well as good bed adhesion, are key aspects to consider in order to anchor the FFF part down and thus limit distortion processes. It has been noted that increasing the deposition bed temperature, the warping becomes less evident. In fact, when the chamber temperature is equal to the glass transition temperature (T_g) of the material the deformation can be considered absent. However, a high chamber temperature results in increased material solidification rate, leading to a possible drop in print quality ¹³⁴. Furthermore, the deformation depends on the length of the printed part. Thus, warping can be reduced by splitting the designed model into several parts ¹³⁵. The likelihood of warping occurring is also influenced by the number of deposited layers during the printing process ¹³⁶. A common trick used to decrease the warping entity consists in designing the FFF part with a larger basis, adding the so-called “skirt”, to increase the printed part adhesion to the deposition bed. The material in excess can easily be removed after the printing.

Layer adhesion

Layer adhesion is a fundamental aspect of the FFF printing process. The extruded filament needs to bond and solidify with the previously printed layers to attain an optimal cohesion of the final printed part. This is achieved by pressing the filament against the already existent layers. The deposition of new melted material makes the previously printed layer re-heat and re-melt. The partial re-melt of the underlying material, together with the pressure applied by the new filament, lead to the bonding of the new layer with the previously printed one. This process also causes the deformation of the deposited filament, which will have an oval shape rather than a circle one (*fig. 19*). As a consequence, the joints between each layer can be described as small valleys (*fig. 20*). These joints also represent stress concentration points, where cracks can form consequently to an applied load, and lead to the well known anisotropic behavior and rougher surface appearance of FFF printed parts.

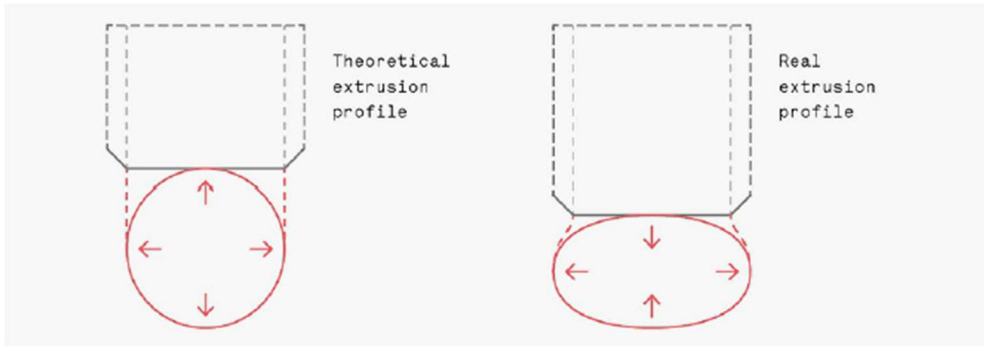


Figure 19. FFF material extrusion profile ¹³².



Figure 20. FFF layer-by-layer construction ¹³².

Support structures

Another important aspect to consider when FFF printing a part is the presence of support structures. Support is essential for any overhanging features that are shallower than 45 degrees relative to the ground plane (*fig. 21*). In those cases, the deposited layers would not be completely supported by the underlying structure and thus a solid scaffold is required to build upon. Support structures allow printing parts with different geometries but decrease the quality of the surface they are in contact with. For this reason, the number of support structures should be reduced to the minimum, and post-processing steps should be considered if a better surface quality of the printed object is needed.

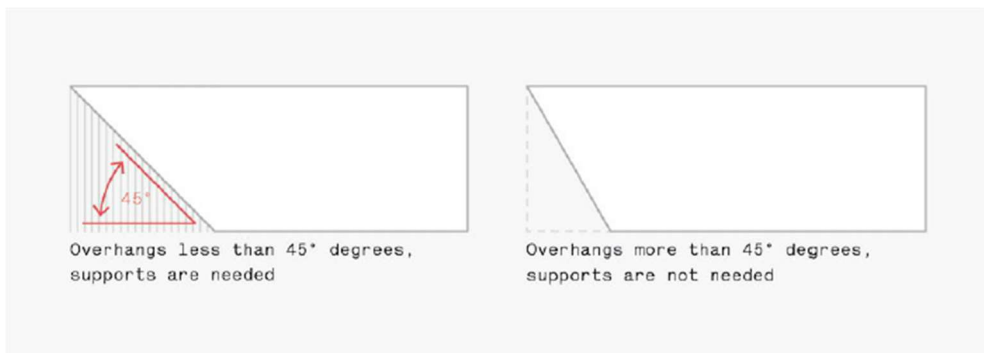


Figure 21. FFF support requirements ¹³².

Many new FFF printers have two extrusion heads, being capable to print using two different materials: one used for the desired object and one for the support structure. Usually, the support is printed using a dissolvable material (generally PVA or HIPS). When using two extrusion heads printers, is fundamental to have good adhesion between the two used materials. The most common FFF dissolvable support/build material combinations are PLA with PVA (dissolved in warm water), and ABS with HIPS (dissolved in a 1:1 ratio of (R)-(+)-Limonene and isopropyl alcohol). The main drawback is represented by the increase in production costs, caused by the high cost of soluble filaments and the increased production times. Therefore, it is preferable to efficiently design the desired part, in order to reduce the support structures needed ¹³⁷. On the other hand, with FFF printers characterized by a single extrusion head, two types of support can be used: accordion and tree-like (*fig. 22*).

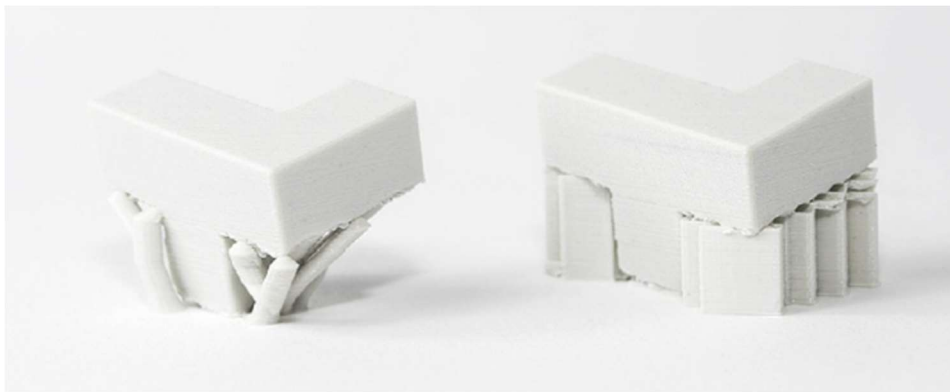


Figure 22. Tree-like support (left) and accordion support (right) ¹³².

The accordion support is more common because of its simple geometry, but requires more material to be built, increasing the production costs. The tree-like support is less expensive (less material required) and has less contact with the print, leading to higher quality printed parts, but it offers less stability, making it unsuitable for complex shape-prints.

Infill

When designing an FFF part, crucial parameters to consider are represented by the infill geometry and percentage. The infill is a low-density structure internal to the printed part that allows saving on material and decreasing building time (*fig. 23*). The infill percentage can be varied based on the application of a part, ranging from 10% for models used for form and fit testing to 80% (or fully dense) for high strength parts. A common infill percentage for FFF printing is 20%. Furthermore, infill geometry also has a considerable impact on the performance of the printed part. Several infill geometries have been developed, with the more common being triangular, rectangular, and honeycomb.



Figure 23. The internal infill geometry of an FFF part ¹³²

Advantages and drawbacks of FFF printing

The FFF printing technology represents a very cost-competitive way to produce custom thermoplastic parts, being characterized by low-cost materials and machines, ease of operation, and absence of production waste. On the contrary to other manufacturing technologies, FFF and other 3D printing technologies can produce the desired part in a single process. STL files can be easily sent through the internet, making the desired object printable from any 3D printer that can satisfy the design parameters. Furthermore, FFF is able to process a broad variety of thermoplastic materials and create different geometries without modifying the printer in any way, making the technique the most popular choice for rapid prototyping, as well as some functional applications.

The main limitation of FFF is represented by the anisotropy of printed parts. The layer-by-layer method of printing results in produced parts that are fundamentally weaker in one direction. Therefore every part must be designed choosing the build direction that will positively, or at least not negatively, impact the final performance. In addition, the productivity of FFF is still much lower than that of classic mass-production processes such as injection molding.

1.6.2 3D printing (Material extrusion) of PLA

Currently, PLA is one of the most used and promising materials for the production of FFF parts. A lot of studies have been conducted on FFF printed PLA parts and they focus on different aspects. An intensive investigation has been carried out to optimize process parameters, aiming to improve interfacial bonding property, mechanical properties, and accuracy. Furthermore, several researchers have focused their studies on the PLA chemical modification, in order to obtain the improvement of mechanical properties of PLA parts through the enhancement of

entanglement state and crystallinity of PLA molecular chains and the application of a reinforced phase. In addition, the functional compounding of PLA can lead to PLA printed parts with interesting characteristics such as heat stability, electrical conductivity, biocompatibility, antistatic property, electromagnetic shielding, and temperature-controlled heating property. In conclusion, these researches are crucial to improve performances, enhance functional applications, and expand or enrich applications of FFF 3D-printed PLA parts.

Apparently, there are some intrinsic limitations corresponding to the use of PLA as print material. One of these is its crystallinity, which results in volume change and residual stress that may affect the dimensional precision of the printing process. Furthermore, the mechanical strength of PLA is lower than that of other polymers such as ABS, PC, or PA. This is mainly caused by the microscopic structure of PLA, consisting of simple linear molecular chains. On the other hand, the available free space between molecular chains, along with the frequency of functional groups, make it possible to easily modify the PLA structure, leading to enhanced mechanical properties. Moreover, several PLA characteristics make it incomparable against other polymeric materials, such as no environmental pollution being (bio)degraded into H₂O and CO₂ and being produced from biotechnological processes; good biocompatibility that makes PLA an excellent candidate for the use as medical suture material, drug sustained-release material, and material for tissue engineering; no degradation in mechanical properties over long-time use.

Interface adhesion property

The mechanical properties of FFF printed PLA parts are practically identical to those of die formed parts when analyzed along the direction in which the filaments are continuously distributed. On the contrary, the other two perpendicular directions present macroscopic interfaces that result in lower mechanical properties (*fig. 24*).

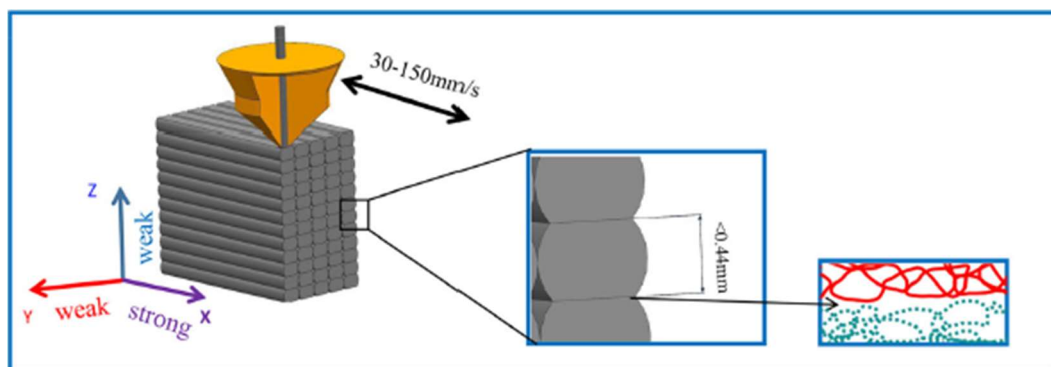


Figure 24. FFF printed PLA parts interface ¹³⁸.

It is evident, as previously mentioned, that the interface is the most fragile position of FFF printed parts ¹³⁹⁻¹⁴¹. Furthermore, it cannot be eliminated since it is a result of the technological principle of FFF process. For this reason, a priority in the development of FFF printed PLA parts should be the enhancement of interface bonding property. The main cause of weak interface bonding, and thus reduced mechanical properties, is the impossibility to maintain enough time the extruded PLA at a temperature above the melting point ^{142, 143}. In fact, the extruded filament, which has a very limited volume, undergoes rapid cooling due to the impact with the external environment. Therefore, molecular chains on the interface do not have the time to diffuse completely and the adjacent filaments cannot be well fused (*fig. 25*).

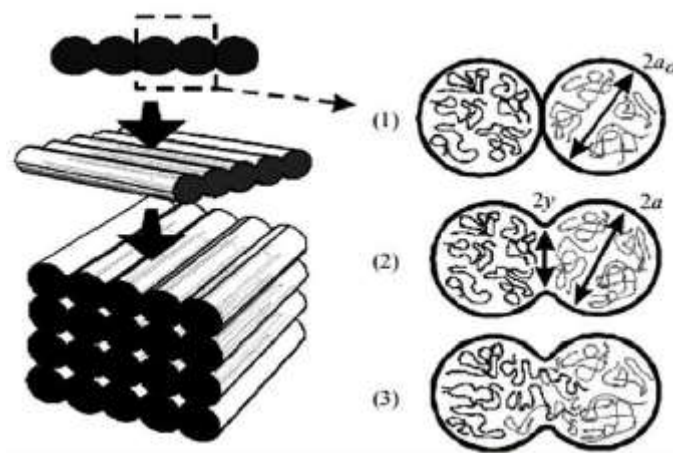


Figure 25. Bond formation process between two PLA filaments: (1) surface contacting; (2) neck growth; (3) molecular diffusion at the interface and randomization ¹³⁸

In the FFF process, a crucial factor for optimized interface bonding is the cooling speed ¹⁴⁴. A too slow cooling can lead to the disorder of fused PLA filaments and evident part shape deformation while a too high cooling speed may result in limited diffusivity of PLA macromolecular chains and, thus, bad interface adhesion. Therefore, a lot of researchers focused their work on the optimization of this parameter.

Partain developed a system to blow heated air through another nozzle directed toward the entire printed PLA part. It has been seen that an air temperature of 65°C would result in interface strength increased by 66% but the method is characterized by some restrictions: the heating of the whole PLA part cannot increase properly the interface bonding and the hot air blown can produce a turbulent flow, causing the disorder of melted PLA filaments and decreasing the dimensional accuracy of the printing process ¹⁴⁵. A local laser heating system of the layered zone near the nozzle has been introduced by Ravi et al. (*fig. 26*).

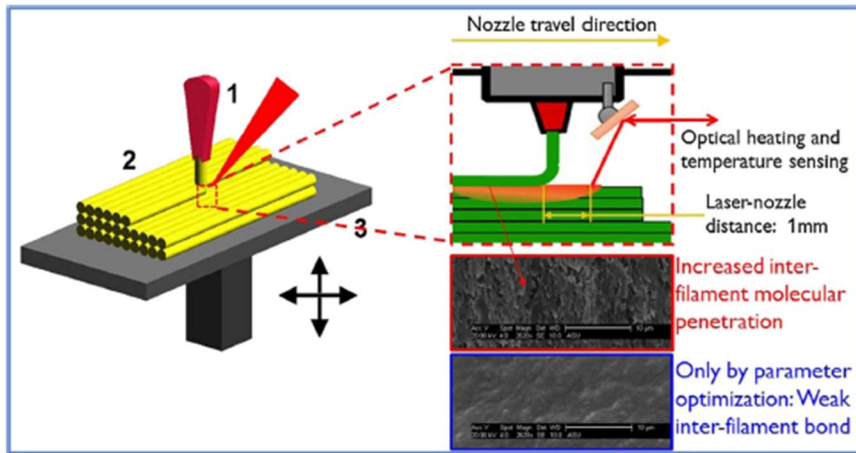


Figure 26. Laser local predeposition heating approach ¹⁴⁶.

The laser has been set to exceed the critical temperature of T_g ($T_g = 60-65^\circ\text{C}$) and results showed an increment of the interface bonding of FFF printed PLA parts and of the infill percentage, the latter probably due to surface reflow ¹⁴⁶. The same idea was adopted by Kishore et al., who realized a synchronous and local heating using infrared rays (*fig. 27*). The system has efficiently lead to an enhancement of interface adhesion, except for infrared rays of 1kW intensity, which, due to the excessive intensity, caused the degradation of PLA, resulting in lower mechanical properties ¹⁴¹.

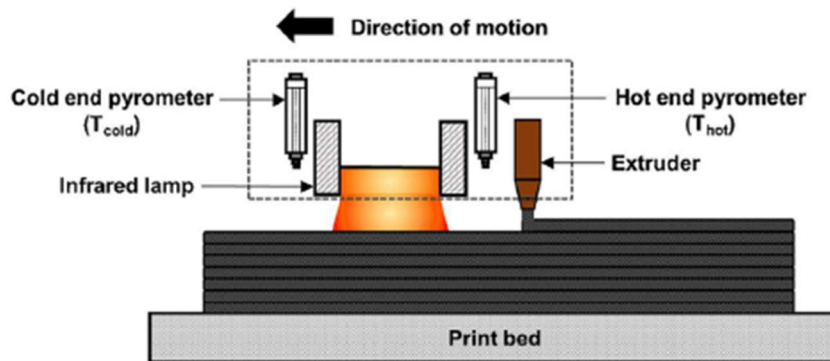


Figure 27. X-ray local predeposition heating approach ¹⁴¹.

In conclusion, the interface of FFF printed PLA parts and, therefore, the mechanical properties of the final objects can be effectively enhanced through a local laser and infrared heating, with better results compared to the whole part heating. However, these systems increase the technological complexity and cost of the FFF process.

Mechanical properties and shape precision

A lot of effort has been put into understanding how the macro-technological parameters affect mechanical properties and shape precision of PLA printed parts ¹⁴⁷. Some macro structuring

rules have been proposed: the printing direction should coincide with the direction of main stretching load (no interfaces present in this direction)¹⁴⁸⁻¹⁵⁰; lower layer height results in better surface quality but inevitably leads to higher printing time¹⁵¹; high infill percentages provide printed parts characterized by better mechanical properties. The FFF printing process inevitably leads, due to his working principle, to a temperature gradient in the PLA parts, causing lower interface bonding and deformation mechanisms like warping, thus resulting in deteriorated mechanical properties. At this moment, the temperature gradient is reduced mainly by controlling plate temperature and printing layer height. From Wang et al., it can be seen that a plate temperature of 160°C and a layer height of 0,2 mm resulted in better bonding and significantly reduced porosity of FFF printed PLA parts. Therefore, better mechanical properties and high shape precision were achieved¹⁵². Other technological parameters that have a large influence on the performance of the printed part and have to be optimized are the infill geometry and percentage, the post-heat processing time, and the printing direction. As an example, Patel et al. printed PLA specimens setting different infill pattern and density and analyzed the tensile strength of the obtained parts¹⁵³. The effect of post-heat processing was studied by Torres et al., who found that a too high or too low post-heat processing temperature result in a decrement of the shear stress property of FFF printed PLA parts¹⁵⁴. Afrose et al. printed PLA parts with different orientations (0°, 45°, 90°) and noted that the FFF printed PLA parts with 45° had the best fatigue property¹⁵⁵. In conclusion, even if several methods are able to optimize the FFF printing process for PLA parts, there are still some intrinsic negative aspects that cannot be eliminated, such as the presence of the interface and the mechanical performance and shape accuracy limitations.

Modified and reinforced PLA filaments for FFF printing

Combining various materials to achieve desired mechanical and functional properties is a promising way to solve all the mentioned problems of FFF printed parts. Therefore, recently, the development of composite materials that are compatible with the available printers has attracted tremendous attention. In particular, many promising results in developing new PLA printable composite materials reinforced by particles, fibers, or nanomaterials have been demonstrated.

Shim et al. developed and characterized an FFF printed polycaprolactone/poly(lactic-co-glycolic acid)/β-tricalcium phosphate (PCL/PLGA/β-TCP) membrane to assess his effectiveness in bone regeneration and osseointegration in areas surrounding implants¹⁵⁶. The feasibility to print a hygromorphic PLA/PHA biocomposite reinforced with recycled wood

fibers was demonstrated by Le Duigou et al. ¹⁵⁷. Postiglione et al. used a home-modified low-cost commercial benchtop 3D printer to produce intrinsically conductive PLA nanocomposite reinforced with multi-walled carbon nanotubes (MWCNTs). Carbon nanotubes (CNTs) were used also by Patanwala et al. to produce PLA composites through FFF printing. Further studies on the nucleation and viscosity of the CNT/PLA composite have been made ¹⁵⁸. Zhang et al. developed PLA/r-GO composite filaments which can be processed through FFF to produce graphene-based flexible circuits ¹⁵⁹. The same material combination was used by Yu et al., who explored the whole mechanical properties besides conductivity. In addition, more polymeric materials such as PE and PLA were modified with metal or ceramic materials (Cu, Al, Al₂O₃) and used to FFF print composites and analyze their properties ¹⁶⁰. Furthermore, other groups mixed some functional materials with PLA, trying to print PLA parts with useful characteristics such as thermal stability, conductivity, biocompatibility, antistatic properties, electromagnetic shielding, and temperature-controlled heating, in order to expand the functional applications of FFF printed PLA parts ¹⁶¹⁻¹⁶⁷.

Carbon fiber reinforced PLA filaments for FFF printing

The use of fiber reinforcements in 3D printing filaments for FFF is a topic of on-going research with both advancements in scientific literature as well as in commercial products. Carbon fiber reinforcement can significantly enhance the mechanical properties of FFF printed parts and the reinforcement may also be used to add extra functionality to the material such as electroconductivity and higher heat conductivity.

Most studies report on the use of short carbon fibers. In this case, before the FFF printing step, polymer pellets and fibers are usually mixed in a blender and then processed with an extruder to fabricate filaments. A second extrusion process could be conducted to increase the fiber homogeneity of the filament. The incorporation of short carbon fibers leads to the production of FFF printed composites with strength and stiffness increased of about 65%, but the obtained mechanical properties are still lower than those of CFRPs produced through traditional manufacturing methods. This is also caused by the high shear mixing, which leads to fiber breakage, reducing their length in the filament and consequently lowering the strength of the printed part ^{116, 168}.

Another promising method to print composites consists in the use of continuous carbon fibers. MarkForged has developed a printer that can produce CFRPs by depositing continuous fibers in a polymeric matrix. The process requires a custom printing head and technique and produces continuous fiber printed parts with mechanical properties which are an order of magnitude

higher than typical FFF printed short fiber-reinforced materials (*fig. 28*). However, even this method is not able to produce parts with performance equal to that of parts produced by traditional manufacturing methods, such as injection moulding.

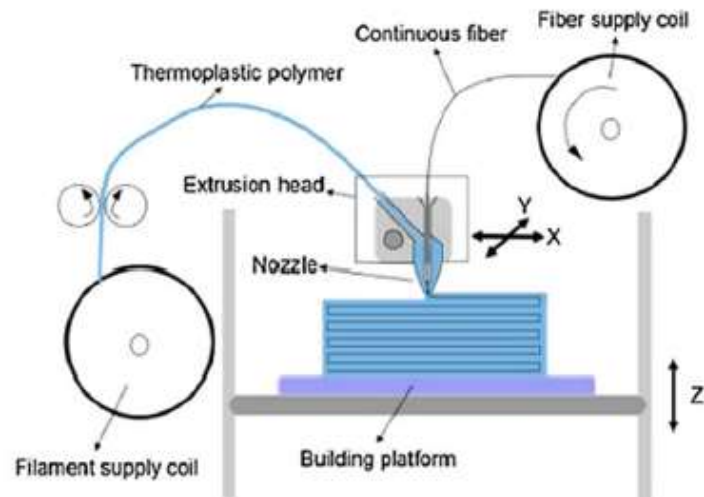


Figure 28. The setup for 3D printing of continuous fiber reinforced composites ¹⁶⁹

Several researchers have focused their studies on the use of carbon fibers for the reinforcement of FFF printed PLA parts.

Ivey et al. produced PLA and short carbon fiber reinforced PLA specimens through FFF printing and compared the mechanical properties of the obtained parts. The results showed a significant improvement in elastic moduli due to the addition of short carbon fibers. Furthermore, the effect of annealing on the printed specimens was assessed. The annealing process led to an increment of crystallinity in both sample groups but no effect on the mechanical properties has been noted ¹⁷⁰. Jiang et al. used short carbon fiber reinforced filaments (PLA, ABS, PETG, and Amphora) to FFF print a series of specimens, in order to assess the effect of CF reinforcement. Test bars were printed with FFF bead orientations at 0° , $\pm 45^\circ$, and 90° with respect to the applied load direction. From the results, it can be seen that the incorporation of carbon fibers caused an increment of tensile modulus at all print orientations while the tensile strength resulted higher only at 0° print direction. Fiber length distribution (FLD) and fiber weight fraction have also been evaluated and it was found that filament extrusion contributes very little to fiber breakage. SEM investigation of fracture surfaces has finally been conducted, showing a reduced void between the beads in the CF reinforced printed parts ¹⁷¹. Tian et al. exploited an FFF modified printing process to obtain continuous carbon fiber reinforced PLA composites. After having systematically investigated

and then optimized the process parameters, 3D printed CFR PLA composites with a fiber content of 27% have been fabricated and analyzed. Flexural strength of 335 MPa and flexural modulus of 30 GPa have been achieved ¹⁷². A further study allowed the development of an innovative method to efficiently recycle the precedently obtained continuous carbon fiber reinforced PLA composites. The original printing trajectory was reversely applied, leading to a 100% recycling of the continuous carbon fiber without any effect on the mechanical properties (fig. 29). For what concerns the matrix, pure PLA was added to the recycled matrix to compensate the aging effects ¹⁷³.

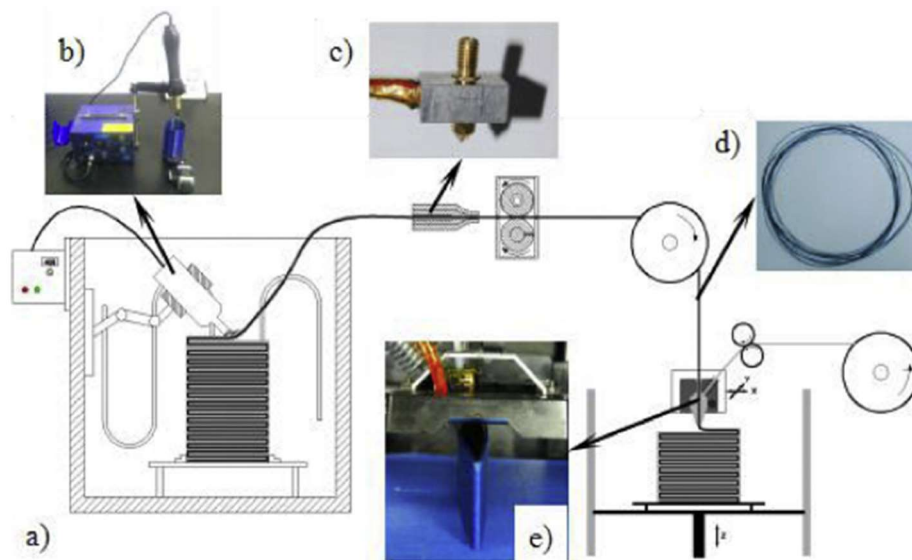


Figure 29. Scheme of recycling and remanufacturing of 3D printed CFRPs. a) key elements for each step. b) hot air gun. c) remolding nozzle. d) recycled impregnated filament. e) remanufacturing process ¹⁷³

Ferreira et al. investigated and compared the properties of FFF printed short carbon fiber reinforced PLA with those of pure PLA. The results showed a sharp increase in the tensile modulus of the printed part (about 2.2 times) along the printing direction, consequently to the addition of carbon fibers. In addition, SEM analysis of the carbon fiber reinforced PLA printed parts revealed that the short carbon fibers were mostly aligned with the direction of printing. For this reason, the biggest increase in stiffness for the composite happened in the printing direction ¹⁷⁴.

2. Thesis object

The increased exploitation of carbon fiber reinforced polymers is inevitably bringing about an increase in production scraps and end-of-life components, resulting in a sharp increase in CFRP waste. Therefore, it is of paramount importance to find efficient ways to reintroduce waste into the manufacturing cycle. At present, several recycling methods for treating CFRPs are available (mechanical, thermal, and chemical recycling), even if all of them still have to be optimized. The step after CFRP recycling, and also the key to build a solid and sustainable CFRP recycling market, is represented by the utilization of Re-CFs. The smartest way to utilize recovered carbon fibers is through the manufacturing of recycled CFRPs, that can be done by re-impregnating the recovered fibers with a new polymeric matrix: however, it has to be highlighted that Re-CFs size will not be the same as in pristine fibers, since this parameter strongly depends on the type and dimension of the recycled CFRP waste. Hence, re-use of Re-CFs needs to imply application where the CF dimension is limited, in order to be able to apply the greatest fraction of recycled product. Currently, there are several processes under development for the processing of recycled carbon fibers (injection molding, nonwoven production, tape development, hybrid yarn technologies, and fused filament fabrication). Fused Filament Fabrication (FFF) is one of the most widely used additive manufacturing (3D printing) techniques that fabricates parts with a polymeric filament deposition process. The filament can also contain fillers or reinforcements such as recycled short carbon fibers and this makes it perfectly compliant with the re-application of the shortened recycled CF. The development of an FFF process which is effectively able to produce printed Re-CFRPs starting from recycled carbon fibers and new polymeric matrixes would not only be extremely important because of the utilization of Re-CFs, but also because fused filament fabrication allows to produce parts adding material layer-by-layer, only where it is needed, saving energy, raw material cost, and waste. Therefore, in this thesis work, carried out in collaboration with Prof. Francesco Picchioni, recycled carbon fibers reinforced PLA composites have been printed exploiting the FFF technology and subsequently characterized, in order to evaluate properties of printed PLA composites containing Re-CFs and compare them with analogues printed using virgin carbon fibers reinforced PLA composites.

3. Results and discussion

3.1 Production of carbon fiber reinforced PLA filament

3.1.1 Carbon fibers pre-treatment

The composite has been prepared using both virgin carbon fibers (V-CFs) and recycled carbon fibers (Re-CFs), in order to compare their properties and assess the feasibility of using Re-CFs in 3D printing applications. Virgin carbon fibers, Toray T700 dry fabrics, have undergone a de-sizing treatment to remove the sizing agent on their surface. Sizing removal treatment is necessary to obtain results that are comparable to those of Re-CFs. Recycled carbon fibers have been obtained in a pyro-gasification pilot plant from Curti, in a semi-industrial process. CFRP treatment has been previously optimized to provide almost complete removal of the polymeric matrix and then manually treated to remove the residual char originating from the pyro-gasification process in which they have been recovered ⁴⁹. The char is a consequence of incomplete matrix degradation and results in lower fiber-matrix adhesion in the composite. Therefore, it is necessary to remove this residue before mixing fibers with the PLA matrix. Carbon fibers treated in the semi-industrial pilot plant show a good mechanical performance, once the plant conditions are optimized, with almost unaffected modulus (about 220GPa for both samples), and a slight embrittlement with σ_b that is almost unaffected (3GPa for both samples) while ε_b that drops from 1.4% down to 1.1% passing from virgin fibers to the recycled ones ⁵⁸. Subsequently, both unsized virgin CFs and recycled CFs have been cut using a chopper gun to obtain fibers with an initial average length of 7 mm (*fig. 30*). The cutting process is crucial to obtain short fibers that can be easily mixed with the thermoplastic matrix, producing a 3D printable material.



Figure 30. Chopped carbon fibers.

3.1.2 Compounding of composite materials

In the compounding step different formulations of the desired composite, using both virgin and recycled carbon fibers, have been produced (*table 5*). The polymer used as matrix is poly(L-lactic acid) (PLLA), a crystallizable polyester that is obtained from renewable resources and is also biodegradable. PLLA, or how it is often referred to, PLA is widely used as 3D printable filament, due to the reasonably low processing temperature - the polymer melts around 170-175°C and can be thus processed in a 180-230°C temperature range - and the easiness of colouring of the polymers. It is also non toxic and biodegradable. However, PLA, as many other aliphatic polyesters, is extremely sensitive to the presence of water when heated above its melting temperature, since water can trigger a random chain scission that will acutely degrade the overall polymer performance.

The first step consists thus in drying starting materials, i.e. fibers and PLA pellets, in order to avoid hydrolysis during further thermomechanic compounding processing.

Table 5. Composite formulations.

		CF content (%wt.)
Recycled CF	PLA-R5	5
	PLA-R10	10
Virgin CF	PLA-V5	5
	PLA-V10	10

After having removed all the residual moisture with the aid of a vacuum oven, the materials have been fed into a twin-screw mixer (Brabender), precedently set at 190°C. This temperature has been chosen because the corresponding viscosity of the PLA is appropriate to guarantee an efficient mixing process and, at the same time, the temperature is not too high to lead to thermal degradation. Another critical parameter that, similarly to the temperature, characterizes the compounding process, is represented by the processing time. After several attempts, the process was optimized to last 12 minutes, 4 minutes allow to melt PLA pellets and the further 8 minutes to mix fibers and PLA. As in the case of the temperature, the optimization of processing time is fundamental to produce a composite characterized by good fiber dispersion and low matrix degradation.

The obtained composites have been ground using an electric grinder to obtain pellets, which have been extruded using a single-screw extruder to produce the desired filaments (*fig. 31*). The employed extruder is equipped with a laser control system that allows to control the filament

diameter during the extrusion. The stability of the filament diameter is a critical parameter to guarantee an efficient feeding of the filament through the extrusion head of the printing machine, allowing a continuous flow of material from the nozzle and thus leading to the production of printed parts without shape defects and avoiding the creation of stress-concentration regions.



Figure 31. Produced filaments.

3.2 Filament characterization

The extruded filaments of all the different formulations have been subjected to TGA analysis to study the effect of fibers on the degradation behavior of PLA. Furthermore, the thermogravimetric analysis allows to investigate the CFs dispersion homogeneity along the filament. Each filament has been subjected to sampling in three different regions, widely distanced one from the other, and results are shown in *figure 33* and summarized in *table 6*. The analysis has been carried out exploiting a method optimized to obtain CF weight fraction for epoxy composites. This method consists of a ramp 20 °C/min to 500 °C in N₂, an isothermal for 15 minutes to allow for pyrolytic degradation of the matrix without affecting the carbon fiber, then a cooling ramp 20 °C/min to 300 °C before switching to air and an isothermal for 5 minutes guarantee that the oxidizing atmosphere will not be aggressive for the graphitic fibers, while a further ramp at 10 °C/min to 500 °C and a final isothermal for 30 minutes in oxidizing environment will boost degradation of the residual resin without affecting carbon fibers, as shown in the PLA-R5 filament analysis (*fig. 32*). The air switch and the following ramp to 500

°C are required to burn the char formed on the fiber surface during the thermal degradation in N₂, in order to obtain a more precise measure of CF wt%. In the case of PLA, the char formation is less favored compared to epoxy matrices because PLA does not contain aromatic moieties like high performance epoxy resins. This has been confirmed by the TGA result of neat PLA (PLA 4043D). In fact, after the first temperature ramp to 500 °C in N₂, the weight percentage reach values close to zero (*fig. 33*). Furthermore, as shown in *figure 32*, calculation of CF weight fraction of composite filaments both after the first ramp in N₂ and after the second ramp in air, show that the first approach provides a value much closer to the expected one: indeed the lack of a protecting char layer, that allows to complete PLA removal in inert atmosphere, favours the attack of the oxidizing environment directly to the CFs surface, as previously demonstrated in the literature, thus eroding their mass. For these reasons, it has been chosen to calculate the carbon fiber weight fraction by taking values obtained directly after the temperature ramp up to 500 °C in N₂ atmosphere, assuming that after this ramp all the polymer matrix has been degraded and volatilized, leaving only the carbon fibers unaltered. *Figure 32* also shows that the weight remains practically constant during the isotherm in N₂, confirming that the first heating ramp is sufficient to degrade all the matrix.

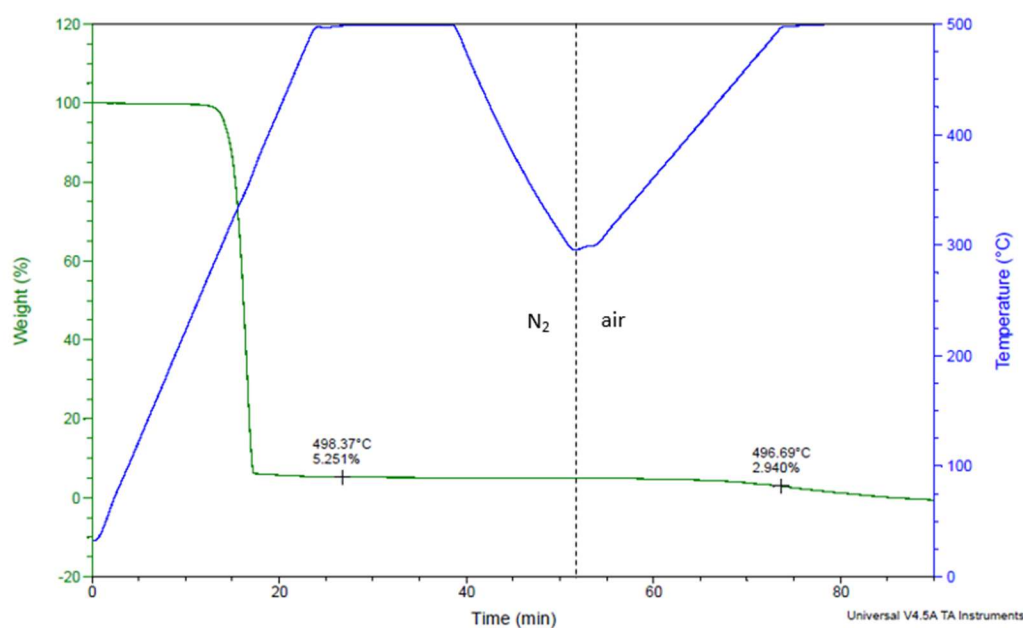


Figure 32. PLA-R5 analysis showing TGA method.

The calculated CF contents for all the filaments are in agreement with the prepared formulations, with values close to 5% for PLA-R5 and PLA-V5 and 10% for PLA-R10 and PLA-V10. It can be seen from *table 6* that the standard deviations of these results are very low, suggesting high homogeneity of fiber inside the filaments. Furthermore, the composite

filaments containing 10 wt% of carbon fibers (PLA-R10 and PLA-V10) show a higher value of onset degradation temperature. This improvement in thermal stability of PLA upon incorporation of carbon fibers could be attributed to their higher thermal conductivity, which facilitates heat dissipation within the composite, preventing the accumulation of heat at certain points and limiting degradation processes ¹⁷⁵.

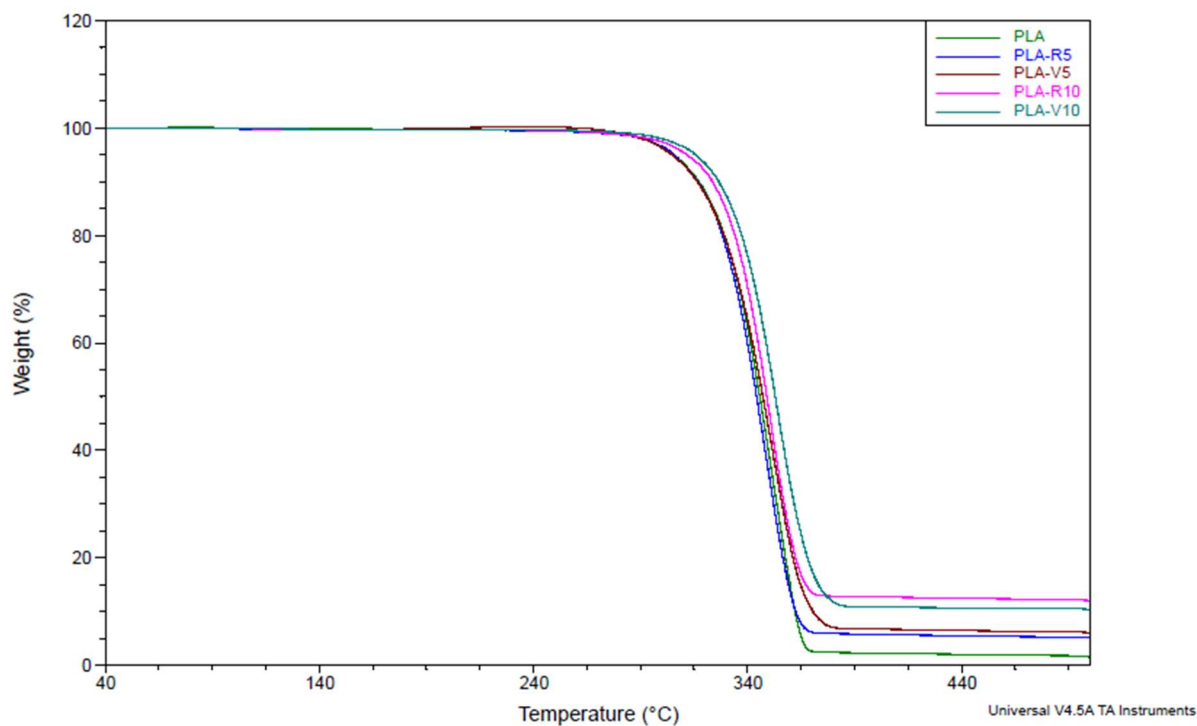


Figure 33. TGA thermogram of filaments.

Table 6. TGA results of filaments.

	CF wt %	Onset (°C)
PLA	/	328 ± 3
PLA-V5	6 ± 1	324 ± 4
PLA-V10	10 ± 1	332 ± 1
PLA-R5	5 ± 1	326 ± 2
PLA-R10	11 ± 1	332 ± 2

A dissolution method based on the use of CHCl_3 has been applied to treat the filaments and remove the PLA matrix. The recovered fibers have been weighted to obtain another estimation of the fiber content on a larger volume than those used for TGA sampling (table 7).

Table 7. Weight percentage of carbon fibers recovered after the CHCl_3 dissolution of the filaments.

	Recovered CF (%wt.)
PLA-V5	8,8
PLA-V10	13,1
PLA-R5	7,3
PLA-R10	12,8

As the table shows, the percentage of fibers recovered after matrix dissolution appears slightly higher than expected (5 wt% for PLA-R5 and PLA-V5 and 10 wt% for PLA-R10 and PLA-V10). This could be attributed to an incomplete matrix dissolution. However, the obtained dried fibers were analyzed with an optical microscope (fig. 34) to obtain an estimate of the effective length of the fibers inside the filament (table 8) after the processing steps in the Brabender mixer and in the extruder. This data is fundamental to assess the printability of produced filaments and, consequently, evaluate the whole processing method in terms of fiber breakage. Results show, as expected, an average length of fibers much lower than that to which fibers have been initially cut (7 mm). However, the processing steps applied seem to have an impact that is not highly dependent on the peculiar situation and, more importantly, on the type of fiber used (virgin or recycled).

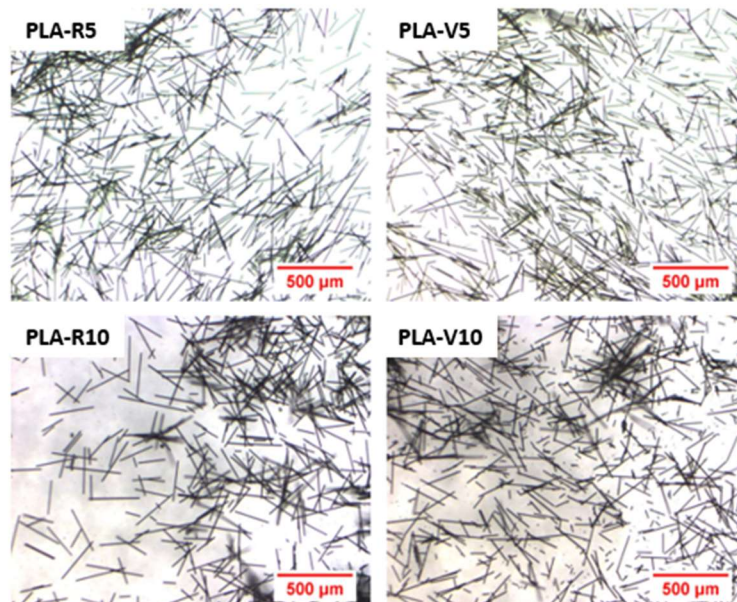


Figure 34. Optical microscope images of fibers recovered after CHCl_3 dissolution of the filaments.

Table 8. Average lengths of fibers inside filaments.

	Fibers length (μm)
PLA-V5	190 \pm 120
PLA-V10	150 \pm 60
PLA-R5	200 \pm 100
PLA-R10	170 \pm 100

Dynamical mechanical analysis (DMA) of the filaments has been carried out and the resulting DMA spectra are shown in *figures 36* and *37*. In *table 9* obtained values of storage modulus (E'), onsets of storage modulus drop, and loss factor ($\tan\delta$) are shown. The storage modulus (E') represents the stiffness of viscoelastic material and is proportional to the elastic modulus. As expected, increasing the fibers content, the stiffness of the composite grows, causing an increment of the storage modulus. From the curves in *figure 36*, it can also be seen that recycled carbon fiber reinforced filaments (PLA-R5 and PLA-R10) have a rigidity that is comparable to that of filaments containing the same weight fraction of virgin carbon fibers (PLA-V5 and PLA-V10). The slight difference could be due to the degradation of the surface of the recycled carbon fibers, caused by the pyro-gasification process. Probably, this led to a reduction of fiber diameter, and thus lower mechanical properties. Furthermore, *table 9* shows that the standard deviation of the average storage modulus, calculated from 3 repetitions of the analysis, is particularly high for PLA-V10 and PLA-R10 samples. A possible cause may be the higher roughness and less stable diameter of the filament containing 10 wt% of carbon fibers (*figure 35*). This increases the difficulty to accurately measure the diameter using a calibre and put the correct value into the software, resulting in higher storage modulus oscillations between different samples.



Figure 35. Optical microscope images of PLA-R5 (on the left) and PLA-R10 (on the right) filaments.

The ratio of the loss modulus (E'') to the storage modulus (E') is the $\tan\delta$ and is often called damping factor. It measures the ability of materials to dissipate energy as heat. *Figure 37* shows that the $\tan\delta$ peak of all the carbon fibers (both recycled and virgin) reinforced PLA filaments dramatically weakened and shifted to a higher temperature when compared to neat PLA. The reduction in the intensity of $\tan\delta$ peak is probably produced by the restriction in chain mobility of PLA by the presence of carbon fibers (stiffening effect)¹⁷⁶. This is an evidence of good interaction between the reinforcement and PLA matrix and, as can be seen from the DMA spectra, the effect is displayed by both virgin and recycled carbon fibers. Furthermore, $\tan\delta$ peak temperature can be considered as a measure of glass transition temperature T_g . The last column of *table 9* shows an increment of $\tan\delta$ peak temperature corresponding to composites with higher CF load. This result confirms that the presence of carbon fibers reduces the mobility of PLA macromolecular chains.

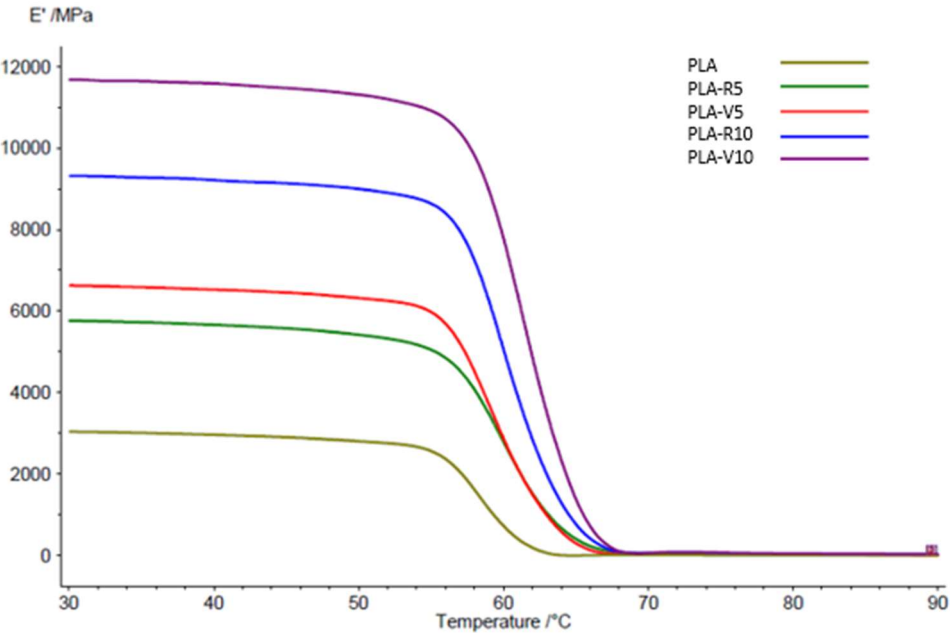


Figure 36. Storage modulus (E') of filaments vs temperature.

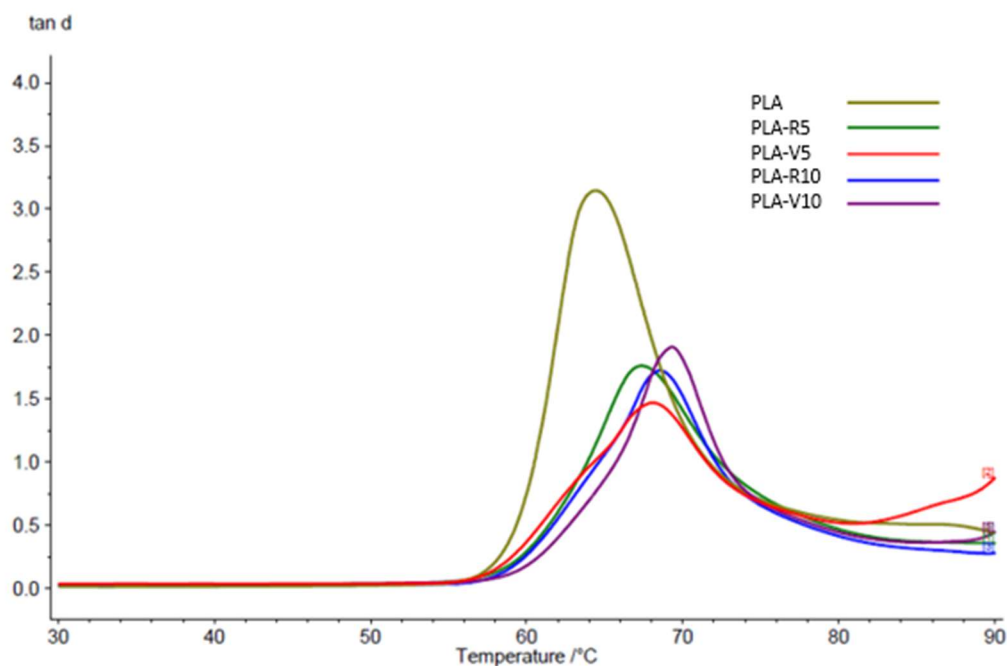


Figure 37. Damping factor ($\tan\delta$) of filaments vs temperature.

Table 9. DMA results of filaments.

	E'30°C (MPa)	Onset (°C)	Tan δ (°C)
PLA	3100 \pm 400	56 \pm 1	65 \pm 1
PLA-V5	6500 \pm 300	56 \pm 0	68 \pm 1
PLA-V10	10000 \pm 1500	58 \pm 0	69 \pm 0
PLA-R5	5900 \pm 400	57 \pm 0	67 \pm 0
PLA-R10	9200 \pm 1100	58 \pm 1	69 \pm 0

Moreover, the obtained filaments have been characterized using Differential Scanning Calorimetry (DSC). The obtained thermograms are shown in *figure 38* and results are summarized in *table 10*. It can be seen that the glass transition temperature (T_g) is not significantly affected by the presence of carbon fibers. In addition, all the curves except that corresponding to PLA native pellets show a negative peak after 100°C. This peak corresponds to the heat generated during the cold crystallization process, which is a crystallization phenomenon that occurs during heating ramps and starts at a temperature above T_g , when rotational movements of macromolecular chains become possible. PLA pellets do not present cold crystallization because they have already developed their maximum crystallinity (χ) before

the analysis, as can be seen from the last column of *table 10*. On the other hand, samples obtained in filament shape via extrusion, they all present cold crystallization because the filament production process involves rapid cooling of the extrudate, which leaves the material in an amorphous state. Furthermore, the χ column of *table 10* shows that the crystallinity of neat PLA filament is slightly higher than that of reinforced filaments. The reason could be attributed to the thermal conductivity of carbon fibers. Probably pure PLA, being less thermal conductive than CF reinforced PLA, can dissipate less heat during the extrusion process to obtain the filament. Thus, the cooling is less rapid and the material has more time to develop crystallinity. Comparing T_{cr} and ΔH_{cr} values of neat PLA and reinforced PLA (PLA-R5, PLA-V5, PLA-R10, PLA-V10) it is evident that the addition of recycled or virgin carbon fibers causes a decrement of cold crystallization temperature, along with an increment of crystallization enthalpy. This can be explained considering the nucleating effect of carbon fibers, which promotes the crystallization process ¹⁷⁷. This effect could be exploited to reduce the annealing time and temperature, considering that introducing carbon fibers, crystallization becomes faster. Carbon fibers seem to alter also the melting process. In fact, filaments containing CFs have, as shown in *table 10*, lower melting temperatures. This can be explained by taking into account the thermal conductivity of carbon fibers, which makes the material heating more efficiently, resulting in lower T_m values. Moreover, as depicted in *figure 38*, the PLA-V5 thermogram shows a double endothermic peak at about 150 °C, which corresponds to the melting process of the material. The presence of a double peak could be due to the presence of two crystalline domains, characterized by crystallites of different dimensions, which consequently melt at different temperatures. Furthermore, all the curves corresponding to the filaments show an endothermic peak at the same temperature of the T_g (around 55 °C). This peak represents an enthalpic stress relaxation accumulated during the production process of the filaments.

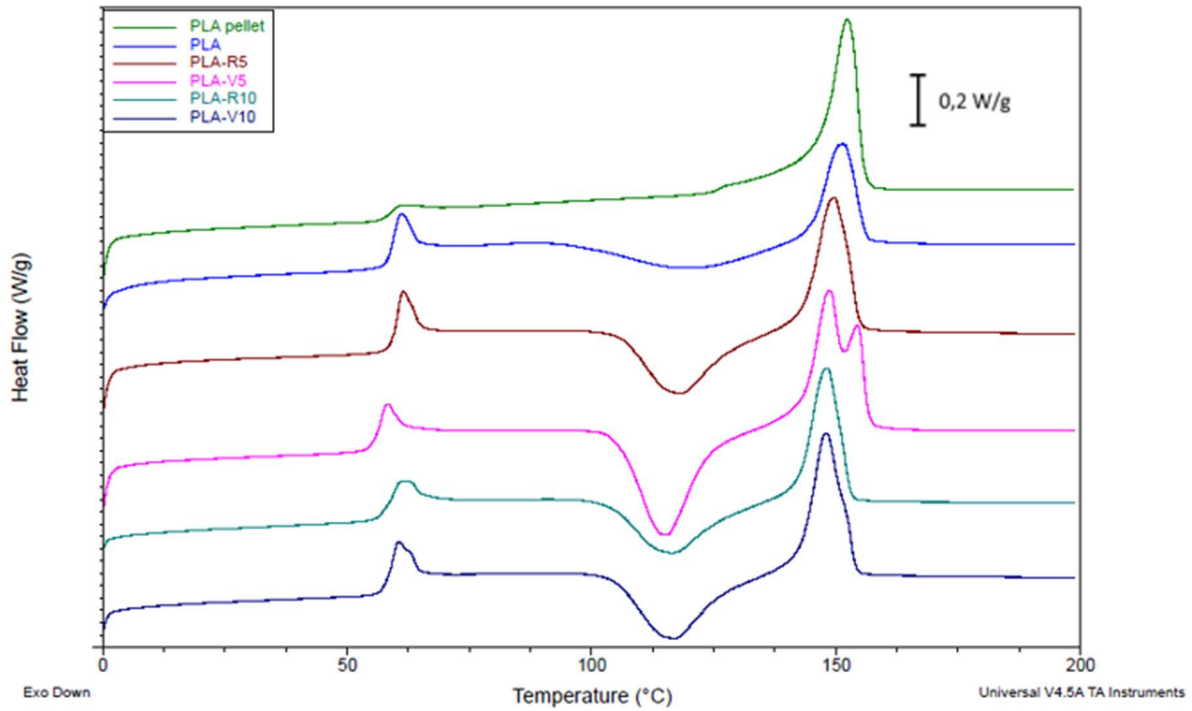


Figure 38. DSC thermograms of filaments (1st heating scan).

Table 10. DSC results of filaments (1st heating scan).

	T_g (°C)	T_{cr} (°C)	ΔH_{cr} (J/g)	T_m (°C)	ΔH_m (J/g)	χ (%)
PLA pellet	59 ± 1	x	0	153 ± 1	$36,0 \pm 0,1$	38 ± 0
PLA	56 ± 1	120 ± 1	15 ± 1	152 ± 1	$18,3 \pm 0,4$	3 ± 1
PLA-V5	54 ± 1	116 ± 1	34 ± 1	148 ± 1	$35,0 \pm 0,3$	1 ± 1
PLA-V10	56 ± 0	117 ± 1	27 ± 0	148 ± 0	$28,6 \pm 0,4$	1 ± 1
PLA-R5	56 ± 0	118 ± 0	26 ± 1	149 ± 1	$27,3 \pm 0,5$	1 ± 1
PLA-R10	56 ± 0	116 ± 0	25 ± 0	148 ± 0	$25,0 \pm 0,4$	1 ± 0

DSC equipment has been also used to measure the specific heat capacity (C_p) of the produced filaments. In particular, C_p value at 30°C has been determined. The specific heat capacity represents the amount of heat that has to be provided to 1 gram of the material in order to cause an increase of 1 °C in its temperature. Considering that carbon fibers are characterized by high thermal conductivity, composites containing CFs are supposed to need less heat to raise their temperature, resulting in lower C_p values. This trend can be clearly observed in *figure 39* and *table 11*, which show that PLA composite filaments containing higher carbon fibers weight fractions have lower values of specific heat capacity.

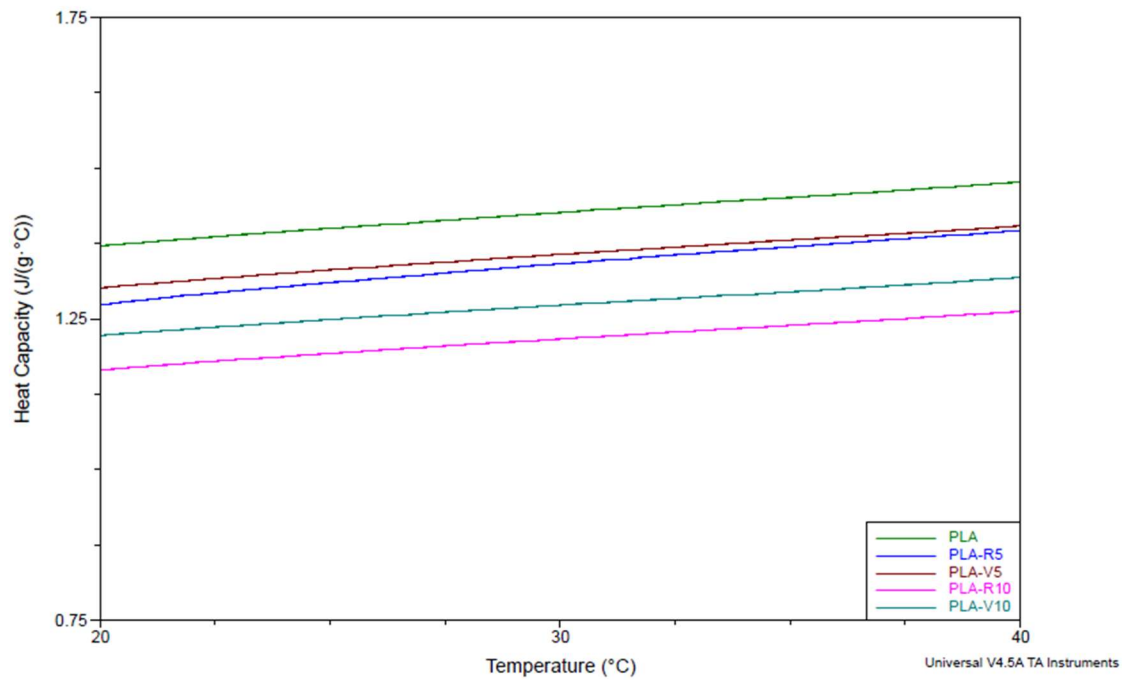


Figure 39. Cp thermograms of filaments.

Table 11. Cp values of filaments at 30°C.

	C_{P,30°C} (J/°C*g)
PLA	1,40 ± 0,07
PLA-V5	1,36 ± 0,01
PLA-V10	1,26 ± 0,04
PLA-R5	1,34 ± 0,08
PLA-R10	1,20 ± 0,05

3.3 3D printing of carbon fiber reinforced PLA

The 3D printer has been used to print DMA specimens, TMA specimens, and dog-bones for mechanical testing (*fig. 40*) starting from neat PLA filament and PLA-R5 filament, containing 5 wt% of recycled carbon fibers. The first step consisted in creating a digital model of the specimens, using the software CAD Inventor and then importing it in the slicer software Simplify 3D, which is interfaced with the printer. Subsequently, using the slicer software all the printing parameters have been optimized to obtain an accurate printing process. Dogbones for mechanical testing have been produced with two different filament deposition patterns, in particular the one at 0° involves filament deposition along the same direction of the applied

load during further mechanical testing, while the 90° sample has filament deposition perpendicular to the specimen drawing in mechanical tests. DMA and TMA specimens instead were all produced with 0° filament orientation.

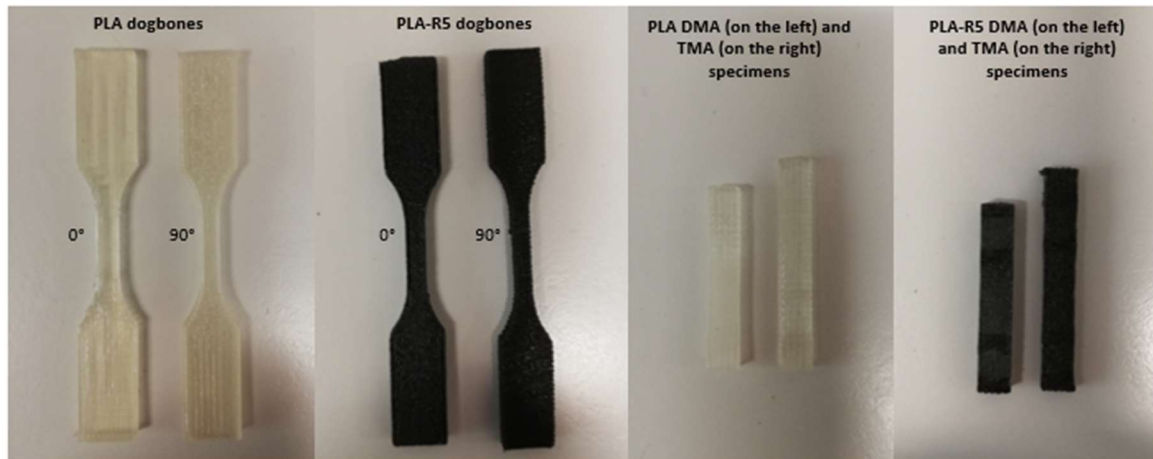


Figure 40. neat PLA and PLA-R5 printed specimens.

3.4 3D-printed specimens characterization

Thermal properties of the printed specimens have been determined by DSC analysis analogously to the previously discussed filament characterization. First scan thermograms are shown in *figure 41* and results summarized in *table 12*. Analyzing the curves and the obtained results, it can be noted that thermal properties of printed specimens are quite similar to those of filaments. Both neat PLA and PLA-R5 curves are characterized by an endothermic peak superimposed to the T_g step. This peak, as in the case of the filaments, corresponds to an enthalpic relaxation of stress accumulated during the manufacturing process. Moreover, comparing ΔH_{cr} of neat PLA and PLA-R5, it can be confirmed that carbon fibers act as nucleating sites, enhancing the cold crystallization process that takes place during the heating scan. It can be also noticed from the last column of *table 12* that printed specimens are almost totally amorphous. The low crystallinity is caused, as in the case of filament production, by the extrusion process, which leads to rapid cooling of the extruded material.

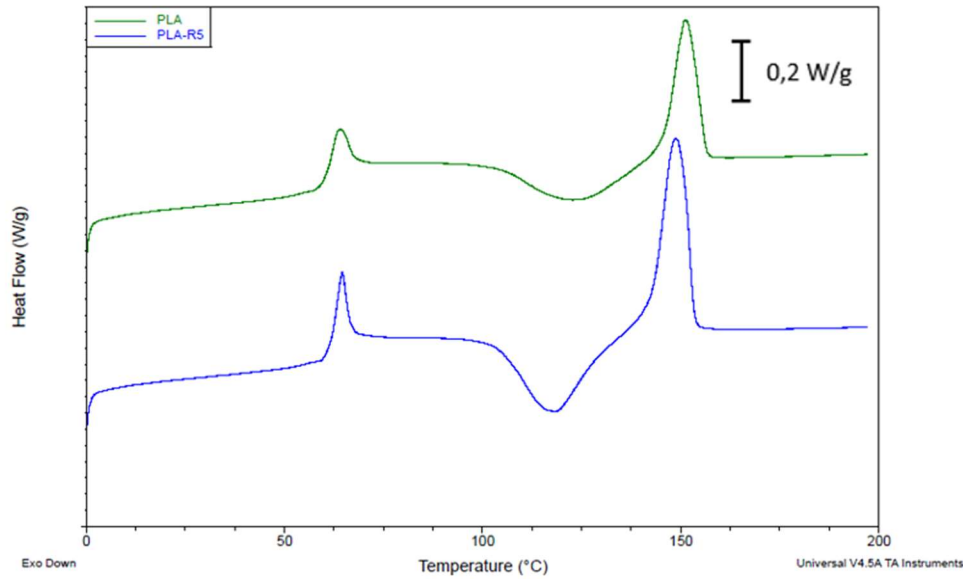


Figure 41. DSC thermograms of printed specimens (1st heating scan).

Table 12. DSC results of printed specimens (1st heating scan)

	T_g (°C)	T_{cr} (°C)	ΔH_{cr} (J/g)	T_m (°C)	ΔH_m (J/g)	χ (%)
PLA	59 ± 1	120 ± 4	18 ± 7	150 ± 2	21 ± 5	4 ± 2
PLA-R5	58 ± 1	120 ± 4	22 ± 7	149 ± 1	25 ± 8	3 ± 1

Dynamic mechanical analysis (DMA) has been carried out to evaluate the viscoelastic properties of printed specimens. *Figure 42* shows that the storage modulus (E') of the composite containing 5 wt% of recycled carbon fibers is, as expected, higher than that of neat PLA. This clearly demonstrates the stiffening effect of recycled carbon fibers on the PLA matrix. Furthermore, the onset temperature of modulus drop shifted from 58°C to 60°C, as it can be observed from *table 13*. Thus, the printed material containing Re-CFs is characterized by a slightly broader range of temperatures in which mechanical properties remain unaltered. $\tan \delta$ curves are shown in *figure 43*. As can be seen, the incorporation of recycled carbon fibers produces a decrement and a concomitant shift of the damping factor peak. The $\tan \delta$ value decrease is a result of the stiffening of the system, which limits the material capability to dissipate energy as heat. The peak temperature shift indicates that carbon fibers probably reduce the chain mobility of PLA.

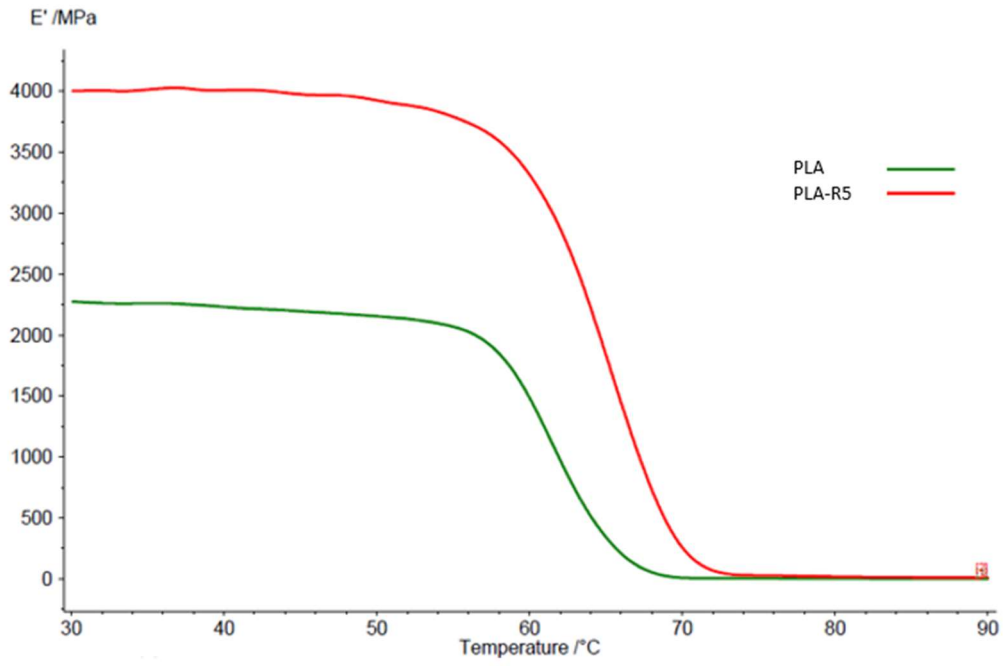


Figure 42. Storage modulus (E') of printed specimens.

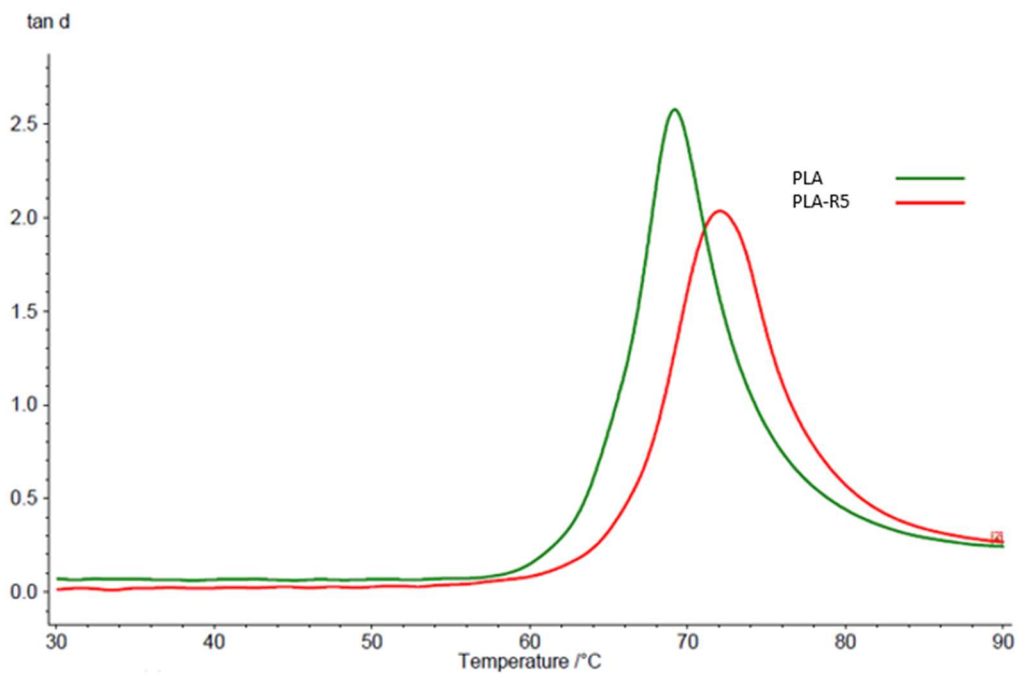


Figure 43. Damping factor ($\tan\delta$) of printed specimens.

Table 13. DMA results of printed specimens.

	E'30°C (MPa)	Onset (°C)	Tan δ (°C)
PLA	2300 ± 400	58 ± 0	69 ± 0
PLA-R5	3800 ± 300	60 ± 0	72 ± 0

DMA has also been conducted setting TMA mode, in order to obtain the Coefficient of Thermal Expansion (CTE) of printed specimens. Therefore, samples clamped in tensile mode have been subjected to a temperature ramp and the probe displacement (dL) along the longer dimension of the specimen has been measured applying an almost null force during the analysis. The dL derivative with respect to the temperature, normalized with respect to the specimen initial length ($dL/dT \cdot L_0$), represents the CTE of the material. *Figure 44* shows two consecutive thermograms of the same PLA-R5 specimen. The curve corresponding to the first heating scan shows an expansion until a temperature close to its T_g , where a peak is observed, after which the material starts to contract. This trend is caused by the relaxation of internal stresses¹⁷⁸, which is a phenomenon that occurs heating printed specimens, as already noted from the DSC thermograms. Therefore, the contraction is probably due to the likeliness of macromolecular chains, previously oriented by the extrusion process, to return in random coil conformation. The curve corresponding to the second heating scan, does not show the same behaviour, indicating that the stress previously detected has been relaxed and the thermal history of the material has been canceled. *Figure 45* shows dL curves of neat PLA and PLA-R5 and the corresponding CTE values, that are also listed in *table 14*. As expected, being carbon fibers dimensionally stable in a broad range of temperatures, the printed composite containing 5 wt% of recycled carbon fibers (PLA-R5) is characterized by lower CTE at temperatures below about 65 °C, where the analysis loses significance due to stress relaxation. The observed CTE trend has a strong relevance when 3D printing is involved, since the dimensional stability of the polymer during the printing process is a key factor in producing items with good dimensional accuracy and further thermal stability.

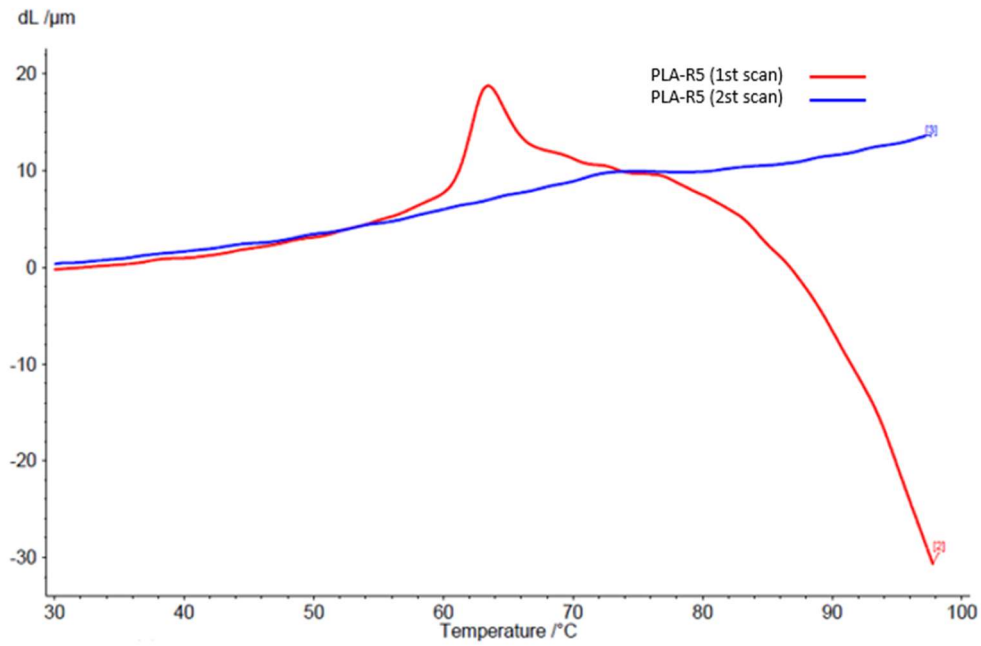


Figure 44. TMA (dL curves) of printed PLA-R5 (1st and 2nd scan)

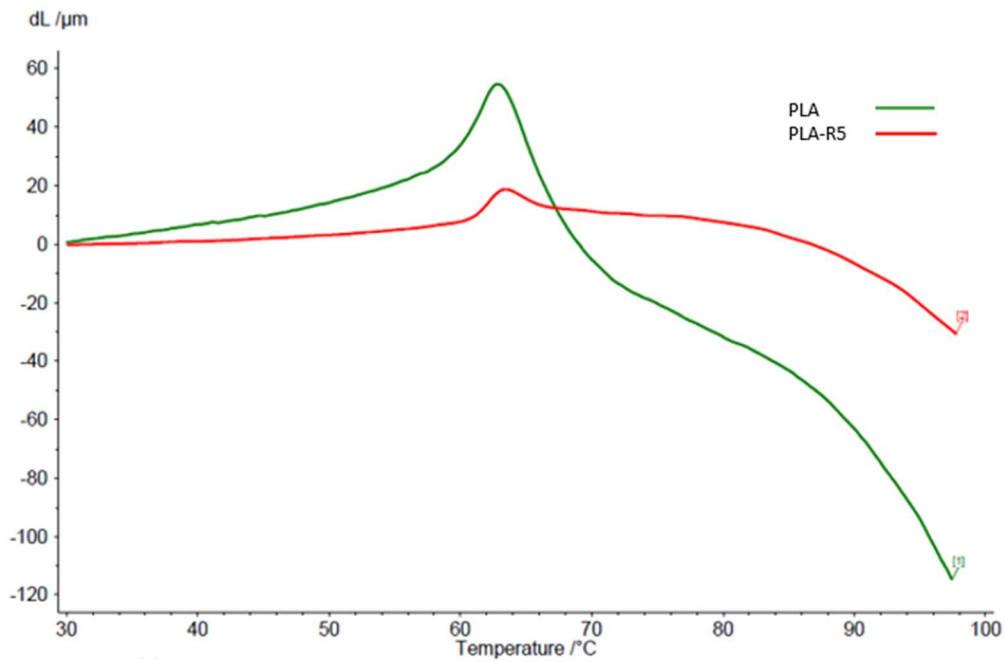


Figure 45. TMA (dL curves) of printed specimens

Table 14. TMA results of printed specimens

	CTE ($10^{-6}/K$)			
	30 °C	40 °C	50 °C	60 °C
PLA	40 ± 10	68 ± 8	110 ± 6	520 ± 50
PLA-R5	20 ± 10	7 ± 2	22 ± 2	130 ± 10

Finally, 3D printed dogbones have been subjected to tensile tests in order to determine their mechanical properties. The collected data have been treated to obtain a stress-strain curve (*fig. 46*), from which Young's Modulus (E), maximum stress, stress at break (σ_b), and elongation at break (ϵ_b) have been calculated. Obtained results have been collected in *table 15*. Comparing curves of neat PLA and PLA-R5 dogbones printed with a deposition angle of 0° , it can be seen that PLA-R5 has a higher modulus and reaches lower values of deformation before breaking, confirming the stiffening effect of recycling carbon fibers on PLA matrix. However, PLA-R5 also reaches lower values of maximum stress compared to neat PLA. This effect could be explained by the presence of a greater quantity of voids inside the printed object, which is probably caused by the presence of recycled carbon fibers and by the rougher surface of the filament. Voids act as stress-concentration points, lowering the maximum stress that the material can bear. Furthermore, curves clearly show a difference between specimens printed with 0° orientations, which have the extruded filament aligned along the load direction, and specimens with 90° orientation: the difference however is minor for neat PLA, while the inclusion of a reinforcement in the filament strongly affect the anisotropy of the system. For both neat PLA and PLA-R5, the dogbone printed with a deposition angle of 0° reaches higher values of maximum stress thanks to the macromolecular orientation along the direction of the applied stress. For PLA-R5, the difference between the two types of specimens is much more evident. In fact, the PLA-R5 dogbone with 90° orientation shows plastic deformation starting at about 6% of strain and reaching values even higher than those reached by neat PLA. The cause of this behavior could be attributed to a scarce interface adhesion between adjacent layers, possibly owing to a partial alignment contribution of the filler component too. Thus, at a stress corresponding to the maximum stress of the curve, layers along the longitudinal direction of the dogbone could begin to detach, leading to plastic deformation. This behavior is not present in the neat PLA specimen printed with a deposition angle of 90° and, therefore, it could be deduced that the presence of recycled carbon fibers increases the anisotropy at the filament level together as decreasing the interlayer adhesion of the printed part.

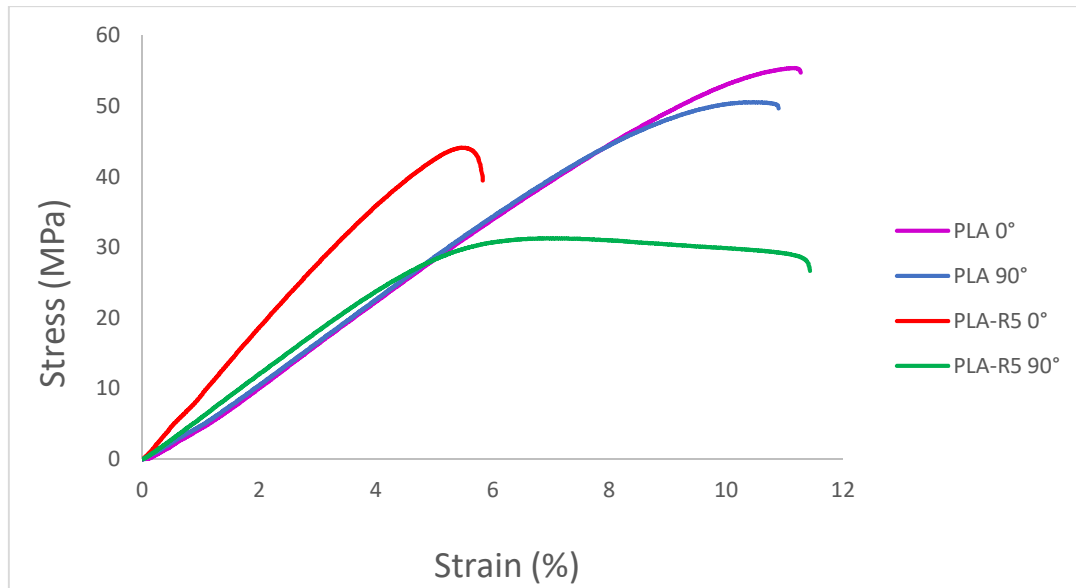


Figure 46. Stress-strain curve of printed dogbones.

Table 15. Tensile test results of dogbones.

	Deposition angle	E (GPa)	Max stress (MPa)	σ_b (MPa)	ϵ_b (%)
PLA	0°	0,62 ± 0,07	55 ± 5	54 ± 6	11 ± 1
	90°	0,61 ± 0,03	50 ± 3	48 ± 4	12 ± 2
PLA-R5	0°	0,96 ± 0,02	45 ± 1	39 ± 1	7 ± 0
	90°	0,62 ± 0,05	33 ± 4	27 ± 5	12 ± 2

4. Conclusions

This thesis work aimed to produce an innovative 3D printable recycled carbon fiber reinforced PLA composite. For this purpose, PLA composite filaments containing different weight fractions of recycled or virgin carbon fibers have been initially produced and characterized. TGA analysis confirmed that the desired reinforcement weight fraction (5 or 10 wt%) has been obtained and demonstrated a slight improvement in PLA thermal stability upon incorporation of carbon fibers. The average length of fibers contained in the filament has been measured with an optical microscope after having dissolved the matrix, showing that the production process led to fiber breakage down to 200 μ m. DSC showed that carbon fibers promote the crystallization of PLA thanks to their nucleating effect. Furthermore, all the analyzed filaments resulted mainly amorphous, probably because of the fast cooling of the extruded during the filament production. Moreover, carbon fibers have been proved to decrease the specific heat capacity (C_p) of PLA. Filaments have also been subjected to DMA and the results demonstrate that the stiffening effect of recycled carbon fibers is comparable to that of virgin carbon fibers. Since no significant difference between virgin and recycled fibers were observed after characterization, neat PLA filament and PLA filament containing 5 wt% of recycled carbon fibers have been used to print dogbones for tensile tests and specimens for DMA and TMA. Dynamic mechanical analysis showed that the addition of recycled carbon fibers results in printed objects characterized by increased stiffness. Moreover, TMA has also been conducted, demonstrating that the coefficient of thermal expansion of printed specimens decreases with the incorporation of recycled carbon fibers. Further investigation of thermal properties has been carried out subjecting samples taken from dogbones to DSC. As in the case of filaments, the crystallinity of printed objected resulted very low. Finally, tensile tests have been run and the results showed that dogbones printed starting from recycled carbon fiber reinforced PLA are effectively stiffer than neat PLA printed dogbones. However, the introduction of recycled carbon fibers produced a decrease in the maximum stress that the material can bear, probably due to an increment of voids quantity inside the printed object. Dogbone specimens printed with a deposition angle of 90° have been also analyzed and in the case of PLA reinforced with recycled carbon fibers plastic deformation, probably caused by low interfacial adhesion between adjacent filaments, has been observed.

5. Experimental procedure

Carbon fibers pre-treatment

The de-sizing process of virgin carbon fibers (Toray T700S 12K) has been carried out by washing the fibers in an acetone bath at reflux for 48h. The recycled carbon fibers, deriving from pyro-gasification of epoxy composite cured samples carried out by Curti s.p.a., have been manually treated to remove the char. Furthermore, both virgin and recycled carbon fibers have been cut with a chopper-gun to produce short 7 mm CFs.

Production of composite filament

Before the compounding step itself, carbon fibers and PLA pellets (Ingeo™ 4043D) have been dried in a vacuum oven set at a temperature of 70 °C for about 16-20 h. Subsequently, fibers (virgin or recycled) and PLA pellets have been weighted using a technical scale to obtain the desired weight fraction in the composite (PLA-R5, PLA-V5, PLA-R10, or PLA-V10). To carry out the compounding step, a twin-screw mixer PLASTI-CORDER® (Brabender™, Germany) has been set at a temperature of 190 °C. The PLA pellets have been fed into the mixer and, after 4 minutes, carbon fibers have been added. The mixing process continued for 8 minutes. After completion, a spatula has been used to remove the produced composite from the screws. The obtained pieces of carbon fiber reinforced PLA composite have been fed into an electric grinding machine (Brabender™, Germany) to obtain pellets. An Advanced 4.0 (3Devo, The Netherlands) single-screw extruder (*fig. 47*) has been used to process composite pellets and neat PLA pellets in order to obtain filaments with an average diameter of 1.75 mm

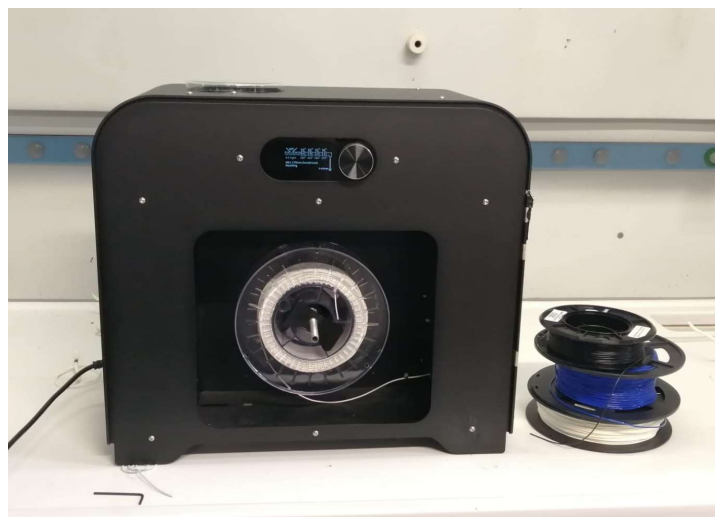


Figure 47. Advanced 4.0 single-screw extruder.

3D printing

A Mustang M400 3D printer (fig. 48) has been used to print dog bones (ASTM D638 TYPE V normative), DMA specimens (25x4,50x2,75 mm), and TMA specimens (30x4,30x2 mm), starting from neat PLA and PLA-R5 filaments. The digital model of the printed objects has been created using the software CAD Inventor and then imported into the slicing program Simplify 3D, which is interfaced with the 3D printer. The printing parameters used for all samples in this study are detailed in *table 16*. All the dogbone samples were printed with an external shell around their perimeter. Furthermore, two series of dogbones have been printed: one with a deposition angle of 0° and the other with a deposition angle of 90°. A 100% infill has been used for all the samples.

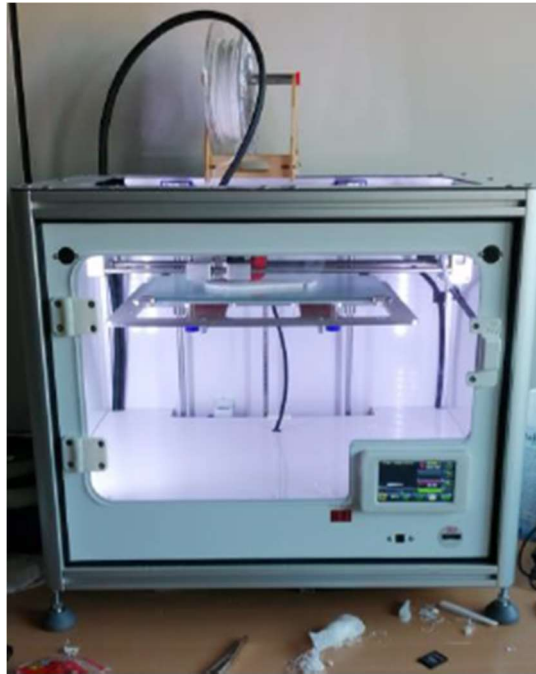


Figure 48. Mustang M400 3D printer

Table 16. Printing parameters.

Nozzle size	0,4 mm
Extruder temperature	230 °C
Bed temperature	60 °C
Printing speed	10 mm/s
Layer height	0,2 mm
Infill percentage	100%

Filaments and 3D printed specimens characterization

To determine the average length of fibers contained in the filaments the latter have been first put in beakers containing CHCl_3 for 8 hours to dissolve the matrix. Then the obtained suspensions of fibers have been filtered and the recovered fibers have been dried for 48 hours. After that, fibers have been weighted with an analytical scale and then analyzed with an optical microscope (Zeiss, Germany).

The thermogravimetric analysis of commercial PLA filament and CF reinforced PLA filaments has been conducted with a TGA model Q600 (TA Instrument, USA). Samples have been obtained cutting small pieces of filament and have been placed into platinum crucibles. The following method has been utilized: ramp $20\text{ }^\circ\text{C}/\text{min}$ to $500\text{ }^\circ\text{C}$; isothermal for 15 minutes; ramp $20\text{ }^\circ\text{C}/\text{min}$ to $300\text{ }^\circ\text{C}$; gas switch N_2/air ; isothermal for 5 minutes; ramp $10\text{ }^\circ\text{C}/\text{min}$ to 500 ; isothermal for 30 minutes. The carbon fibers weight percentage has been calculated at the end of the first ramp to $500\text{ }^\circ\text{C}$.

Thermal properties of filaments and printed specimens have been evaluated using a differential scanning calorimetry DSC Q2000 (TA Instrument, USA). Samples have been prepared weighting material quantities of 3-5 mg with an analytical scale and placing them into aluminum pans. The following method has been utilized to analyze filaments and pellets: ramp $10\text{ }^\circ\text{C}/\text{min}$ from 0°C to $200\text{ }^\circ\text{C}$; ramp $10\text{ }^\circ\text{C}/\text{min}$ to 0°C ; ramp $10\text{ }^\circ\text{C}/\text{min}$ to 200 . Printed specimens have been analyzed setting a single ramp $10\text{ }^\circ\text{C}/\text{min}$ from $0\text{ }^\circ\text{C}$ to $200\text{ }^\circ\text{C}$.

The DSC has also been used to measure the heat capacity at constant pressure (C_p) of the materials. The analysis has been conducted with a temperature ramp of $10\text{ }^\circ\text{C}/\text{min}$ from $10\text{ }^\circ\text{C}$ to $50\text{ }^\circ\text{C}$ and a sampling interval of 1 sec/pt. The C_p value has been measured at an intermediate temperature of $30\text{ }^\circ\text{C}$. Before starting the analysis, the DSC has been calibrated using a sapphire.

The dynamic mechanical analysis of both filaments and printed specimens has been carried out using a DMA model 242 E Artemis (Netzsch, Germania). The DMA has been equipped with tensile geometry and caliber has been used to obtain the dimensions of each sample. Tests have been run starting from a temperature of $30\text{ }^\circ\text{C}$ and reaching a temperature of $100\text{ }^\circ\text{C}$ with a ramp of $3\text{ }^\circ\text{C}/\text{min}$ and applying an oscillation frequency of 1 Hz.

The coefficient of thermal expansion (CTE) has been measured using the DMA pre-setted in TMA mode, using a tensile geometry. Printed specimens have been subjected to a static force of 0,05 N during a temperature ramp of $3\text{ }^\circ\text{C}/\text{min}$ from $30\text{ }^\circ\text{C}$ to $100\text{ }^\circ\text{C}$ and the probe

displacement (dL) has been measured. The derivate $dL/(dT*L_0)$ represents the CTE. The analysis required calibration in TMA mode, which has been done using a steel specimen.

Mechanical properties of printed specimens (dogbones) have been measured using a dynamometer Remet TC10, with a load cell of 1 kN. Tensile tests have been run following the ASTM D638 TYPE V normative, setting the strain rate to 1 mm/min. The produced data (applied stress and crosshead displacement) has been treated and normalized using the cross-section area and the length of the reduced section of the specimens to obtain the stress-strain curves, from which elastic modulus (E), ultimate strength (σ), stress at break (σ_b), and elongation at break (ϵ_b) have been calculated.

Bibliography

1. Chung, D. D. L., Processing-structure-property relationships of continuous carbon fiber polymer-matrix composites. *Materials Science and Engineering: R: Reports* **2017**, *113*, 1-29.
2. Koumoulos, E. P.; Trompeta, A.-F.; Santos, R.-M.; Martins, M.; Santos, C.; Iglesias, V.; Böhm, R.; Gong, G.; Chiminelli, A.; Verpoest, I.; Kiekens, P.; Charitidis, C. A., Research and Development in Carbon Fibers and Advanced High-Performance Composites Supply Chain in Europe: A Roadmap for Challenges and the Industrial Uptake. *Journal of Composites Science* **2019**, *3*, 86.
3. Naqvi, S. R.; Prabhakara, H. M.; Bramer, E. A.; Dierkes, W.; Akkerman, R.; Brem, G., A critical review on recycling of end-of-life carbon fibre/glass fibre reinforced composites waste using pyrolysis towards a circular economy. *Resources, Conservation and Recycling* **2018**, *136*, 118-129.
4. Witten, E.; Kraus, T.; Kühnel, M., Composite Market Report-Market developments, trends, outlook and challenges. *Study by AVK and Carbon Composites* **2016**.
5. Sauer, M.; Kühnel, M.; Witten, E.; Mathes, V., Composites market report 2018—market developments, trends, outlook and challenges. *Germany: AVK-TV Industrievereinigung verstrkte Kunststoffe Carbon Composite* **2018**.
6. Meng, F.; Olivetti, E. A.; Zhao, Y.; Chang, J. C.; Pickering, S. J.; McKechnie, J., Comparing Life Cycle Energy and Global Warming Potential of Carbon Fiber Composite Recycling Technologies and Waste Management Options. *ACS Sustainable Chemistry & Engineering* **2018**, *6* (8), 9854-9865.
7. Lefevvre, A.; Garnier, S.; Jacquemin, L.; Pillain, B.; Sonnemann, G., Anticipating in-use stocks of carbon fiber reinforced polymers and related waste flows generated by the commercial aeronautical sector until 2050. *Resources, Conservation and Recycling* **2017**, *125*, 264-272.
8. Hagnell, M.; Åkermo, M., The economic and mechanical potential of closed loop material usage and recycling of fibre-reinforced composite materials. *Journal of cleaner production* **2019**, *223*, 957-968.
9. Rybicka, J.; Tiwari, A.; Del Campo, P. A.; Howarth, J., Capturing composites manufacturing waste flows through process mapping. *Journal of Cleaner Production* **2015**, *91*, 251-261.
10. Shuaib, N. A.; Mativenga, P. T.; Kazie, J.; Job, S., Resource efficiency and composite waste in UK supply chain. *Procedia CIRP* **2015**, *29*, 662-667.
11. Hall, S., End-of-life recycling options for glass fibre reinforced polymers. **2016**.
12. Hadi, P.; Ning, C.; Ouyang, W.; Xu, M.; Lin, C. S.; McKay, G., Toward environmentally-benign utilization of nonmetallic fraction of waste printed circuit boards as modifier and precursor. *Waste Management* **2015**, *35*, 236-246.
13. Liu, P.; Meng, F.; Barlow, C. Y., Wind turbine blade end-of-life options: An eco-audit comparison. *Journal of Cleaner Production* **2019**, *212*, 1268-1281.
14. Pillain, B.; Loubet, P.; Pestalozzi, F.; Woidasky, J.; Erriguible, A.; Aymonier, C.; Sonnemann, G., Positioning supercritical solvolysis among innovative recycling and current waste management scenarios for carbon fiber reinforced plastics thanks to comparative life cycle assessment. *Journal of Supercritical Fluids* **2019**, *154*.
15. Li, X.; Bai, R.; McKechnie, J., Environmental and financial performance of mechanical recycling of carbon fibre reinforced polymers and comparison with conventional disposal routes. *Journal of Cleaner Production* **2016**, *127*, 451-460.
16. Princaud, M.; Aymonier, C.; Loppinet-Serani, A.; Perry, N.; Sonnemann, G., Environmental Feasibility of the Recycling of Carbon Fibers from CFRPs by Solvolysis Using Supercritical Water. *ACS Sustainable Chemistry & Engineering* **2014**, *2* (6), 1498-1502.
17. Nunes, A. O.; Viana, L. R.; Guineheuc, P. M.; Moris, V. A. D.; de Paiva, J. M. F.; Barna, R.; Soudais, Y., Life cycle assessment of a steam thermolysis process to recover carbon fibers from carbon fiber-reinforced polymer waste. *International Journal of Life Cycle Assessment* **2018**, *23* (9), 1825-1838.
18. Witik, R. A.; Teuscher, R.; Michaud, V.; Ludwig, C.; Månson, J.-A. E., Carbon fibre reinforced composite waste: an environmental assessment of recycling, energy recovery and landfilling. *Composites Part A: Applied Science and Manufacturing* **2013**, *49*, 89-99.
19. Mazzocchetti, L.; Merighi, S.; Benelli, T.; Giorgini, L. In *Evaluation of Tryptophan-Late curing agent systems as hardener for epoxy resin*, AIP Conference Proceedings, AIP Publishing LLC: 2018; p 020170.

20. Auvergne, R.; Caillol, S.; David, G.; Boutevin, B.; Pascault, J.-P., Biobased thermosetting epoxy: present and future. *Chemical reviews* **2014**, *114* (2), 1082-1115.
21. Bobade, S. K.; Paluvai, N. R.; Mohanty, S.; Nayak, S., Bio-based thermosetting resins for future generation: a review. *Polymer-Plastics Technology and Engineering* **2016**, *55* (17), 1863-1896.
22. Mustapha, R.; Rahmat, A. R.; Abdul Majid, R.; Mustapha, S. N. H., Vegetable oil-based epoxy resins and their composites with bio-based hardener: a short review. *Polymer-Plastics Technology and Materials* **2019**, *58* (12), 1311-1326.
23. Baroncini, E. A.; Kumar Yadav, S.; Palmese, G. R.; Stanzione III, J. F., Recent advances in bio-based epoxy resins and bio-based epoxy curing agents. *Journal of Applied Polymer Science* **2016**, *133* (45).
24. Solmi, S.; Rozhko, E.; Malmusi, A.; Tabanelli, T.; Albonetti, S.; Basile, F.; Agnoli, S.; Cavani, F., The oxidative cleavage of trans-1, 2-cyclohexanediol with O₂: Catalysis by supported Au nanoparticles. *Applied Catalysis A: General* **2018**, *557*, 89-98.
25. Paone, E.; Tabanelli, T.; Mauriello, F., The rise of lignin biorefinery. *Current Opinion in Green and Sustainable Chemistry* **2020**, *24*, 1-6.
26. Tabanelli, T.; Paone, E.; Blair Vásquez, P.; Pietropaolo, R.; Cavani, F.; Mauriello, F., Transfer Hydrogenation of Methyl and Ethyl Levulinate Promoted by a ZrO₂ Catalyst: Comparison of Batch vs Continuous Gas-Flow Conditions. *ACS Sustainable Chemistry & Engineering* **2019**, *7* (11), 9937-9947.
27. Sisti, L.; Belcari, J.; Mazzocchetti, L.; Totaro, G.; Vannini, M.; Giorgini, L.; Zucchelli, A.; Celli, A., Multicomponent reinforcing system for poly (butylene succinate): composites containing poly (l-lactide) electrospun mats loaded with graphene. *Polymer Testing* **2016**, *50*, 283-291.
28. Mazzocchetti, L.; Sandri, S.; Scandola, M.; Bergia, A.; Zuccheri, G., Radiopaque organic-inorganic hybrids based on poly (D, L-lactide). *Biomacromolecules* **2007**, *8* (2), 672-678.
29. Sisti, L.; Totaro, G.; Vannini, M.; Giorgini, L.; Ligi, S.; Celli, A., Bio-based PA11/graphene nanocomposites prepared by in situ polymerization. *Journal of nanoscience and nanotechnology* **2018**, *18* (2), 1169-1175.
30. Giorgini, L.; Benelli, T.; Brancolini, G.; Mazzocchetti, L., Recycling of carbon fiber reinforced composites waste to close their Life Cycle in a Cradle-to-Cradle approach. *Current Opinion in Green and Sustainable Chemistry* **2020**, 100368.
31. Zhang, J.; Chevali, V. S.; Wang, H.; Wang, C. H., Current status of carbon fibre and carbon fibre composites recycling. *Composites Part B-Engineering* **2020**, 193.
32. Oliveux, G.; Dandy, L. O.; Leeke, G. A., Current status of recycling of fibre reinforced polymers: Review of technologies, reuse and resulting properties. *Progress in Materials Science* **2015**, *72*, 61-99.
33. Pickering, S. J., Recycling technologies for thermoset composite materials—current status. *Composites Part A: applied science and manufacturing* **2006**, *37* (8), 1206-1215.
34. Pimenta, S.; Pinho, S. T., Recycling carbon fibre reinforced polymers for structural applications: Technology review and market outlook. *Waste Management* **2011**, *31* (2), 378-392.
35. Gopalraj, S. K.; Kärki, T., A review on the recycling of waste carbon fibre/glass fibre-reinforced composites: fibre recovery, properties and life-cycle analysis. *Sn Applied Sciences* **2020**, *2* (3), 1-21.
36. Khurshid, M. F.; Hengstermann, M.; Hasan, M. M. B.; Abdkader, A.; Cherif, C., Recent developments in the processing of waste carbon fibre for thermoplastic composites - A review. *Journal of Composite Materials*.
37. Rybicka, J.; Tiwari, A.; Leeke, G. A., Technology readiness level assessment of composites recycling technologies. *Journal of Cleaner Production* **2016**, *112*, 1001-1012.
38. Holmes, M., Recycled carbon fiber composites become a reality. *Reinforced Plastics* **2018**, *62* (3), 148-153.
39. Amaechi, C. V.; Odijie, A. C.; Orok, E. O.; Ye, J., Economic aspects of fiber reinforced polymer composite recycling. **2020**.
40. Kaya, M., Recovery of metals and nonmetals from electronic waste by physical and chemical recycling processes. *Waste management* **2016**, *57*, 64-90.
41. Schinner, G.; Brandt, J.; Richter, H., Recycling carbon-fiber-reinforced thermoplastic composites. *Journal of Thermoplastic Composite Materials* **1996**, *9* (3), 239-245.

42. Roux, M.; Eguémann, N.; Dransfeld, C.; Thiébaud, F.; Perreux, D., Thermoplastic carbon fibre-reinforced polymer recycling with electrodynamical fragmentation: From cradle to cradle. *Journal of Thermoplastic Composite Materials* **2017**, *30* (3), 381-403.
43. Palmer, J.; Ghita, O. R.; Savage, L.; Evans, K. E., Successful closed-loop recycling of thermoset composites. *Composites Part A: Applied Science and Manufacturing* **2009**, *40* (4), 490-498.
44. Nekouei, R. K.; Pahlevani, F.; Rajarao, R.; Golmohammadzadeh, R.; Sahajwalla, V., Two-step pre-processing enrichment of waste printed circuit boards: Mechanical milling and physical separation. *Journal of cleaner production* **2018**, *184*, 1113-1124.
45. Wang, H.; Zhang, G.; Hao, J.; He, Y.; Zhang, T.; Yang, X., Morphology, mineralogy and separation characteristics of nonmetallic fractions from waste printed circuit boards. *Journal of Cleaner Production* **2018**, *170*, 1501-1507.
46. Pickering, S. J.; Kelly, R. M.; Kennerley, J.; Rudd, C.; Fenwick, N., A fluidised-bed process for the recovery of glass fibres from scrap thermoset composites. *Composites Science and Technology* **2000**, *60* (4), 509-523.
47. Jiang, G.; Pickering, S. J.; Walker, G. S.; Wong, K. H.; Rudd, C. D., Surface characterisation of carbon fibre recycled using fluidised bed. *Applied Surface Science* **2008**, *254* (9), 2588-2593.
48. Dong, P. A. V.; Azzaro-Pantel, C.; Cadene, A.-L., Economic and environmental assessment of recovery and disposal pathways for CFRP waste management. *Resources, Conservation and Recycling* **2018**, *133*, 63-75.
49. Mazzocchetti, L.; Benelli, T.; D'Angelo, E.; Leonardi, C.; Zattini, G.; Giorgini, L., Validation of carbon fibers recycling by pyro-gasification: The influence of oxidation conditions to obtain clean fibers and promote fiber/matrix adhesion in epoxy composites. *Composites Part a-Applied Science and Manufacturing* **2018**, *112*, 504-514.
50. Giorgini, L.; Benelli, T.; Mazzocchetti, L.; Leonardi, C.; Zattini, G.; Minak, G.; Dolcini, E.; Cavazzoni, M.; Montanari, I.; Tosi, C., Recovery of carbon fibers from cured and uncured carbon fiber reinforced composites wastes and their use as feedstock for a new composite production. *Polymer Composites* **2015**, *36* (6), 1084-1095.
51. Meng, F.; McKechnie, J.; Pickering, S. J., An assessment of financial viability of recycled carbon fibre in automotive applications. *Composites Part A: Applied Science and Manufacturing* **2018**, *109*, 207-220.
52. López, F. A.; Rodríguez, O.; Alguacil, F. J.; García-Díaz, I.; Centeno, T. A.; García-Fierro, J. L.; González, C., Recovery of carbon fibres by the thermolysis and gasification of waste prepreg. *Journal of analytical and applied pyrolysis* **2013**, *104*, 675-683.
53. Giorgini, L.; Leonardi, C.; Mazzocchetti, L.; Zattini, G.; Cavazzoni, M.; Montanari, I.; Tosi, C.; Benelli, T., Pyrolysis of fiberglass/polyester composites: recovery and characterization of obtained products. *FME Transactions* **2016**, *44* (4), 405-414.
54. Meyer, L. O.; Schulte, K.; Grove-Nielsen, E., CFRP-Recycling Following a Pyrolysis Route: Process Optimization and Potentials. *Journal of Composite Materials* **2009**, *43* (9), 1121-1132.
55. Onwudili, J. A.; Miskolczy, N.; Nagy, T.; Lipóczy, G., Recovery of glass fibre and carbon fibres from reinforced thermosets by batch pyrolysis and investigation of fibre re-using as reinforcement in LDPE matrix. *Composites Part B: Engineering* **2016**, *91*, 154-161.
56. Giorgini, L.; Benelli, T.; Leonardi, C.; Mazzocchetti, L.; Zattini, G.; Cavazzoni, M.; Montanari, I.; Tosi, C., EFFICIENT RECOVERY OF NON-SHREDDDED TIRES VIA PYROLYSIS IN AN INNOVATIVE PILOT PLANT. *Environmental Engineering & Management Journal (EEMJ)* **2015**, *14* (7).
57. Neri, E.; Passarini, F.; Vassura, I.; Berti, B.; Giorgini, L.; Zattini, G.; Tosi, C.; Cavazzoni, M., APPLICATION OF LCA METHODOLOGY IN THE ASSESSMENT OF A PYROLYSIS PROCESS FOR TYRES RECYCLING. *Environmental Engineering & Management Journal (EEMJ)* **2018**, *17* (10).
58. Mazzocchetti, L.; Benelli, T.; Zattini, G.; Maccaferri, E.; Brancolini, G.; Giorgini, L. In *Evaluation of carbon fibers structure and morphology after their recycling via pyro-gasification of CFRPs*, AIP Conference Proceedings, AIP Publishing LLC: 2019; p 020036.
59. Zattini, G.; Mazzocchetti, L.; Benelli, T.; Maccaferri, E.; Brancolini, G.; Giorgini, L. In *Mechanical Properties and Fracture Surface Analysis of Vinyl Ester Resins Reinforced with Recycled Carbon Fibres*, Key Engineering Materials, Trans Tech Publ: 2020; pp 110-115.

60. Kim, K. W.; Lee, H. M.; An, J. H.; Chung, D. C.; An, K. H.; Kim, B. J., Recycling and characterization of carbon fibers from carbon fiber reinforced epoxy matrix composites by a novel superheated-steam method. *Journal of Environmental Management* **2017**, *203*, 872-879.
61. Limburg, M.; Stockschläder, J.; Quicker, P., Thermal treatment of carbon fibre reinforced polymers (Part 1: Recycling). *Waste Management & Research* **2019**, *37* (1_suppl), 73-82.
62. Jody, B. J.; Pomykala, J. A.; Daniels, E. J.; Greminger, J. L., A process to recover carbon fibers from polymer-matrix composites in end-of-life vehicles. *JOM* **2004**, *56* (8), 43-47.
63. Asmatulu, E.; Twomey, J.; Overcash, M., Recycling of fiber-reinforced composites and direct structural composite recycling concept. *Journal of Composite Materials* **2014**, *48* (5), 593-608.
64. Lee, C.-K.; Kim, Y.-K.; Pruitichaiwiboon, P.; Kim, J.-S.; Lee, K.-M.; Ju, C.-S., Assessing environmentally friendly recycling methods for composite bodies of railway rolling stock using life-cycle analysis. *Transportation Research Part D: Transport and Environment* **2010**, *15* (4), 197-203.
65. Lee, S. H.; Choi, H. O.; Kim, J. S.; Lee, C. K.; Kim, Y. K.; Ju, C. S., Circulating flow reactor for recycling of carbon fiber from carbon fiber reinforced epoxy composite. *Korean Journal of Chemical Engineering* **2011**, *28* (2), 449-454.
66. Meng, F.; McKechnie, J.; Turner, T.; Wong, K. H.; Pickering, S. J., Environmental aspects of use of recycled carbon fiber composites in automotive applications. *Environmental science & technology* **2017**, *51* (21), 12727-12736.
67. Ma, J. H.; Wang, X. B.; Li, B.; Huang, L. N. In *Investigation on recycling technology of carbon fiber reinforced epoxy resin cured with amine*, Advanced materials research, Trans Tech Publ: 2009; pp 409-412.
68. Das, M.; Varughese, S., A novel sonochemical approach for enhanced recovery of carbon fiber from CFRP waste using mild acid-peroxide mixture. *ACS Sustainable Chemistry & Engineering* **2016**, *4* (4), 2080-2087.
69. Xu, P.; Li, J.; Ding, J., Chemical recycling of carbon fibre/epoxy composites in a mixed solution of peroxide hydrogen and N, N-dimethylformamide. *Composites science and technology* **2013**, *82*, 54-59.
70. Li, J.; Xu, P.-L.; Zhu, Y.-K.; Ding, J.-P.; Xue, L.-X.; Wang, Y.-Z., A promising strategy for chemical recycling of carbon fiber/thermoset composites: self-accelerating decomposition in a mild oxidative system. *Green Chemistry* **2012**, *14* (12), 3260-3263.
71. Das, M.; Chacko, R.; Varughese, S., An efficient method of recycling of CFRP waste using peracetic acid. *ACS Sustainable Chemistry & Engineering* **2018**, *6* (2), 1564-1571.
72. Morin, C.; Loppinet-Serani, A.; Cansell, F.; Aymonier, C., Near- and supercritical solvolysis of carbon fibre reinforced polymers (CFRPs) for recycling carbon fibers as a valuable resource: State of the art. *Journal of Supercritical Fluids* **2012**, *66*, 232-240.
73. Jiang, G.; Pickering, S. J.; Lester, E. H.; Warrior, N. A., Decomposition of epoxy resin in supercritical isopropanol. *Industrial & engineering chemistry research* **2010**, *49* (10), 4535-4541.
74. Piñero-Hernanz, R.; García-Serna, J.; Dodds, C.; Hyde, J.; Poliakov, M.; Cocero, M. J.; Kingman, S.; Pickering, S.; Lester, E., Chemical recycling of carbon fibre composites using alcohols under subcritical and supercritical conditions. *The Journal of Supercritical Fluids* **2008**, *46* (1), 83-92.
75. Harbers, T.; Ebel, C.; Drechsler, K.; Endres, A.; Muller, G., Highly Efficient Production and Characterization of CFRP Made from Recycled Carbon Fibers. *Sampe Journal* **2014**, *50* (3), 7-13.
76. Lawrence, C. A., *Fundamentals of spun yarn technology*. Crc Press: 2003.
77. Pimenta, S.; Pinho, S. T., The effect of recycling on the mechanical response of carbon fibres and their composites. *Composite Structures* **2012**, *94* (12), 3669-3684.
78. Dauguet, M.; Mantoux, O.; Perry, N.; Zhao, Y. F., Recycling of CFRP for high value applications: Effect of sizing removal and environmental analysis of the SuperCritical Fluid Solvolysis. *Procedia Cirp* **2015**, *29*, 734-739.
79. Altay, L.; Seki, Y.; Sever, K.; Sen, I.; Uysalman, T.; Atagur, M.; Seydibeyoglu, O.; Sarikanat, M., Effect of Compatibilizer on Morphology, Thermal and Mechanical Properties of Recycled Carbon Fiber Reinforced Polypropylene Composites. *Acta Physica Polonica A* **2018**, *134* (1), 196-199.
80. Altay, L.; Bozaci, E.; Atagur, M.; Sever, K.; Tantug, G. S.; Sarikanat, M.; Seki, Y., The effect of atmospheric plasma treatment of recycled carbon fiber at different plasma powers on recycled carbon fiber and its polypropylene composites. *Journal of Applied Polymer Science* **2019**, *136* (9).

81. Lee, H.; Ohsawa, I.; Takahashi, J., Effect of plasma surface treatment of recycled carbon fiber on carbon fiber-reinforced plastics (CFRP) interfacial properties. *Applied Surface Science* **2015**, *328*, 241-246.
82. Lee, H.; Wei, H. W.; Takahashi, J., The influence of plasma in various atmospheres on the adhesion properties of recycled carbon fiber. *Macromolecular Research* **2015**, *23* (11), 1026-1033.
83. Chen, Y.; Wang, X. D.; Wu, D. Z., Recycled carbon fiber reinforced poly(butylene terephthalate) thermoplastic composites: fabrication, crystallization behaviors and performance evaluation. *Polymers for Advanced Technologies* **2013**, *24* (4), 364-375.
84. Feng, N.; Wang, X. D.; Wu, D. Z., Surface modification of recycled carbon fiber and its reinforcement effect on nylon 6 composites: Mechanical properties, morphology and crystallization behaviors. *Current Applied Physics* **2013**, *13* (9), 2038-2050.
85. Greco, A.; Maffezzoli, A.; Buccoliero, G.; Caretto, F.; Cornacchia, G., Thermal and chemical treatments of recycled carbon fibres for improved adhesion to polymeric matrix. *Journal of Composite Materials* **2013**, *47* (3), 369-377.
86. Han, H. Y.; Wang, X. D.; Wu, D. Z., Preparation, crystallization behaviors, and mechanical properties of biodegradable composites based on poly(L-lactic acid) and recycled carbon fiber. *Composites Part a-Applied Science and Manufacturing* **2012**, *43* (11), 1947-1958.
87. Han, H. Y.; Wang, X. D.; Wu, D. Z., Mechanical properties, morphology and crystallization kinetic studies of bio-based thermoplastic composites of poly(butylene succinate) with recycled carbon fiber. *Journal of Chemical Technology and Biotechnology* **2013**, *88* (7), 1200-1211.
88. Nie, W. Z.; Qi, K.; Li, S. F.; Zhang, L. J., Mechanical enhancement, morphology, and crystallization kinetics of polyoxymethylene-based composites with recycled carbon fiber. *Journal of Thermoplastic Composite Materials* **2016**, *29* (7), 935-950.
89. Qian, Z. Q.; Wang, Y. T.; Li, J. H.; Wang, X. D.; Wu, D. Z., Development of sustainable polyoxymethylene-based composites with recycled carbon fibre: mechanical enhancement, morphology, and crystallization kinetics. *Journal of Reinforced Plastics and Composites* **2014**, *33* (3), 294-309.
90. Huan, X. H.; Shi, K.; Yan, J. Q.; Lin, S.; Li, Y. J.; Jia, X. L.; Yang, X. P., High performance epoxy composites prepared using recycled short carbon fiber with enhanced dispersibility and interfacial bonding through polydopamine surface-modification. *Composites Part B-Engineering* **2020**, *193*.
91. Li, M. G.; Li, S. Q.; Liu, J.; Wen, X.; Tang, T., Striking effect of epoxy resin on improving mechanical properties of poly(butylene terephthalate)/recycled carbon fibre composites. *Composites Science and Technology* **2016**, *125*, 9-16.
92. Montes, S. M. G.; Ibarra, R. M.; Loera, A. F. G., Carbon nanotubes synthesized on the surface of recycled carbon fibers by catalytic chemical vapor deposition for revalorization of degraded composite materials. *Journal of Nanoparticle Research* **2020**, *22* (1).
93. Szpieg, M.; Wysocki, M.; Asp, L. E., Mechanical performance and modelling of a fully recycled modified CF/PP composite. *Journal of Composite Materials* **2012**, *46* (12), 1503-1517.
94. Wong, K. H.; Mohammed, D. S.; Pickering, S. J.; Brooks, R., Effect of coupling agents on reinforcing potential of recycled carbon fibre for polypropylene composite. *Composites Science and Technology* **2012**, *72* (7), 835-844.
95. Pickering, S. In *Carbon fibre recycling technologies: what goes in and what comes out*, Carbon fibre recycling and reuse 2009 conference, IntertechPira, Hamburg, Germany, 2009.
96. Warrior, N.; Turner, T.; Pickering, S. In *AFRECAR and HIRECAR Project results*, Carbon fibre recycling and reuse 2009 conference, IntertechPira, Hamburg, Germany, 2009.
97. Russell, S. J., *Handbook of nonwovens*. Woodhead Publishing: 2006.
98. Akonda, M. H.; Lawrence, C. A.; Weager, B. M., Recycled carbon fibre-reinforced polypropylene thermoplastic composites. *Composites Part a-Applied Science and Manufacturing* **2012**, *43* (1), 79-86.
99. Giannadakis, K.; Szpieg, M.; Varna, J., Mechanical Performance of a Recycled Carbon Fibre/PP Composite. *Experimental Mechanics* **2011**, *51* (5), 767-777.
100. Szpieg, M.; Wysocki, M.; Asp, L. E., Reuse of polymer materials and carbon fibres in novel engineering composite materials. *Plastics, rubber and composites* **2009**, *38* (9-10), 419-425.
101. Shah, D. U.; Schubel, P. J., On recycled carbon fibre composites manufactured through a liquid composite moulding process. *Journal of Reinforced Plastics and Composites* **2016**, *35* (7), 533-540.

102. Turner, T. A.; Warrior, N. A.; Pickering, S. J., Development of high value moulding compounds from recycled carbon fibres. *Plastics Rubber and Composites* **2010**, 39 (3-5), 151-156.
103. Goergen, C.; May, D.; Mitschang, P., Integration of rCF in resin transfer pressing process. *Journal of Reinforced Plastics and Composites* **2020**, 39 (9-10), 361-372.
104. Tse, B.; Yu, X. L.; Gong, H.; Soutis, C., Flexural Properties of Wet-Laid Hybrid Nonwoven Recycled Carbon and Flax Fibre Composites in Poly-Lactic Acid Matrix. *Aerospace* **2018**, 5 (4).
105. Van de Werken, N.; Reese, M. S.; Taha, M. R.; Tehrani, M., Investigating the effects of fiber surface treatment and alignment on mechanical properties of recycled carbon fiber composites. *Composites Part a-Applied Science and Manufacturing* **2019**, 119, 38-47.
106. Wei, H. W.; Nagatsuka, W.; Lee, H.; Ohsawa, I.; Sumimoto, K.; Wan, Y.; Takahashi, J., Mechanical properties of carbon fiber paper reinforced thermoplastics using mixed discontinuous recycled carbon fibers. *Advanced Composite Materials* **2018**, 27 (1), 19-34.
107. Wei, H. W.; Nagatsuka, W.; Ohsawa, I.; Sumimoto, K.; Takahashi, J., Influence of small amount of glass fibers on mechanical properties of discontinuous recycled carbon fiber-reinforced thermoplastics. *Advanced Composite Materials* **2019**, 28 (3), 321-334.
108. Wong, K. H.; Pickering, S. J.; Rudd, C. D., Recycled carbon fibre reinforced polymer composite for electromagnetic interference shielding. *Composites Part a-Applied Science and Manufacturing* **2010**, 41 (6), 693-702.
109. Bachmann, J.; Wiedemann, M.; Wierach, P., Flexural Mechanical Properties of Hybrid Epoxy Composites Reinforced with Nonwoven Made of Flax Fibres and Recycled Carbon Fibres. *Aerospace* **2018**, 5 (4).
110. Wei, H.; Lee, H.; Nagatsuka, W.; Ohsawa, I.; Kawabe, K.; Murakami, T.; Sumitomo, K.; Takahashi, J., Systematic comparison between carding and paper-making method for producing discontinuous recycled carbon fiber reinforced thermoplastics. *ICCM20, Copenhagen, Denmark* **2015**.
111. Yin, G.; Cai, G.; Wei, H.; Nagatsuka, W.; Kohira, T.; Morisawa, J.; Takahashi, J. In *Novel carding process to improve mechanical properties of recycled carbon fiber card web reinforced thermoplastics*, Proceedings of 21st international conference on composite materials, 2017.
112. Lützkendorf, R.; Reussmann, T.; Danzer, M., Hybrid composites with recycled carbon fibres. *Lightweight Design worldwide* **2017**, 10 (2), 16-19.
113. Cornacchia, G.; Galvagno, S.; Portofino, S.; Caretto, F.; Giovanni, C.; Matera, D.; Donatelli, A.; Iovane, P.; Martino, M.; Civita, R. In *Carbon fiber recovery from waste composites: an integrated approach for a commercially successful recycling operation*, SAMPE'09 Conference. SAMPE, Baltimore, MD, USA, 2009.
114. Xiao, B.; Zaima, T.; Shindo, K.; Kohira, T.; Morisawa, J.; Wan, Y.; Yin, G. H.; Ohsawa, I.; Takahashi, J., Characterization and elastic property modeling of discontinuous carbon fiber reinforced thermoplastics prepared by a carding and stretching system using treated carbon fibers. *Composites Part a-Applied Science and Manufacturing* **2019**, 126.
115. Sathishkumar, T.; Naveen, J. a.; Satheeshkumar, S., Hybrid fiber reinforced polymer composites—a review. *Journal of Reinforced Plastics and Composites* **2014**, 33 (5), 454-471.
116. Longana, M. L.; Ong, N.; Yu, H. N.; Potter, K. D., Multiple closed loop recycling of carbon fibre composites with the HiPerDiF (High Performance Discontinuous Fibre) method. *Composite Structures* **2016**, 153, 271-277.
117. Tapper, R. J.; Longana, M. L.; Yu, H.; Hamerton, I.; Potter, K. D., Development of a closed-loop recycling process for discontinuous carbon fibre polypropylene composites. *Composites Part B: Engineering* **2018**, 146, 222-231.
118. Akonda, M. H.; Stefanova, M.; Potluri, P.; Shah, D. U., Mechanical properties of recycled carbon fibre/polyester thermoplastic tape composites. *Journal of Composite Materials* **2017**, 51 (18), 2655-2663.
119. Khurshid, M.; Abdkader, A.; Cherif, C. In *Process development for uni directional tape structure based on recycled carbon fiber and thermoplastic fibers for fiber reinforced plastics*, 19th World textile conference on textiles at the crossroads, 2019; pp 1-6.
120. Hehl, J., Erforschung eines verfahrens zur konsolidierung von carbonfasertapes aus recycelten carbonfasern zur herstellung von faserverbundbauteilen. *University of Denkdorf DITF Deutschland* **2017**.

121. Horrocks, A. R.; Anand, S. C., *Handbook of Technical Textiles: Technical Textile Processes*. Woodhead Publishing: 2015.
122. Hasan, M.; Nitsche, S.; Abdkader, A.; Cherif, C., Carbon fibre reinforced thermoplastic composites developed from innovative hybrid yarn structures consisting of staple carbon fibres and polyamide 6 fibres. *Composites Science and Technology* **2018**, *167*, 379-387.
123. Hengstermann, M.; Raithel, N.; Abdkader, A.; Hasan, M. M. B.; Cherif, C., Development of new hybrid yarn construction from recycled carbon fibers for high performance composites. Part-I: basic processing of hybrid carbon fiber/polyamide 6 yarn spinning from virgin carbon fiber staple fibers. *Textile Research Journal* **2016**, *86* (12), 1307-1317.
124. Goergen, C.; Schommer, D.; Duhovic, M.; Mitschang, P., Deep drawing of organic sheets made of hybrid recycled carbon and thermoplastic polyamide 6 staple fiber yarns. *Journal of Thermoplastic Composite Materials* **2020**, *33* (6), 754-778.
125. Hengstermann, M.; Hasan, M. M. B.; Abdkader, A.; Cherif, C., Development of a new hybrid yarn construction from recycled carbon fibers (rCF) for high-performance composites. Part-II: Influence of yarn parameters on tensile properties of composites. *Textile Research Journal* **2017**, *87* (13), 1655-1664.
126. Hengstermann, M.; Hasan, M. M. B.; Scheffler, C.; Abdkader, A.; Cherif, C., Development of a new hybrid yarn construction from recycled carbon fibres for high-performance composites. Part III: Influence of sizing on textile processing and composite properties. *Journal of Thermoplastic Composite Materials* **2019**, 0892705719847240.
127. Miyake, T.; Imaeda, S., A dry aligning method of discontinuous carbon fibers and improvement of mechanical properties of discontinuous fiber composites. *Advanced Manufacturing-Polymer & Composites Science* **2016**, *2* (3-4), 117-123.
128. Hasan, M. M. B.; Hengstermann, M.; Dilo, R.; Abdkader, A.; Cherif, C., Investigations on the manufacturing and mechanical properties of spun yarns made from staple CF for thermoset composites. *Autex Research Journal* **2017**, *17* (4), 395-404.
129. Alagirusamy, R.; Das, A., *Technical textile yarns*. Elsevier: 2010.
130. Hasan, M.; Nitsche, S.; Abdkader, A.; Cherif, C. In *Properties of CF/PA6 friction spun hybrid yarns for textile reinforced thermoplastic composites*, IOP conference series: materials science and engineering, 2017; p 042013.
131. Abdkader, A.; Hengstermann, M.; Badrul Hasan, M. M.; Hossain, M.; Cherif, C.; Weber, D., Evaluation of spinning methods for production of hybrid yarns from rCF for CFRP components. *Melliand International* **2017**, (4).
132. Redwood, B.; Schffer, F.; Garret, B., *The 3D printing handbook: technologies, design and applications*. 3D Hubs: 2017.
133. Comb, J.; Priedeman, W.; Turley, P. W. In *FDM® Technology process improvements*, 1994 International Solid Freeform Fabrication Symposium, 1994.
134. Wang, T.-M.; Xi, J.-T.; Jin, Y., A model research for prototype warp deformation in the FDM process. *The International Journal of Advanced Manufacturing Technology* **2007**, *33* (11-12), 1087-1096.
135. Guerrero-de-Mier, A.; Espinosa, M.; Domínguez, M., Bricking: A new slicing method to reduce warping. *Procedia Engineering* **2015**, *132*, 126-131.
136. Sood, A. K.; Ohdar, R. K.; Mahapatra, S. S., Parametric appraisal of mechanical property of fused deposition modelling processed parts. *Materials & Design* **2010**, *31* (1), 287-295.
137. Vanek, J.; Galicia, J. A. G.; Benes, B. In *Clever support: Efficient support structure generation for digital fabrication*, Computer graphics forum, Wiley Online Library: 2014; pp 117-125.
138. Liu, Z.; Wang, Y.; Wu, B.; Cui, C.; Guo, Y.; Yan, C., A critical review of fused deposition modeling 3D printing technology in manufacturing polylactic acid parts. *The International Journal of Advanced Manufacturing Technology* **2019**, *102* (9-12), 2877-2889.
139. Cui, M. A.; Snyder, J.; Elliott, A. M.; Romero, N.; Kannan, S.; Halada, G. P., Impact of the fused deposition (FDM) printing process on polylactic acid (PLA) chemistry and structure. *Applied Sciences* **2017**, *7* (6), 579.
140. Gu, P.; Li, L., Fabrication of biomedical prototypes with locally controlled properties using FDM. *CIRP Annals* **2002**, *51* (1), 181-184.

141. Kishore, V.; Ajinjeru, C.; Nycz, A.; Post, B.; Lindahl, J.; Kunc, V.; Duty, C., Infrared preheating to improve interlayer strength of big area additive manufacturing (BAAM) components. *Additive Manufacturing* **2017**, *14*, 7-12.
142. Sun, Q.; Rizvi, G.; Bellehumeur, C.; Gu, P. In *Experimental Study of the Cooling Characteristics of Polymer Filaments in FDM and Impact on the Mesostructures and Properties of Prototypes 313*, 2003 International Solid Freeform Fabrication Symposium, 2003.
143. Sun, Q.; Rizvi, G.; Bellehumeur, C.; Gu, P., Effect of processing conditions on the bonding quality of FDM polymer filaments. *Rapid Prototyping Journal* **2008**.
144. Bellehumeur, C.; Li, L.; Sun, Q.; Gu, P., Modeling of bond formation between polymer filaments in the fused deposition modeling process. *Journal of manufacturing processes* **2004**, *6* (2), 170-178.
145. Partain, S. C. Fused deposition modeling with localized pre-deposition heating using forced air. Montana State University-Bozeman, College of Engineering, 2007.
146. Ravi, A. K.; Deshpande, A.; Hsu, K. H., An in-process laser localized pre-deposition heating approach to inter-layer bond strengthening in extrusion based polymer additive manufacturing. *Journal of Manufacturing Processes* **2016**, *24*, 179-185.
147. Bahnini, I.; Rivette, M.; Rechia, A.; Siadat, A.; Elmesbahi, A., Additive manufacturing technology: the status, applications, and prospects. *The International Journal of Advanced Manufacturing Technology* **2018**, *97* (1-4), 147-161.
148. Torres, J.; Cole, M.; Owji, A.; DeMastry, Z.; Gordon, A. P., An approach for mechanical property optimization of fused deposition modeling with polylactic acid via design of experiments. *Rapid Prototyping Journal* **2016**.
149. Rajpurohit, S. R.; Dave, H. K., Analysis of tensile strength of a fused filament fabricated PLA part using an open-source 3D printer. *The International Journal of Advanced Manufacturing Technology* **2019**, *101* (5-8), 1525-1536.
150. Yang, J.-H.; Zhao, Z.-j.; Park, S.-H. In *Evaluation of directional mechanical properties of 3D printed polymer parts*, 2015 15th International Conference on Control, Automation and Systems (ICCAS), IEEE: 2015; pp 1952-1954.
151. Vaezi, M.; Chua, C. K., Effects of layer thickness and binder saturation level parameters on 3D printing process. *The International Journal of Advanced Manufacturing Technology* **2011**, *53* (1-4), 275-284.
152. Wang, L.; Gramlich, W. M.; Gardner, D. J., Improving the impact strength of Poly (lactic acid)(PLA) in fused layer modeling (FLM). *Polymer* **2017**, *114*, 242-248.
153. Patel, D., Effects of infill patterns on time, surface roughness and tensile strength in 3D printing. *Int. J. Eng. Dev. Res* **2017**, *5*, 566-569.
154. Torres, J.; Cotelto, J.; Karl, J.; Gordon, A. P., Mechanical property optimization of FDM PLA in shear with multiple objectives. *Jom* **2015**, *67* (5), 1183-1193.
155. Afrose, M. F.; Masood, S.; Iovenitti, P.; Nikzad, M.; Sbarski, I., Effects of part build orientations on fatigue behaviour of FDM-processed PLA material. *Progress in Additive Manufacturing* **2016**, *1* (1-2), 21-28.
156. Shim, J.-H.; Won, J.-Y.; Sung, S.-J.; Lim, D.-H.; Yun, W.-S.; Jeon, Y.-C.; Huh, J.-B., Comparative efficacies of a 3D-printed PCL/PLGA/ β -TCP membrane and a titanium membrane for guided bone regeneration in beagle dogs. *Polymers* **2015**, *7* (10), 2061-2077.
157. Le Duigou, A.; Castro, M.; Bevan, R.; Martin, N., 3D printing of wood fibre biocomposites: From mechanical to actuation functionality. *Materials & Design* **2016**, *96*, 106-114.
158. Patanwala, H. S.; Hong, D.; Vora, S. R.; Bognet, B.; Ma, A. W., The microstructure and mechanical properties of 3D printed carbon nanotube-polylactic acid composites. *Polymer Composites* **2018**, *39* (S2), E1060-E1071.
159. Zhang, D.; Chi, B.; Li, B.; Gao, Z.; Du, Y.; Guo, J.; Wei, J., Fabrication of highly conductive graphene flexible circuits by 3D printing. *Synthetic Metals* **2016**, *217*, 79-86.
160. Yu, W. W.; Zhang, J.; Wu, J. R.; Wang, X. Z.; Deng, Y. H., Incorporation of graphitic nano-filler and poly (lactic acid) in fused deposition modeling. *Journal of Applied Polymer Science* **2017**, *134* (15).

161. Liu, W. a. Z. J. a. L. Y. a. W. J. a. X. J., Influence of addition of ATBC on the preparation and properties of PLA/PCL filaments for FDM 3D printing. *Gongneng Cailiao/Journal of Functional Materials* **2017**, *48*, 11168-11173.
162. Haq, R. H. A.; Rahman, M. N. A.; Ariffin, A. M. T.; Hassan, M. F.; Yunus, M. Z.; Adzila, S. In *Characterization and mechanical analysis of PCL/PLA composites for FDM feedstock filament*, IOP Conference Series: Materials Science and Engineering, 2017; pp 120-138.
163. Mao, D.; Li, Q.; Li, D.; Chen, Y.; Chen, X.; Xu, X., Fabrication of 3D porous poly (lactic acid)-based composite scaffolds with tunable biodegradation for bone tissue engineering. *Materials & Design* **2018**, *142*, 1-10.
164. Kennedy, Z.; Christ, J.; Evans, K.; Arey, B.; Sweet, L.; Warner, M.; Erikson, R.; Barrett, C., 3D-printed poly (vinylidene fluoride)/carbon nanotube composites as a tunable, low-cost chemical vapour sensing platform. *Nanoscale* **2017**, *9* (17), 5458-5466.
165. Arun, K.; Aravindh, K.; Raja, K.; Jeeva, P.; Karthikeyan, S., Metallization of PLA plastics prepared by FDM-RP process and evaluation of corrosion and hardness characteristics. *Materials Today: Proceedings* **2018**, *5* (5), 13107-13110.
166. Yang, Y.; Chen, Y.; Wei, Y.; Li, Y., 3D printing of shape memory polymer for functional part fabrication. *The International Journal of Advanced Manufacturing Technology* **2016**, *84* (9-12), 2079-2095.
167. Daniel, F.; Patoary, N. H.; Moore, A. L.; Weiss, L.; Radadia, A. D., Temperature-dependent electrical resistance of conductive polylactic acid filament for fused deposition modeling. *The International Journal of Advanced Manufacturing Technology* **2018**, *99* (5-8), 1215-1224.
168. Fu, S.-Y.; Lauke, B., Effects of fiber length and fiber orientation distributions on the tensile strength of short-fiber-reinforced polymers. *Composites Science and Technology* **1996**, *56* (10), 1179-1190.
169. Wang, X.; Jiang, M.; Zhou, Z.; Gou, J.; Hui, D., 3D printing of polymer matrix composites: A review and prospective. *Composites Part B: Engineering* **2017**, *110*, 442-458.
170. Ivey, M.; Melenka, G. W.; Carey, J. P.; Ayranci, C., Characterizing short-fiber-reinforced composites produced using additive manufacturing. *Advanced Manufacturing: Polymer & Composites Science* **2017**, *3* (3), 81-91.
171. Jiang, D.; Smith, D. E., Anisotropic mechanical properties of oriented carbon fiber filled polymer composites produced with fused filament fabrication. *Additive Manufacturing* **2017**, *18*, 84-94.
172. Tian, X.; Liu, T.; Yang, C.; Wang, Q.; Li, D., Interface and performance of 3D printed continuous carbon fiber reinforced PLA composites. *Composites Part A: Applied Science and Manufacturing* **2016**, *88*, 198-205.
173. Tian, X. Y.; Liu, T. F.; Wang, Q. R.; Dilmurat, A.; Li, D. C.; Ziegmann, G., Recycling and remanufacturing of 3D printed continuous carbon fiber reinforced PLA composites. *Journal of Cleaner Production* **2017**, *142*, 1609-1618.
174. Ferreira, R. T. L.; Amatte, I. C.; Dutra, T. A.; Bürger, D., Experimental characterization and micrography of 3D printed PLA and PLA reinforced with short carbon fibers. *Composites Part B: Engineering* **2017**, *124*, 88-100.
175. Huxtable, S. T.; Cahill, D. G.; Shenogin, S.; Xue, L.; Ozisik, R.; Barone, P.; Usrey, M.; Strano, M. S.; Siddons, G.; Shim, M., Interfacial heat flow in carbon nanotube suspensions. *Nature materials* **2003**, *2* (11), 731-734.
176. Paiva, M. C.; Mano, J. F., Interfacial studies of carbon fibre/polycarbonate composites using dynamic mechanical analysis. *e-Polymers* **2005**, *5* (1).
177. Chen, R.; Misra, M.; Mohanty, A. K., Injection-moulded biocomposites from polylactic acid (PLA) and recycled carbon fibre: Evaluation of mechanical and thermal properties. *Journal of Thermoplastic Composite Materials* **2014**, *27* (9), 1286-1300.
178. Test, D. C. I. T. C., IPC-TM-650 TEST METHODS MANUAL.